AD-A137 881 THE EFFECT OF VERTICAL DATUM INCONSISTENCIES ON THE DETERMINATION OF GRAV..(U) OHIO STATE UNIV COLUMBUS DEPT OF GEODETIC SCIENCE AND SUREEYI.. P LASKOWSKI

UNCLASSIFIED AUG 83 OSU/DGSS-349 AFGL-TR-83-0228 F/G 8/5 NL

1/2

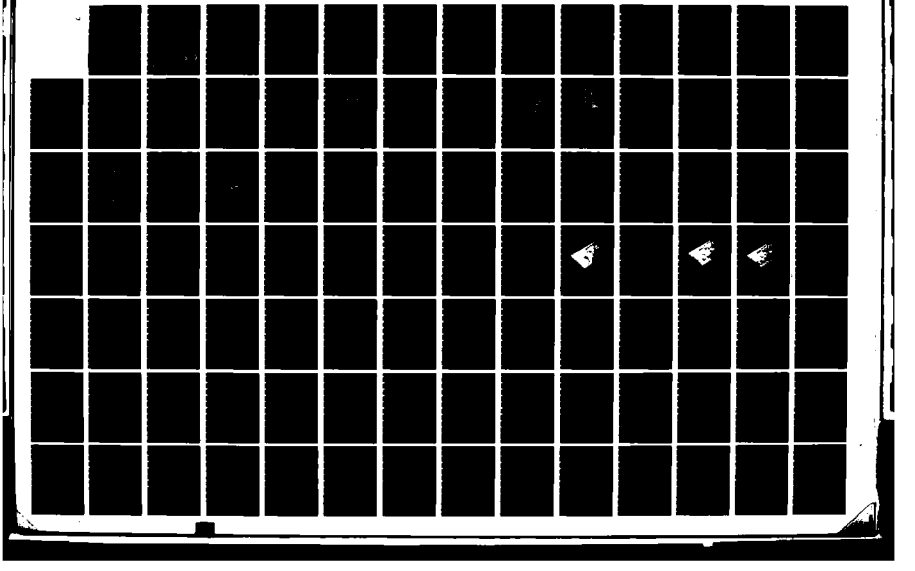

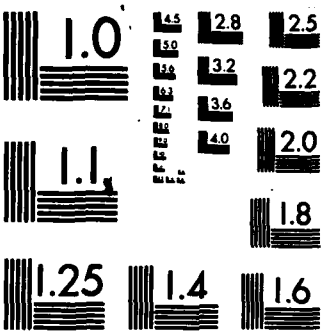

MICROCOPY RESOLUTION TEST CHART
NATIONAL BUREAU OF STANDARDS-1963-A

AFGL-TR-83-0228

12

THE EFFECT OF VERTICAL DATUM INCONSISTENCIES ON THE DETERMINATION OF GRAVITY RELATED QUANTITIES

Piotr Laskowski

The Ohio State University
Research Foundation
Columbus, Ohio 43212

August, 1983

Scientific Report No. 4

AIR FORCE GEOPHYSICS LABORATORY
AIR FORCE SYSTEMS COMMAND
UNITED STATES AIR FORCE
HANSCOM AFB, MASSACHUSETTS 01731

CONTRACTOR REPORTS

This report has been reviewed by the ESD Public Affairs Office (PA) and is releasable to the National Technical Information Service (NTIS).

This technical report has been reviewed and is approved for publication.

CHRISTOPHER JEKELI
Contract Manager

THEODORE E. WIRTANEN
Acting Chief, Geodesy & Gravity Branch

FOR THE COMMANDER

DONALD H. ECKHARDT
Director
Terrestrial Sciences Division

Qualified requestors may obtain additional copies from the Defense Technical Information Center. All others should apply to the National Technical Information Service.

If your address has changed, or if you wish to be removed from the mailing list, or if the addressee is no longer employed by your organization, please notify AFGL/DAA, Hanscom AFB, MA 01731. This will assist us in maintaining a current mailing list.

Do not return copies of this report unless contractual obligations or notices on a specific document requires that it be returned.

SECURITY CLASSIFICATION OF THIS PAGE (When Data Entered)

REPORT DOCUMENTATION PAGE		READ INSTRUCTIONS BEFORE COMPLETING FORM
1. REPORT NUMBER AFGL-TR-83-0228	2. GOVT ACCESSION NO. AD-A137 881	3. RECIPIENT'S CATALOG NUMBER
4. TITLE (and Subtitle) THE EFFECT OF VERTICAL DATUM INCONSISTENCIES ON THE DETERMINATION OF GRAVITY RELATED QUANTITIES		5. TYPE OF REPORT & PERIOD COVERED Scientific Report No. 4 6. PERFORMING ORG. REPORT NUMBER OSU/DGSS-349
7. AUTHOR(s) Piotr Laskowski		8. CONTRACT OR GRANT NUMBER(s) F19628-82-K- 0022
9. PERFORMING ORGANIZATION NAME AND ADDRESS The Ohio State University Research Foundation 1958 Neil Avenue, Columbus, Ohio 43210		10. PROGRAM ELEMENT, PROJECT, TASK AREA & WORK UNIT NUMBERS 61102F 2309G1BC
11. CONTROLLING OFFICE NAME AND ADDRESS Air Force Geophysics Laboratory Hanscom AFB, Massachusetts 01730 Monitor/Christopher Jekeli/LWG		12. REPORT DATE August 1983 13. NUMBER OF PAGES 94
14. MONITORING AGENCY NAME & ADDRESS(if different from Controlling Office)		15. SECURITY CLASS. (of this report) Unclassified 15a. DECLASSIFICATION/DOWNGRADING SCHEDULE

16. DISTRIBUTION STATEMENT (of this Report)

Approved for public release; distribution unlimited

17. DISTRIBUTION STATEMENT (of the abstract entered in Block 20, if different from Report)

18. SUPPLEMENTARY NOTES

19. KEY WORDS (Continue on reverse side if necessary and identify by block number)

Vertical datum, sea surface topography, potential coefficients, gravity anomalies, mean sea level

20. ABSTRACT (Continue on reverse side if necessary and identify by block number)

Three different models of inconsistencies in the world vertical datum due to the Sea Surface Topography problem are constructed.

A spherical harmonic decomposition of different models of global vertical datum inconsistencies into a set of potential coefficients up to degree and order 180 is described. The effect of datum inconsistency is found significant at low degree harmonics and negligible above degree 60. The maximum relative

DD FORM 1 JAN 73 1473 EDITION OF 1 NOV 65 IS OBSOLETE UNCLASSIFIED

SECURITY CLASSIFICATION OF THIS PAGE (When Data Entered)

20. (cont.)

error (by degree variances of coefficients) is estimated as 1%. In terms of the error in geoid undulation the absolute cumulative effect of datum inconsistency can be of the order of 0.5 m which is of the order of the amplitude of Sea Surface Topography variation. In terms of the error in gravity anomaly, the cumulative effect can be of the order of 0.1 mgal.

The effect of the internal distortion of the North Americal vertical datum due to the overconstrained adjustment of the 1929 levelling net is found to produce the cumulative error in geoid undulation of the order of 2 millimeters, and in terms of gravity anomaly this error is estimated as 0.0001 mgals.

Since the propagated datum inconsistency error affects mostly a few low degree harmonics, the recommendation is made toward the substitution of those contaminated coefficients derived from the terrestrial gravity anomalies data by satellite derived harmonics. Some remarks are made on the choice of appropriate splitting degree.

The secondary effect on the zero-degree undulation term when the gravity anomaly data in the spherical cap are used through the Stokes' equation to produce the geoid undulation field is found to be of the order of 1 cm for most practical applications.

Also, the total effect due to vertical datum inconsistencies associated with the practical procedure of geoid undulation computation based on the terrestrial gravity data in a spherical cap was found to be of the order of 7 to 19 cm for most practical applications.

Foreword

This report was prepared by Piotr Laskowski, Graduate Research Associate, Department of Geodetic Science and Surveying, The Ohio State University, under Air Force Contract No. F19628-82-K-0022, The Ohio State University Research Foundation Project No. 714274. This project is under the supervision of Professor Richard H. Rapp. The contract covering this research is administered by the Air Force Geophysics Laboratory, Hanscom Air Force Base, Massachusetts, with Dr. Christopher Jekeli, Scientific Program Officer.

Acknowledgements

I am in debt to my advisor, Professor Richard H. Rapp, for his guidance and help during the work that this report describes and for his patience and guidance during the improvement and writing of this report.

I am grateful to my wife Iwona for constant support, pre-typing the manuscript, help with the computer-related operations and with editing the successive versions of this report.

I would like to thank Professor Dhaneshwar Hajela for serving on the reading committee for the Thesis examination. His comments were greatly appreciated.

Miss Laura Brumfield did an excellent job in typing this thesis and to her I am greatly in debt.

I can not stress enough the degree to which I have relied on work from previous vertical datum projects in the Department of Geodetic Science and Surveying. Especially the use of computer subroutine HARMIN by O. Colombo and subroutine LISITZ by Kostas Katsambalos greatly simplified my work.

This study has also been submitted to the Graduate School of The Ohio State University in partial fulfillment of the requirements for the degree Master of Science.

TABLE OF CONTENTS

LIST OF FIGURES

LIST OF TABLES

1. INTRODUCTION

The primary reference surface for heights is the geoid. The geoid is defined as the equipotential surface of earth's actual gravity field which most closely approximates mean sea level in the spatial least squares sense. Historically the geoid has played an important conceptual role in vertical datum work. A practical realization of the geoid was brought about by tide gauge measurements at selected points. The effects of tides, and of other periodic variations, can be filtered out using appropriate numerical filters. The result is supposed to yield the mean sea level at a given site. Now, to establish a vertical network origin it was only necessary to define this point to have an elevation zero. From this point levelling can proceed to determine potential differences, or orthometric heights, of all other points in the vertical datum. The heights then refer to a specific vertical datum by the mean sea level at the origin.

The usual assumption made in the past was that the mean sea level was a unique equipotential surface. It is now well recognized that this is not the case and that the vertical datums of the world are not in a uniform system due to the effects of sea surface topography. The sea surface topography is the departure of the mean sea level from the geoid. The causes of sea surface topography include ocean currents, water density variations as well as air pressure and wind stress. In addition, close to the shore the sea-bed topography and river discharge may also play a significant role.

It thus follows that heights given on one vertical datum are not compatible with heights on another datum. Fortunately, this incompatibility is not large since the effects of sea surface topography are of the order of 2 meters. Nevertheless, there are applications where a consistent height system to a decimeter level is desired. For example, in the calculation of free air gravity anomalies to match today's accuracy of gravity measurments (0.02 mgal) we should know the height of the point to 6 cm which is a much stronger requirement than can currently be reached due to the variety of local vertical datums.

The variable sea surface topography can cause problems even within a single vertical datum. It has been the practice in some countries to connect precise levelling nets to several tide gauges, widely dispersed around the perimeter of the net. The sea surface topography at each tide gauge is different, and resulting adjustment of the levelling data to fit these different mean sea levels can lead, and led, to distortions in the levelling networks.

In many computations a precise knowledge of a set of spherical harmonic coefficients of the earth's disturbing potential T is required. The coefficients can be derived from a combination of satellite derived potential coefficients, $1° \times 1°$ terrestrial gravity anomalies, and $1° \times 1°$ anomalies derived from Seasat altimeter data. In the case of the terrestrial data, systematic errors may be caused by inconsistencies between

different vertical datums, so that gravity anomalies after reduction do not refer to a single equipotential surface.

The purpose of the present work is to evaluate the magnitude of the errors in the potential coefficients caused by the inconsistencies in the world's vertical datum. Due to the insufficient information on the levelling networks in most of the areas of the earth's land surface, the technique of numerical simulation was applied. It should be mentioned however, that the model height-error function (used as the basis for this study) was constructed in such a way as to get the best approximation of the reality from the information available. The contribution of the computed error in the potential coefficients to the geoid undulations and gravity anomalies is also given here.

The technique of numerical simulation was also applied to the problem of modelling distortions in the levelling net which were introduced during the least squares adjustment, when more than one coastal height was constrianed to zero. The example of the levelling net of the United States was chosen here because such procedure actually took place during the 1929 General Adjustment, and all heights being used today are possibly affected by the error of this kind. The distortions were modelled using the adjustment of the simulated network of the United States and were included in the basic height-error function.

Summarizing, the results obtained in these studies refer to two different sources of errors. The first is the error caused by the world's inconsistent height datums, the second is the error introduced by improper data reduction (forcing the height of more than one coastal point to zero). Both sources of errors are present in the actual vertical datum work, and both propagate on to any derived gravimetric quantity related to gravity anomalies, such as the disturbing potential, geoid undulations, deflections of vertical and others.

2. SEA SURFACE TOPOGRAPHY PROBLEM

Classically the undisturbed ocean surface has been taken as the geoid, that is the unique equipotential surface of the actual gravity field. Unfortunately such a surface does not exist and the actual ocean surface can serve only as an approximation of the geoid. The departure of the mean sea level (MSL) from the equipotential surface is called sea surface topography (SST). The MSL is constantly changing with time, as is the SST (Merry and Vanicek, 1982). The MSL variations are mainly due to salinity differences, temperature differences, atmospheric pressure changes, winds, crustal movements, eustatic changes, and river discharge. Also, the global mean sea surface appears to be rising at a rate of approximately 0.5 cm/year (Frasetto, 1970). Nevertheless, we make an assumption here that all time dependent components have been filtered out and that SST implied by such idealized MSL is independent of time.

It is general practice to choose the average physical water surface as the reference level not only for measurements of altitude on land, but also for all depth determinations at sea. Oceanography studies of the MSL require the determination of the relative topography of the physical water surface (Lisitzin, 1974). Different authors have chosen a definite constant depth as reference. Some important names worth mentioning here are: Dietrich (1937), Defant (1941), Lacombe (1951), Reid (1961), Stommel (1965), Lisitzin (1965), Sturges (1974), and Levitus (1982). Other oceanographers have chosen a rather different approach to the problem, endeavoring to determine for every part of the ocean the layer of 'no motion' or, more precisely, the layer of minimum water motion. The first important contribution to this problem was done by Dietrich in 1937.

Lisitzin (1965) computed the MSL in dynamic cm, relative to the 4000-decibar dynamic depth. According to the standard textbooks, the dynamic depth D of an isobaric surface is computed in two parts: fixed, 'standard ocean' part D (35, 0, p) of uniform 35% salinity and 0° C temperature (for a given pressure level p), and the 'anomaly of dynamic depth' ΔD. Therefore, the oceanic graphics (like those given by Lisitzin, 1965) represent the height surplus of the actual mean sea level (or zero-decibar surface) over the theoretical zero-decibar surface of the standard ocean. This height surplus is usually expressed in dynamic cm, where (according to the standard definition) 1 dyn.cm is the unit of potential corresponding to the work required to move a unit mass approximately 1 cm in vertical direction. The surface of equal dynamic depth is thus the equipotential surface, although without any geodetic significance. Figure 1 shows Lisitzin's world oceanic chart of the Sea Surface Topography. The sea surface variation (in dyn. cm) was computed relative to the 4000-dbar dynamic depth at open deep regions of oceans. The chart reveals that for all latitudes the mean sea level is lowest in the Atlantic Ocean, while the highest values, generally, are to be found in the Pacific Ocean. As an average, the Pacific Ocean stands 72 dyn.cm higher than the Atlantic Ocean and 36 dyn.cm higher than the Indian Ocean. This is strongly connected to the variation of water density between the different oceans. The highest mean sea level occurs in the western parts of all oceans, at the latitudes of approximately 20° to 30° in both hemispheres. From this highest position the MSL slopes steeply towards the poles. The lowest values occur in the higher latitudes of the two hemispheres and there is a secondary minimum in the zones around the equator.

The average sea level for all the deep-sea regions of the oceans considered in Figure 1 is 289 dyn.cm (Lisitzin, 1965). The MSL in the adjacent and Mediterranean seas is generally lower than that in the oceans (Lisitzin, 1965). Therefore, as a first approximation of global average Lisitzin proposed the value of 280 dyn.cm. This value will be used in the sequel.

If we had reliable values of SST we could correct MSL heights to get the geoid. Unfortunately, the complexity of SST problem does

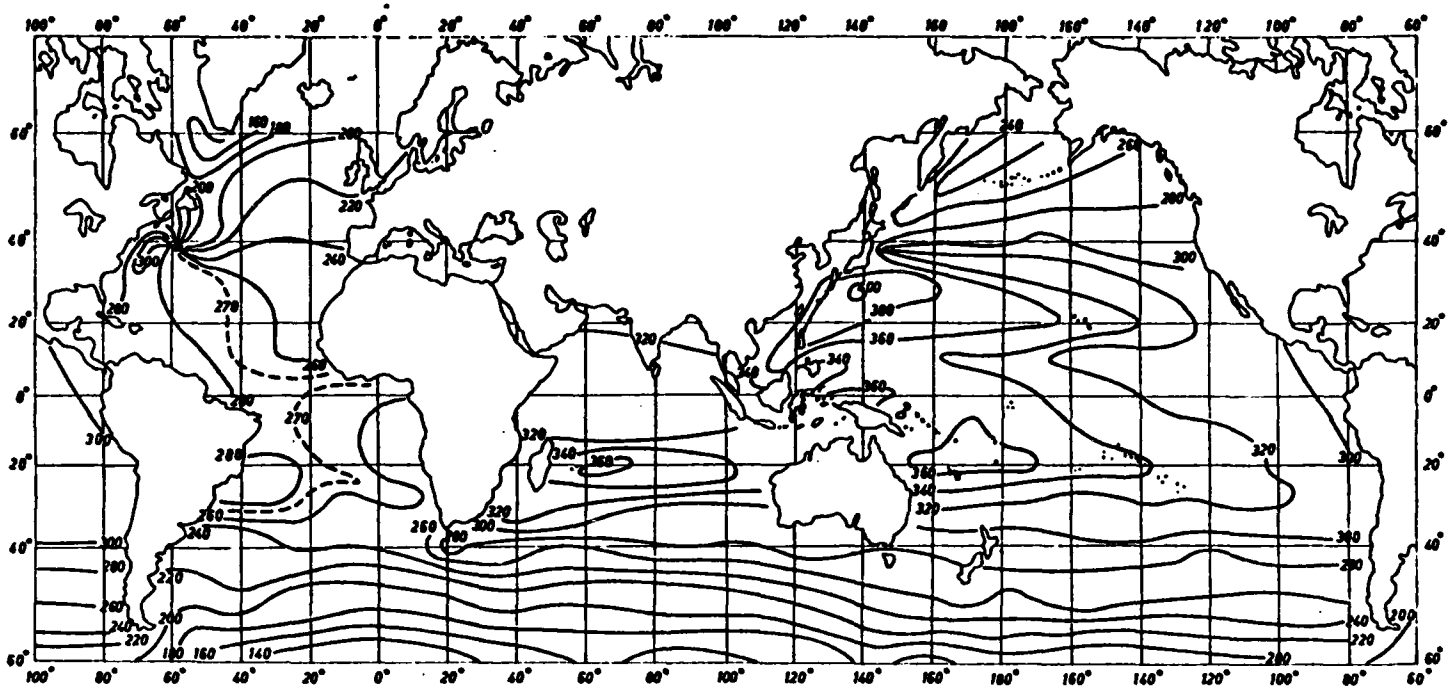

Figure 1. The distribution of Sea Surface Topography (in dyn.cm) in the world oceans, with the average value of 280 dyn.cm
From: (Lisitzin, 1974)

not allow for realistic approximation of the geoid at the sub-decimeter level, and the unification of all vertical datums is not possible today. Instead based on the existing incomplete information on SST, we can try to model the spatial interrelations between different levelling nets. Extrapolating SST from deep-ocean regions to continental shore-lines and utilizing available information on the levelling techniques and adjustment procedures at different vertical networks we can construct the spatial height-error function. This function would reflect the relative location of different vertical datums with respect to the idealized geoid. For the purpose of this study the reference geoid is that implied by the Lisitzin's global average value of SST, that is 280 dyn.cm. The magnitude of our height-error function would not exceed the amplitude of the SST, that is 2 m. In the next chapter we examine how the error of this magnitude propagates on to the spherical harmonic coefficients of the disturbing potential derived from the terrestrial gravity anomaly data.

3. SST AND DIFFERENT VERTICAL NETWORK PROCEDURES

In this chapter vertical network procedures in different parts of the world are examined. The information given here is by no means complete. Of main interest to us is the incorrect assumption that MSL coincides with the geoid, and its implication on the magnitude of the relative spatial inconsistencies between different levelling datums. Such an estimation was possible after extrapolating the values of SST from the deep-ocean regions to the continental shore-lines. This sort of procedure is by no means accurate but is expected to provide a sufficient approximation for the purpose of our model studies. The Sea Surface Topography on continental shelves is affected by the sea-bed topography, river discharge, wind stress and other factors (Lisitzin, 1965) and, therefore, might significantly differ from the values estimated on the basis of extrapolation from the deep ocean regions. Nevertheless, we use this technique since we believe it assures sufficient accuracy for the purpose of this investigation.

The main source of information on SST is the Lisitzin's world-chart of mean sea level variations relative to the 4000-dbar isobaric surface shown on Figure 1. To relate the extrapolated SST values with the vertical datum's zero-level and levelling network procedures, it is essential to know the spatial distribution of tide-gauge stations which were set to zero-height during the adjustment of particular levelling network. Unfortunately, such information was not available on all continents so that at some of them we had to assume that a unified continental vertical network was adjusted with a hypothetical single master tide-gauge station constrained to zero-height at an arbitrary fixed location. From this point of view our studies are purely modelling ones with the intention, however, to produce a realistic range of the resultant contribution to the set of spherical harmonics, and other gravimetric quantities derived from gravity data referred to these datums. On the other hand, wherever possible we reconstruct the spatial interrelations between different vertical datums as realistically as the available data allow.

3.1 Classical Vertical Datum Procedures in the United States and Canada

The present vertical reference system of the United States is based on the 1929 General Adjustment (Lippold, 1980). This adjustment contained a total of 107000 km of levelling in the U.S. and Canada (Figure 2). The 1929 datum was obtained by holding the fixed zero-elevations at 26 tide gauge sites; 21 of these spread along East, West and Gulf Coast of the U.S., and 5 lie in Canada. The distribution of primary tide gauge stations used as the reference in 1929 adjustment is shown on Figure 2. The resulting height system was designated the Sea Level Datum of 1929. This name was later changed to the National Geodetic Vertical Datum of 1929 (NGVD 29).

Canada did not adopt this datum, because values from a 1928 adjustment had been published the previous year. Therefore, the present Canadian vertical system is based on the first continental adjustment carried out in 1928 and realized through the fixed zero-height values at 3 Atlantic and 2 Pacific tidal stations (Lachapelle, 1978). Those five primary stations plus Rouses Point (located south of Montreal on the U.S.-Canadian border and connected to the Atlantic Ocean) form the set of 6 zero-height constraints applied during the 1928 adjustment. Figure 3 shows the Canadian vertical framework of 1928 (Lachapelle, 1978).

In the early 50's a new adjustment of the entire Canadian levelling network was made by the Geodetic Survey. Differences with the 1928 adjustment attained about 15 cm., but no changes were introduced to the 1928 datum. Summarizing, Canadian and U.S. vertical networks are on different vertical reference systems. The maximum differences reach 10 cm for points along the border.

Generally, the latest adjustment of the North American Network in 1929 was based on the four incorrect assumptions (Vanicek, Castle, Balazs, 1980):

1. MSL at the 26 utilized tide stations coincides with the geoid (the height set equal to zero);
2. Observed elevation differences between benchmark pairs are affected by only random error characterized by a symmetrical distribution of probability;
3. There was crustal stability during the development of the network;
4. Orthometric correction computed for normal gravity instead of the actual gravity were used.

In this study we focus only on the first assumption: the MSL at primary tide stations is affected by the irregular SST. Forcing the heights at all 26 stations to be zero causes the distortions in the resultant vertical datum. Later we will evaluate the possible magnitude of this distortion. Of course the distortion will contribute to an error in spherical harmonic coefficients and therefore, will be incoporated into our global model of height-error function introduced in Chapter 2.

The distribution of SST values around the North American Continent together with the location of 26 primary tide gauges used as a reference

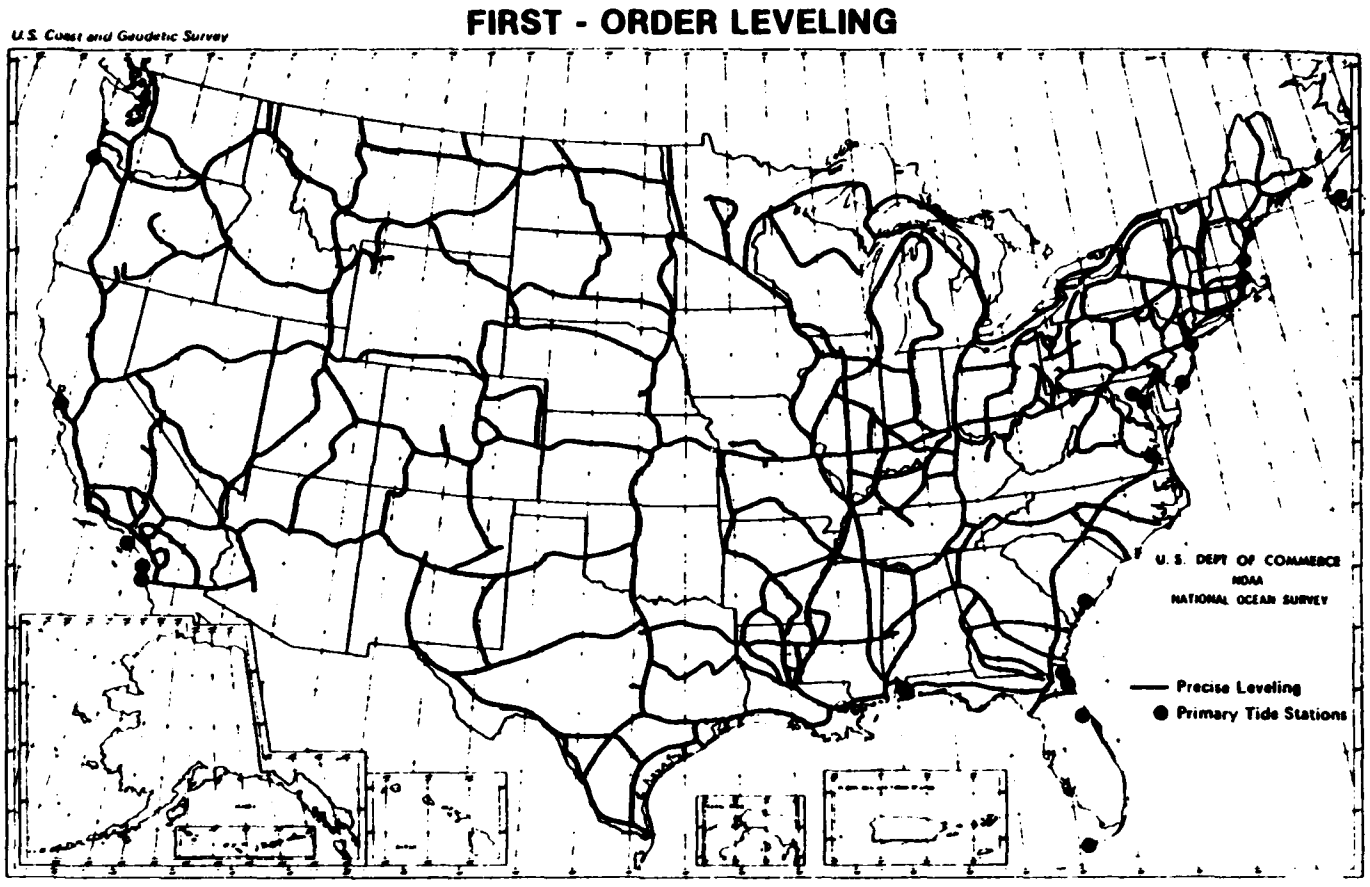

Figure 2. Primary tide gauge stations and vertical control used in 1929 adjustment of the levelling net in the United States. From: (Lippold, 1980)

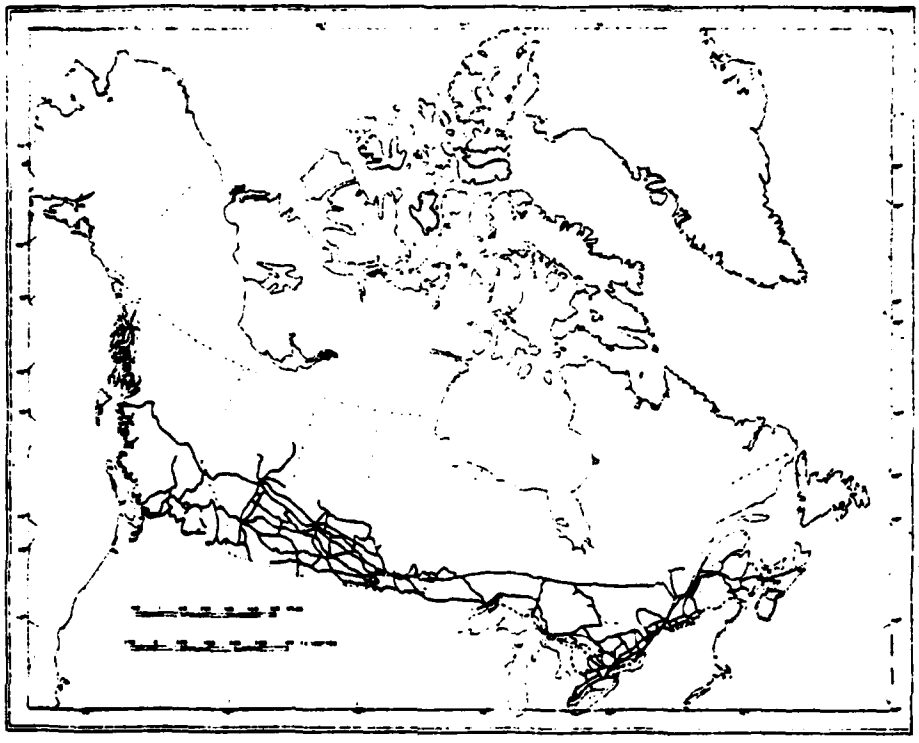

Figure 3. Canadian vertical framework used in the 1928 adjustment.
From: (Lachapelle, 1978)

in 1929 adjustment is shown in Figure 4. The SST was extrapolated from the deep-ocean regions as presented by Lisitzin (1965). It is based on 4000 dbar isobaric deep-sea level. The units are dynamic centimeters. The global average of 280 dyn.cm was subtracted from Lisitzin's values in order to produce results with respect to our model geoid implied by this value.

3.2 Vertical Datum Procedures in Australia

On the Australian continent the Division of National Mapping has conducted a programme of tidal readings at 30 tide gauges around the continent between 1966 and 1968 (Leppert, 1970). In 1971 the simultaneous adjustment was done holding MSL for 1966-1968 fixed at zero at the above mentioned 30 stations. Figure 5 shows the levelling network used in 1971 adjustment together with 30 primary tide gauges which were constrained to zero-height. The net is split into 5 regional nets which were adjusted separately.

As we see, in the case of Australian continent the coincidence of MSL with the geoid was assumed. This incorrect assumption will lead to distortions in the adjusted vertical datum. The distortions will again propagate on to the spherical harmonics coefficients. Another incorrect assumption was made, when (in the orthometric correction formula) the theoretical gravity was used instead of the actual gravity.

On the other hand, the adjustment programs used in the 1971 procedure allowed the difference in height (at each tide gauge) between the bench mark and sea level to be allocated any weight between zero and infinity. By setting weights to zero Mitchell (1972) calculated the free network with a single constraint at the fundamental tide station, Jervis Bay (Mitchell, 1972), (Angus-Leppan, Rizos, 1980). As will be pointed out later, the only acceptable way to adjust a levelling net is to use a single MSL-value constrained to zero-height. Such treatment leads to the so called free network, which could be further block-shifted up or down to obtain the best weighted least squares fit to the MSL at tide guages. For the purpose of this study, we assume that one of the free-network solutions will be chosen in the future to represent the vertical datum of Australia. The extrapolated value of SST at the fundamental tide station in Jervis Bay is 0.3 ±0.2 m (Angus-Leppan, Rizos, 1980).

Figure 6 shows the distribution of SST values around the Australian continent together with the location of 30 primary tide-station held fixed to zero-height during the 1971 adustment. The SST values are estimated from Lisitzin's map (Lisitzin, 1965). They are based on the 4000 dbar isobaric level and the global average of 280 dyn.cm was taken out in order to get the dynamic heights with respect to our model geoid implied by this value.

3.3 Vertical Datum Procedure in Europe

The first adjustment of a combined European Levelling Network was presented by Helmert in 1881. In this computation the mean sea

Figure 4: Variation of Sea Surface Topography around North America with respect to the 280 dyn.cm average given in (Lisitzin, 1974)
Units are dyn.cm.

●- tide gauge stations used as a reference

Figure 5: Australian vertical framework of 1971, showing division into 5 regional nets and the location of tide gauges used as a reference.
From: (Leppert, 1974)

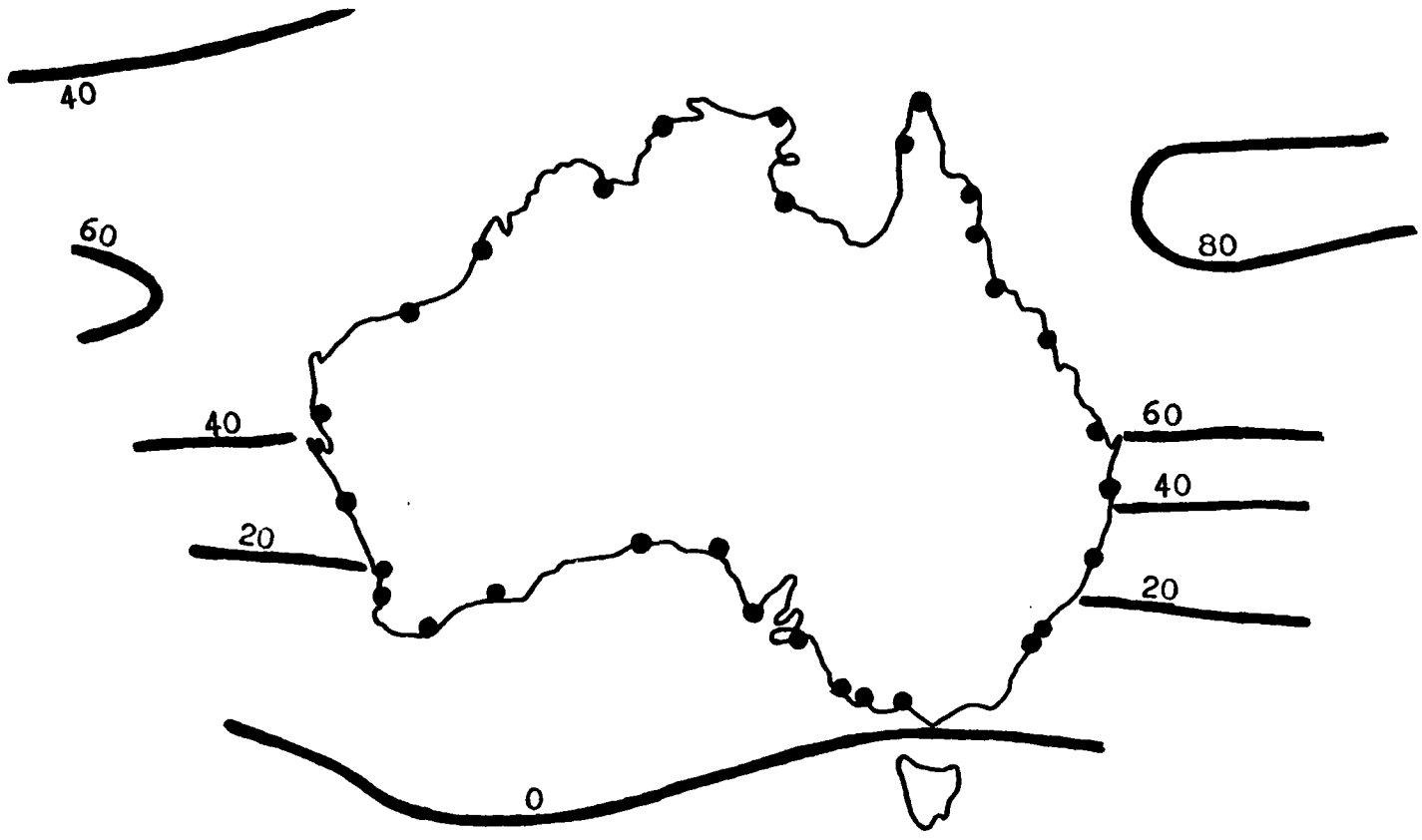

Figure 6. Variation of Sea Surface Topography (Lisitzin, 1965) around Australia in dyn.cm (relative to 280 dyn.cm average)
● - tide gauge stations

Figure 7. UELN-73 - national blocks and tidal stations
From: (Kok, J., Ehrnsperger, W., Rietveld, H., 1980)

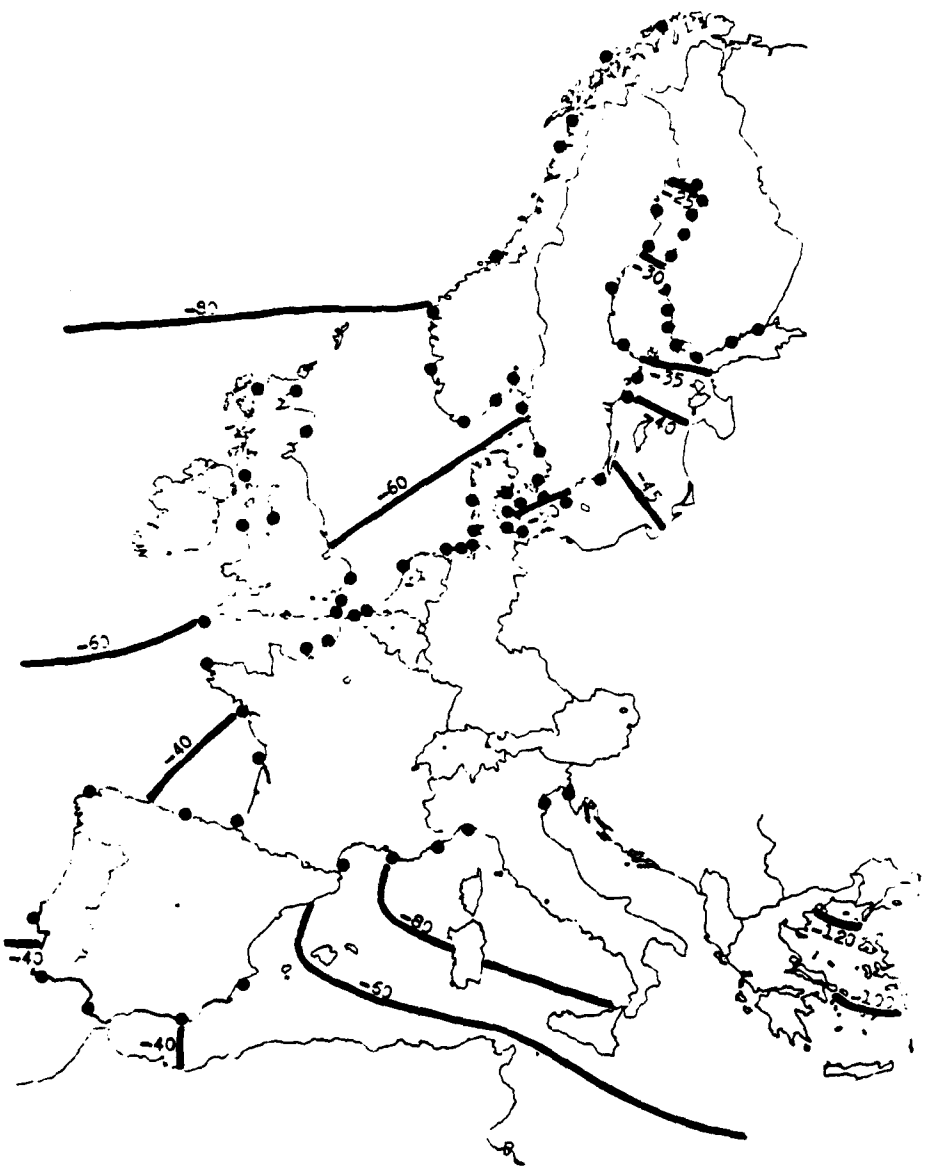

Figure 8. Variation of Sea Surface Topography around Europe (Lisitzin, 1965) in dyn.cm (relative to 280 dyn.cm average). Location of tide gauges, in UELN-73 from (Kok, J., Ehrnsperger, W., Rietveld, M., 1980).

levels and the national levelling networks of Central Europe were for the first time related to one common levelling datum (Heer and Niemeier, 1982). In 1955, the International Commission for the Adjustment of the United European Levelling Network (UELN) was established in Florence. The final results of this so-called UELN-55 adjustment, including Fennoscandia, Central- and South-Western Europe, were published in 1960.

In 1981 a combined adjustment of levelling data from the continental countries and the United Kingdom was carried out. As the new IAG sub-commission for UELN was established in 1973, this new network is called UELN-73. The configuration of the national blocks and tidal stations are shown on Figure 7 (Kok, F., Ehrnsperger, W., Rietveld, H., 1980). To avoid difficulties with the various definitions of heights, in the adjustment of UELN-73 only geopotential numbers or geopotential units (gpu) were introduced as parameters representing the 'heights' of all surface points, and geopotential differences were introduced as observations. In phase I of this new computation the free adjustment of the levelling networks was performed, without incorporating any information on MSL. At first, the data of the 14 West European countries participating in the net were adjusted separately. After these preliminary computations a combined adjustment was carried out, from which the geopotential numbers of the included reference points and their standard deviations were taken. A single datum point in this adjustment is the Normal Amsterdam Piel (NAP) represented in UELN-73, by point No. 4019 (Kok, Ehrnsperger, Rietveld, 1980). Gravity data was based on the International Gravity Standardization Net 1971 (IGSN 71). The method of observation equations was used. The 79 tidal stations are connected to the net, but the information on MSL was not used as constraints, allowing for the free adjustment dependent only on the geopotential number of the datum point at NAP.

In phase II of UELN-73 it is planned to perform statistical testing of adjusted heights of tidal stations against the oceanographic definition of MSL. In the future, based on such tests the whole block of adjusted values obtained in the free adjustment of phase I could be shifted in vertical direction in order to obtain an optimal least squares fit to the oceanographic MSL-values at tide stations. After removing the average value of SST from coastal heights such optimal fit would ultimately produce the geoid, at the resolution of the magnitude of uncertainty to which the values of SST are known.

Figure 8 shows the distribution of SST values around Europe together with the location of tide gauges connected (passively) to the net (Kok, J. Ehrnsperger, W. Rietveld, H., 1980). The SST heights are estimated from Lisitzin's map and the global average of 280 dyn.cm was taken out in order to produce the dynamic heights with respect to our model geoid implied by this value.

Since no constraints have been imposed on heights at coastal point, the UELN-73 datum is free of internal distortions caused by the departure

of MSL from the geoid. However, the systematic error exists in all values and is equal to the SST value at the datum point (NAP). This value could be estimated from Figure 8 as about -50 cm (Lisitzin, 1974, p. 1963).

3.4 The SST Estimates Along Other Countries

The Lisitzin's world's oceanic chart (Figure 1) can serve as a basis for extrapolation of the SST values along the coasts of other continental blocks. The values of SST are based on the 4000 dbar isobaric level and the global average of 280 dyn.cm was taken out.

Figure 9 shows the distribution of SST around Asia, Figure 10 around the coasts of South America, and Figure 11 around Africa. The units for Sea Surface Topography variation are dynamic centimeters.

4. THE DISTORTIONS IN A VERTICAL DATUM DUE TO THE ZERO-CONSTRAINTS AT SEVERAL TIDE GAUGES

As we know today, the classical assumption that the Mean Sea Level coincides with the geoid is not valid. However, even today it remains a common practice to assign the zero-heights to coastal points connected to the levelling net. These so-called zero-constraints introduce inherent distortions in the adjusted vertical datum. The magnitude of this distortion depends mainly on the configuration of tide gauges which were constrained to zero-height with respect to the particular distribution of SST along the perimeter of the net. The distortions introduced at tidal stations can, therefore, reach the amplitude of variation of SST along the ocean boundaries of the given network. During the adjustment process those distortions propagate inside the net and all the interior nodes will be affected by this displacement. In this chapter we want to evaluate the magnitude of this displacement on the example of the levelling net of the United States.

All heights on the North American continent are based on the National Geodetic Vertical Datum of 1929. Therefore, the North American vertical datum is basically warped due to the 26 zero-constraints at tide gauges incorporated to the net during adjustment. The magnitude and spatial behaviour of this distortion is of great importance to our present problem. We will model this distortion and next evaluate its effect on potential coefficient together with the effects resulting from the SST problem.

4.1 The General Approach to the Problem

In order to evaluate the distortions in the levelling net the method of numerical simulation was used.

First, we design a simplified regular grid to model the 1929-levelling net of the U.S. Our numerical approximations to the actual network will be constructed as a regular grid inside the rectangle

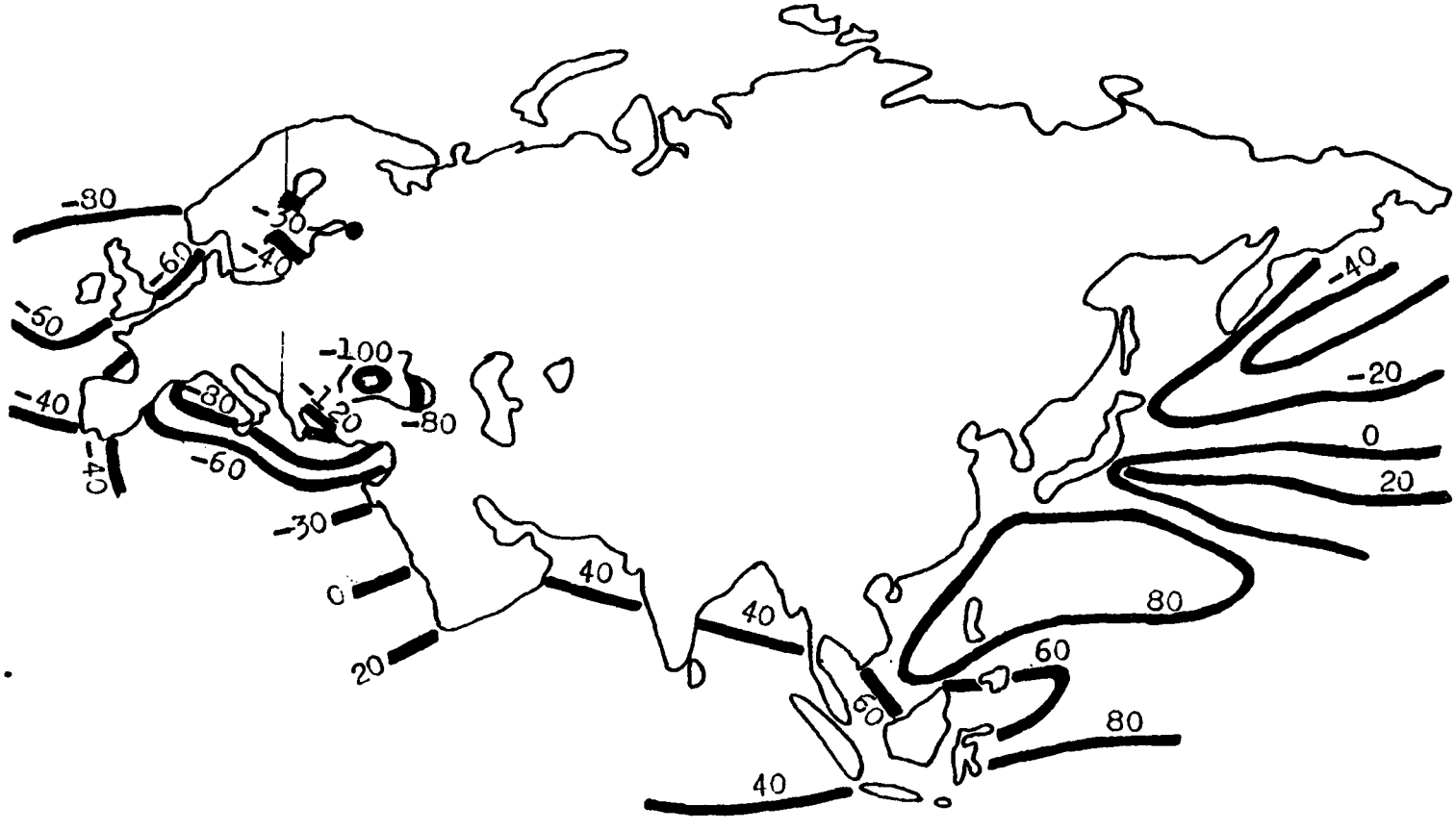

Figure 9. Variation of Sea Surface Topography around Asia (Lisitzin, 1965) in dyn.cm (relative to 280 dyn.cm average)

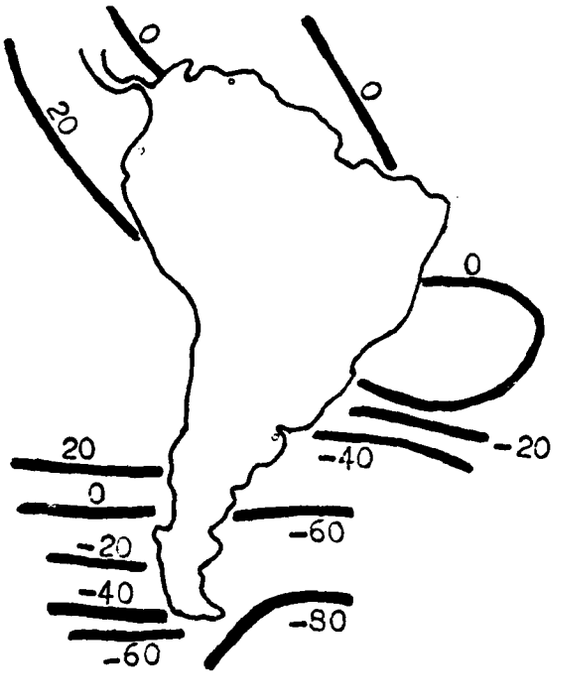

Figure 10. Variation of Sea Surface Topography around South America (Lisitzin, 1965), in dyn.cm. (relative to 280 dyn.cm average)

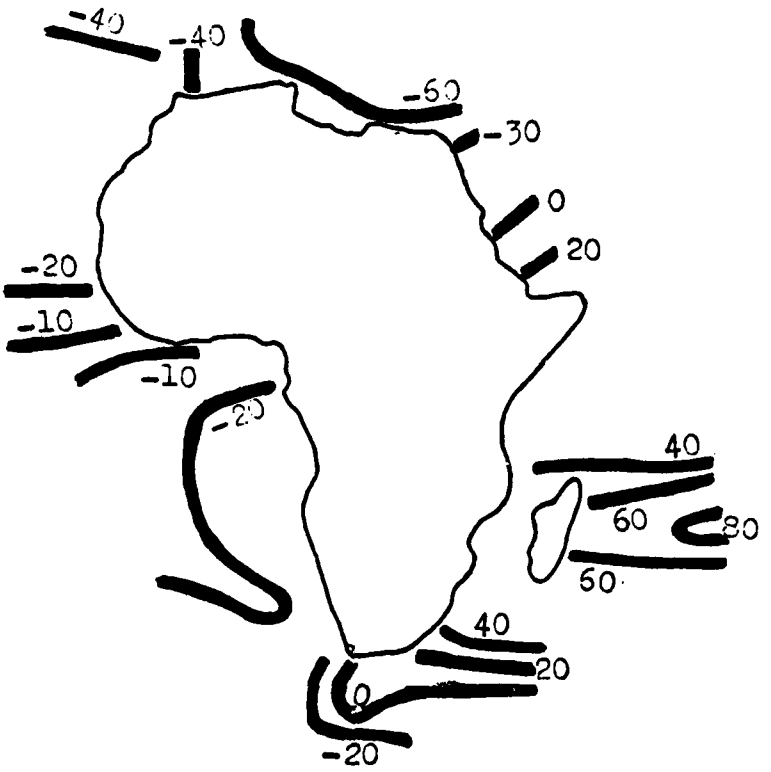

Figure 11. Variation of Sea Surface Topography around Africa (Lisitzin, 1965) in dyn.cm. (relative to 280 dyn.cm)

1920 km NS and 4000 km EW, which more or less approximates the actual boundaries of the U.S. Figure 12 shows the example of such network for the case of 36(=6x6) grid points. The net basically consists of 25 rectangular loops, each 384 km in North-South direction and 800 km in East-West. Each grid-point represents the unknown height, therefore, there are 36 unknowns in this example. In the actual vertical datum work the observations are taken as height differences between points in the net. In the example we assume there is one observation (height difference) between each pair of adjacent points giving 60 observation equations. It means no observation stretches over more than one segment in the net.

As in the case of actual adjustment of the 1929 levelling net, each segment between 'bench marks' in the example provides one linear observation equation of the type

$$h_j - h_i = \Delta h_{ij} \tag{1}$$

or

$$Ah = \Delta h \tag{2}$$

In order to simulate the set of observations Δh_{ij} we first assign heights (from a topographic map) to all grid points $h_1^0, h_2^0, \ldots, h_n^0$. The grid points are ordered as shown on Figure 12, which assures a regular structure of the linear system of observation equations. At this stage we assign the sea surface topography heights to 'coastal' points marked on Figure 12. The values of SST with respect to 280 dyn.cm global average can be estimated from Lisitzin's chart (Figure 4). Now, starting from those reference heights, we can compute the set of observations Δh_{ij} using (1). At this point we have the right-hand side and the design matrix A of formula (2). The standard deviations of our synthetic observations were assigned according to the usual formula (Milbert, 1980):

$$\sigma_{ij} = \sigma_0 \sqrt{L_{ij}}$$

where L_{ij} - section length (in km) between bench marks i and j and $\sigma_0 = 0.3$ cm. In our simple example it gives the values:

$$\sigma_{ij} = \begin{cases} 8.49 \text{ cm in East-West direction} \\ 5.88 \text{ cm in North-South direction} \end{cases}$$

Now, we solve the system of observation equations (2) using the method of linear least squares with linear equality constraints by downweighting. A brief description of the method together with some accuracy considerations will be given in the next section. We can obtain the solution with different sets of constraints. Since in the 1929 adjustment of the levelling net of the U.S. each geodetically connected tide gauge provided a zero-height constraint, in our model-studies we also attached a set of linear constraints of the type:

$$h_i = 0, \; i = 1, \ldots, k$$

to the grid points representing 'tide gauges' along the West Coast, the East Coast, and the Gulf Coast. In our 6 by 6 example we have 13 constraints equations, forcing the least squares solution to assume zero-height values at 13 grid points marked on Figure 12. Let this solution be denoted by $\hat{h}$.

Now we can subtract our reference "true" heights h^0 from the constrained least squares solution $\hat{h}$:

$$d = \hat{h} - h^0 \qquad (3)$$

The function d represents the vertical datum distortion caused by the zero-constraints imposed on heights at tidal stations. This function should be understood in the spatial sense - the distortion varies from point to point forming a more or less irregular but continuous surface. The shape and the amplitude of this function is of particular importance. We can assume that heights in the United States, and most likely in the entire N. American Continent that are used today, are contaminated by distortion of this type. The North American vertical datum is warped and this deformation can be quantitatively modeled by our function d. The contribution of this distortion to the error in spherical harmonic coefficients can be now evaluated on performing the Fourier analysis of the distortion function d as will be described later.

4.2 The Software Considerations

A method of linear least squares with linear equality constraints by downweighting was used to solve for the distortion function d in our model studies. This method which is based on orthogonal decomposition is numerically more stable than the usual methods based on normal equations approach. For this reason it was used to handle our problem. The Householder orthogonal decomposition plays a major role in this technique, therefore we start from a brief summary of some algebraic principles behind this approach.

4.2.1 Householder Orthogonal Decomposition for Least Squares Problems and Disadvantages of Normal Equations Method

We begin with some basic definitions:

An orthgonal decomposition of mxn matrix A of rank k means to find an mxm orthogonal matrix H, an mxn matrix of the form

$$R = \begin{bmatrix} R_{11} & 0 \\ 0 & 0 \end{bmatrix}$$

and an nxn orthogonal matrix K, so that $A=HRK^T$ and R_{11} is a kxk matrix of rank k.

An important property of the orthogonal matrix: if Q is orthogonal, then we have:

- preservation of Euclidean length (norm) under multiplication $\|Qy\| = \|y\|$
- stability in computation with regard to propagating data errors or uncertainty.

Householder transformation (Householder, 1958).

Given a m-vector $v \neq 0$, there exists an orthogonal matrix Q such that

$Qv = -\sigma \|v\| e_1$ with

$$e_1 = \begin{bmatrix} 1 \\ 0 \\ . \\ . \\ . \\ 0 \end{bmatrix} \quad \text{and} \quad \sigma = \begin{cases} +1 & \text{if } v_1 \geq 0 \\ -1 & \text{if } v_1 < 0 \end{cases} \quad \text{where } v = \begin{bmatrix} v_1 \\ v_2 \\ . \\ . \\ . \\ v_m \end{bmatrix}$$

It turns out that $Q = I_m - \frac{2uu^T}{u^Tu}$, where $u = v + \sigma \|v\| e_1$, and I_m - identity matrix.

Geometric interpretation of Householder transformation:

it represents a reflection in the (m-1) - dimensional subspace, S, orthogonal to the vector u. By this it is meant that $Qu = u$ and $Qs = s$ for all $s \in S$.

At this stage, we can formulate the least squares problem (Lawson and Hanson, 1974).

For an equation

$$Ax \cong b \qquad (4)$$

with a real mxn matrix A of rank $k \leq \min(m,m)$ and a real m-vector b, find a real n-vector x minimizing the euclidean length of Ax-b. Additionally, we explicitly assume that the numerical data that constitute A and b have only a limited number of accurate digits. This assumption reflects the usual situation in numerical handling of data. In our modelling studies the set of observation equations (2) will be considered a least squares problem.

Next we briefly describe the numerical properties of the algorithm to solve problem least squares by orthogonal decomposition using Householder transformations (Golub and Businger (1965), Hanson and Lawson (1969)). Depending on the rank of the design matrix A of a least squares problem $Ax \cong b$ the algorithm takes the following actions:

- if matrix A is well conditioned (full rank) this algorithm finds a standard, unique least squares solution x that minimizes $Ax - b$.
- if matrix A is rank-deficient the algorithm determines the effective rank k of matrix A and finds the so called minimum length solution x that minimizes both: $\|Ax - b\|$ and $\|x\|$. This solution is also unique. The effective rank k is the rank of the matrix $\tilde{A}$ that replaces A as a result of a specific computational algorithm.
- if matrix A has theoretically full rank, but inevitable small changes in the data of the order of magnitude of data uncertainty could convert the matrix to one of deficient rank the algorithm replaces A by a 'nearby' rank-deficient matrix, say, $\tilde{A}$, (Lawson and Hanson, 1974, p. 79, eq. 14.8), and then computes a minimum length solution to the slightly different problem $\tilde{A}x \cong b$.

The last case is the ill-conditioned case and is traditionally disregarded by standard algorithms that solve least squares problems. Indeed, it is a difficult problem to handle numerically, and (if not properly treated) can lead to very unstable, inaccurate solutions. The rank of the matrix $\tilde{A}$ that replaces A as a result of a specific computational procedure is called the pseudorank of A. Pseudorank (or effective rank) is not a unique property of Matrix A, but also depends on the details of computational algorithm, the values of assumed tolerance parameters and the effects of machine round-off errors.

Generally, the algorithm (Lawson and Hanson, 1974, p. 78) determines the orthogonal matrices Q, K and the permutation matrix P in the following steps:

DECOMPOSITION
a) find orthogonal matrices Q, P such that

$$A = Q^T R P^T, \text{ or}$$

$$QAP = R = \begin{matrix} \left[\begin{matrix} R_{11} & R_{12} \\ 0 & R_{22} \end{matrix}\right] \begin{matrix} \} k \\ \} m-k \end{matrix} \\ \underbrace{}_{k} \quad \underbrace{}_{n-k} \end{matrix}$$

where, R is upper triangular, R_{11} is nonsingular and k = pseudorank of A.

b) construct vector

$$Qb = c = \begin{bmatrix} c_1 \\ c_2 \end{bmatrix} \begin{matrix} \} \, k \\ \} \, m-k \end{matrix}$$

c) find an orthogonal matrix K such that

$$A = Q^T \begin{bmatrix} W & 0 \\ 0 & R_{22} \end{bmatrix} \begin{bmatrix} K^T & 0 \\ 0 & I_{n-k} \end{bmatrix} P^T$$

or

$$[R_{11} : R_{12}]K = [\underbrace{W}_{k} : \underbrace{0}_{n-k}] \} \, k$$

where W is nonsingular, upper triangular matrix.

SOLUTION

a) solve for the unique k-vector y_1 from the nonsingular equation

$$Wy_1 = c_1$$

and set y_2 arbitrary

b) the solution vector $\hat{x}$ is found as follows:

$$\hat{x} = P \begin{bmatrix} K & 0 \\ 0 & I_{n-k} \end{bmatrix} \begin{bmatrix} y_1 \\ y_2 \end{bmatrix} \begin{matrix} \} \, k \\ \} \, n-k \end{matrix}$$

c) the residual norm can then be computed as $\|b-Ax\| = \|c_2\|$.

d) the variance-covariance matrix of the solution vector $\hat{x}$ for the full rank case (k=n) is proportional to

$$C := PR^{-1} (R^{-1})^T P^T$$

(Lawson and Hanson, 1974, p. 68, eq. 12.10)

Both orthogonal matrices Q and K are products of a number of elementary Householder transformations.

Remarks on the algorithms:

- The described algorithm solves directly the original least squares problem, it means the system of observation equation with rectangular design matrix A: $Ax \cong b$. (the formulation of the so-called normal equations is avoided).
- Because the orthogonal decomposition of A is found, there is no (explicit) matrix - inversion.

One may think that using a general inverses approach (presented by Householder method) one has to resign from statistical indicators as covariance matrices (which are formally related to the normal matrices (symmetric, positive definite)). This is not true, as can be found in Lawson and Hanson (1974, pp. 67-73). It turns out that using the computed components of the Householder's orthogonal decomposition, one can construct the required covariance matrices in a cheap, effective and stable way.

4.2.2 Method of Linear Least Squares with Linear Equality Constraints by Downweighting.

During the 1929 adjustment of the levelling net of the U.S. the heights at each of the 26 geodetically connected tide gauges were constrained to zero through a linear equation of the type

$h_i = 0$, i=1, 2, ..., k (h_i stands for the height at tide station i)

or generally

$$Ch = f \qquad (5)$$

In the adjustment of our model-net we also wish to impose zero-constraints on grid points bordering upon the sea. As can be found in Lawson and Hanson (1974), this can be done simply by entering the associated constraints equations (5) before our original observation

equation system (2) or (4). Next, the set of the original observation equations (4) should be downweighted by premultiplying by some small quantity ε to be chosen by the user. This quantity establishes the compromise between the usual least squares solution of the unconstrained system (4) and the closeness of fit to the prescribed constraints (5). However, the internal relative importance of each equation in the unconstrained system (4) expressed by the weights associated with the original observations (Section 4.1) is preserved during this downweighting operation. Summarizing, we combine observation equations $Ah = \Delta h$ and constraints equations $Ch = f$ into one linear system:

$$\begin{bmatrix} C \\ \varepsilon A \end{bmatrix} h = \begin{bmatrix} f \\ \varepsilon \Delta h \end{bmatrix} \qquad (6)$$

This system can be solved for the height vector h using the method of Householder orthogonal decomposition described in the previous section.

It should be mentioned, that in our case of zero-constraints vector f in (6) is set to 0.

Altogether, this numerical procedure is called in the literature, the least squares method with linear equality constraints by downweighting (Lawson and Hanson, 1974, p. 148-158). And as mentioned already, the small parameter ε expresses the compromise between the closeness of fit to the values prescribed by the constraints and fidelity to the unconstrained least squares solution of the original system.

$$Ah = \Delta h$$

Powell and Reid (1968) have proven the stability of this method, provided the Householder transformations are used, and constraint equations are placed on the top of the original system (2).

4.2.3 Comparison with Normal Equations Method

It can be shown (Lawson and Hanson (1974), p. 122) that for a mxn matrix A the Householder method applied directly to least square problem $Ax = b$, requires $mn^2 + m^3/3$ operations (by an operation we mean a pair: addition - multiplication). The traditional method by normal equations requires $mn^2/2$ operations to form the normal equations $A^tAx = A^tb$, and $n^3/6$ operations to solve normal equations using Cholesky's method. Therefore, Householder method is twice as expensive as the traditional normal equation method. On the other hand using computer arithmetic of the given precision the Householder method produces twice as many significant digits in the solution as the normal equation method does. In other words, to assure the same quality of results we have to double the computer precision while using

normal equations method. For large systems of equations it leads quickly to computer-storage problems.

Conclusion: on a given computer the Householder method can handle larger problems than the normal equation method can.

Lawson and Hanson (1974) give the following simple example of the loss of significant digits using normal equations method:

$$A = \begin{bmatrix} 1 & 1 \\ 1 & 1 \\ 1 & 1-\varepsilon \end{bmatrix}$$

The normal equations matrix $A^T A$ is to be formed on the computer with the relative precision η. Suppose the value of ε is such, that it is significant to the problem, $\varepsilon > 100\eta$ say, but $\varepsilon^2 < \eta$, so that $1-\varepsilon \neq 1$ but $3+\varepsilon^2$ is computed as 3. Thus, instead of computing

$$A^T A = \begin{bmatrix} 3 & 3-\varepsilon \\ 3-\varepsilon & 3-2\varepsilon+\varepsilon^2 \end{bmatrix}$$

we shall compute the matrix

$$\begin{bmatrix} 3 & 3-\varepsilon \\ 3-\varepsilon & 3-2\varepsilon \end{bmatrix}$$

Further computation of Cholesky decomposition of this matrix into the product $R^T R$, gives

$$R = \begin{bmatrix} r_{11} & r_{12} \\ 0 & r_{22} \end{bmatrix}$$

where
$r_{11} = \sqrt{3}$, $r_{12} = (3-\varepsilon)/\sqrt{3}$, $r_{22}^2 = 3-2\varepsilon - (9-6\varepsilon)/3 = 0$, while the correct result at this point would be

$$r_{22}^2 = 2\varepsilon^2/3 \neq 0.$$

Therefore, in the precision η no significant digits are obtained in the element r_{22}. Consequently the matrix R is computed as singular. On the other hand, when the Householder transformation is applied to triangularize A directly, without forming A^TA, we get the matrix

$$R = \begin{bmatrix} -\sqrt{3} & \frac{\varepsilon - 3}{\sqrt{3}} \\ 0 & \frac{-\varepsilon\sqrt{6}}{3} \end{bmatrix}$$

which is nonsingular.

The important point in the Householder routine is that components of R were computed as the difference of quantities of order of magnitude unity. Thus, using η-precision arithmetic, these components are not lost in the round-off errors.

4.3 The Results of Simulation of the North American Vertical Datum Distortion Function for Different Densities of Model Networks

In Figure 12 we see the example of a synthetic network for the array of 6x6 grid points. Points are regularly distributed and ordered row-wise so that the densification of the net could be easily programmed. The least squares method with linear constraints by downweighting was used to obtain the solution to the combined system of observation equations together with constraints equations as was described in previous section. We denote this solution by $\hat{h}$, the actual dimensions of linear system to be solved were for this case: 36 unknown heights and 73 equations (60 observations + 13 constraints). The difference: constrained solution $\hat{h}$ minus the original reference heights h^0 described in Section 4.1, gives the distortion function of the vertical datum.

$$d = \hat{h} - h^0$$

Figure 13 shows the contour map of the distortion function d for the 6x6 network, together with the 3-dimensional view of this function. The units are cm and contour interval is equal to 2 cm. The downweighting parameter ε has the value 0.1 which is sufficient to constrain the zero-height at tide gauges with tolerance of 2 mm. From the contour map we see that the distortions assume the extremal values at tide stations, where the zero-constraints were forced. The minimum occurs at the south part of the West Coast, the maximum at East Coast, near Florida. From South-West Coast the distortion function increases gradually toward East. Approximately in the middle of the continent

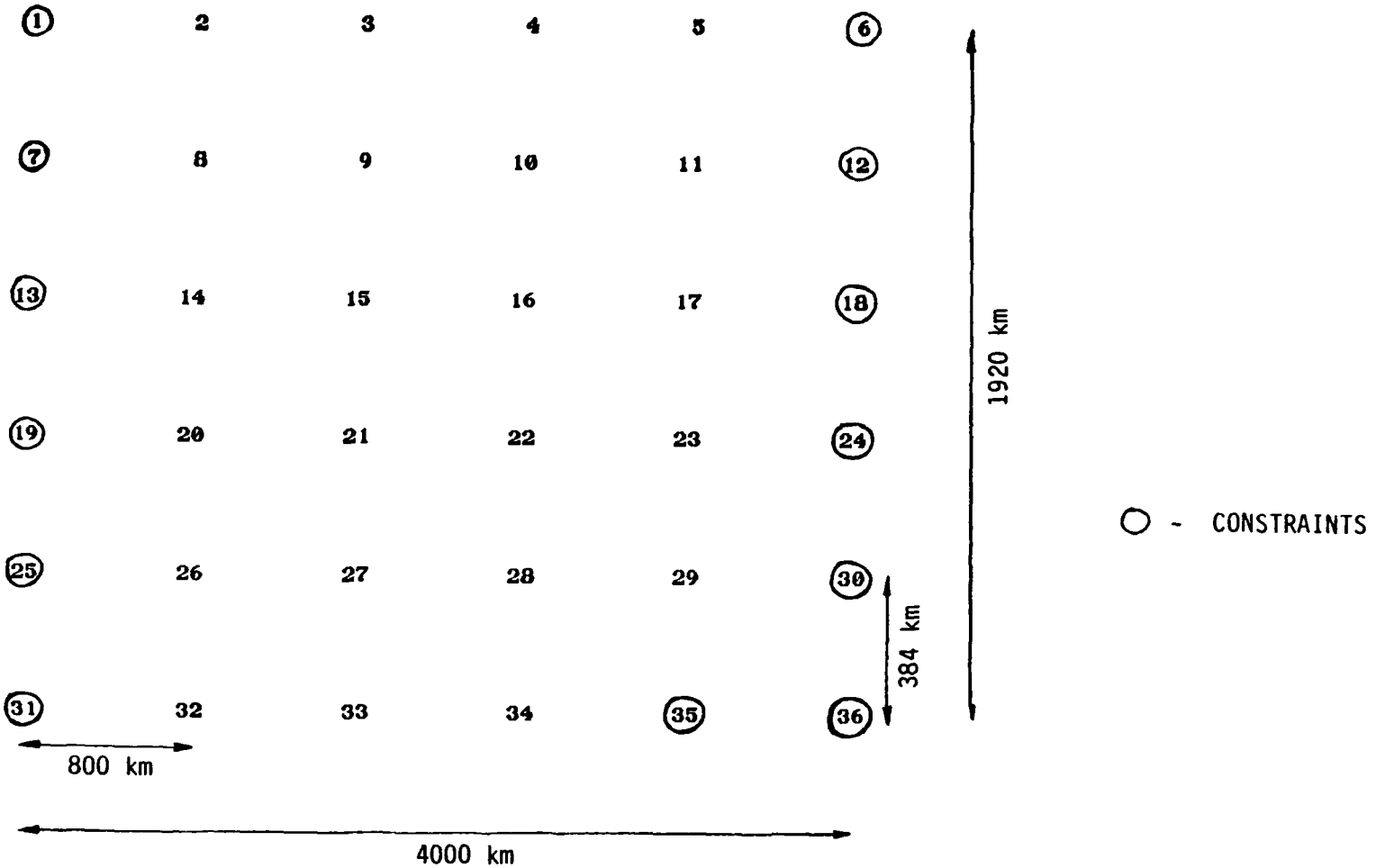

Figure 12. Example of the 6x6 rectangular grid approximating the 1929 Levelling Net in the U.S.A., showing the order of unknowns and the constrained heights (in circles).

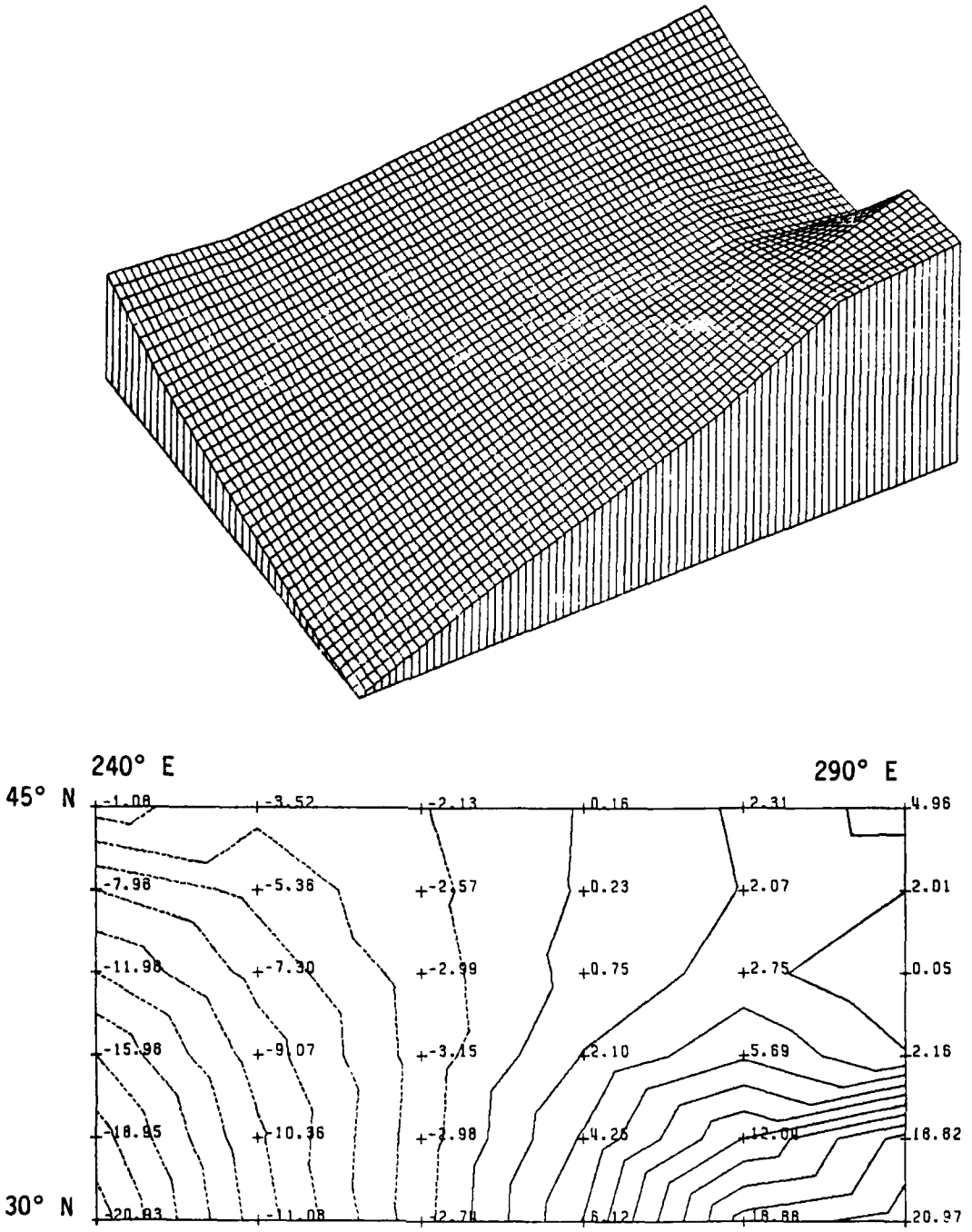

Figure 13. Contour map and the 3-D view of the distortion function d (eq. 3) for the case of the 6x6 Digital Surface Model.
The units are cm and contour interval is equal to 2 cm.

the distortions diminish to zero and the line of no distortion passes across the continent almost exactly in the North-South direction. From here distortions increase again towards East and South. Of course this particular shape of the distortion function d is a result of a specific distribution of sea surface topography around North-American continent shown on Figure 4. It can not be generalized to any other continent or location.

In the next stage we densify the model levelling-network. For the case of a 10x10 regular grid the dimensions of the linear system are: 100 unknown heights, and 204 equations (180 observations + 24 constraints). Figure 14 shows the contour map and the 3 dimensional view of the distortion function d for this case. The contour interval is equal to 2 cm and the downweighting parameter ε=0.1, which is enough to constrain the heights to zero at 24 'tide gauges' with the tolerance of 1 mm. The distribution of the distortions over the continent is very similar to the previous case.

Finally, in Figure 15 the contour map and the 3-dimensional view of the distortion function for the 15x 15 grid is shown. Units are cm and contour interval is equal to 2 cm. The downweighting parameter ε is equal to 0.2 which is sufficient to constrain the heights to zero at 35 'tide gauges' with the tolerance of 1 mm. For this case the system of 445 equations with 225 unknowns was solved. The general behaviour of distortion function is again similar to the previous examples.

Summarizing the above results we can formulate the following general remarks:

- the maximum (in magnitude) distortions in the vertical datum occur at the tide gauges, where incorrect zero-constraints were forced:
- the extreme distortions values are: -20 cm at the South part of West Coast and +21 cm at the South Part of the East Coast;
- in the center of the continent the distortions never exceed those at the tide gauges;
- the shape of the distortion function is not sensitive to the density of grid, it is a result of a particular distribution of the SST along the coasts of the continent;
- the line of no distortion passes through the middle of the continent in the meridional direction;
- the vertical datum was warped in a smooth way, which means there is no unexpected extremes (local minimums or maximums) in the center of continent, and there is no long or short-wavelength periodic effects.

The last remark may come from the fact that our synthetic network was very sparse, which is equivalent to the smoothing effect. On the other hand, the general shape of continental topography (which is imaged in the input data) is very unsymmetric, with high mountains on West Side and plains on East. Nevertheless, the topography does not seem to affect the shape of the distortion function.

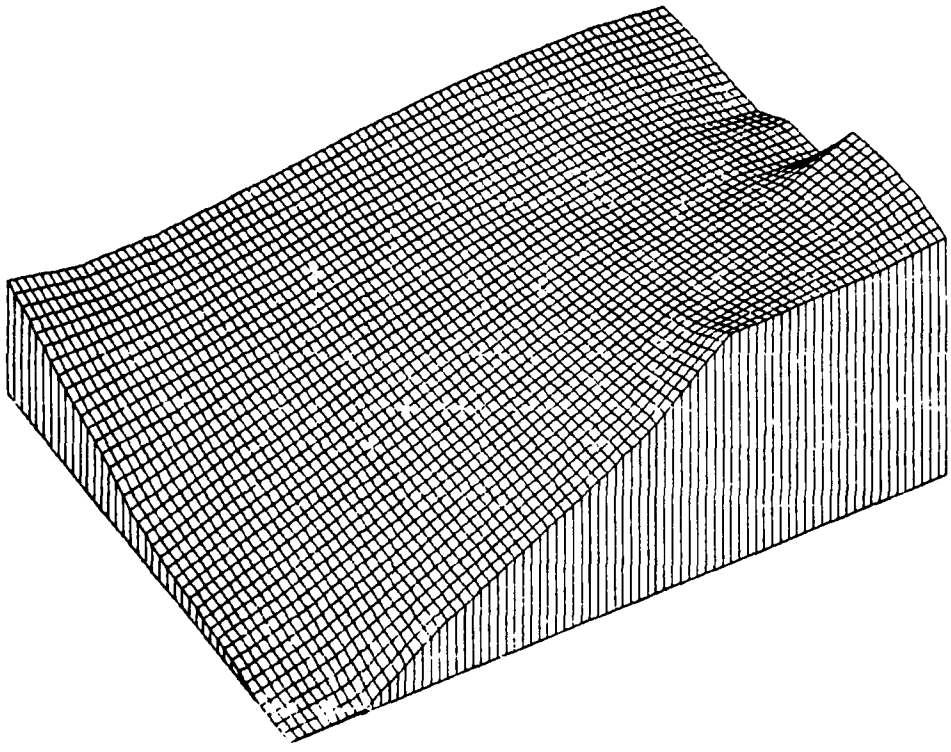

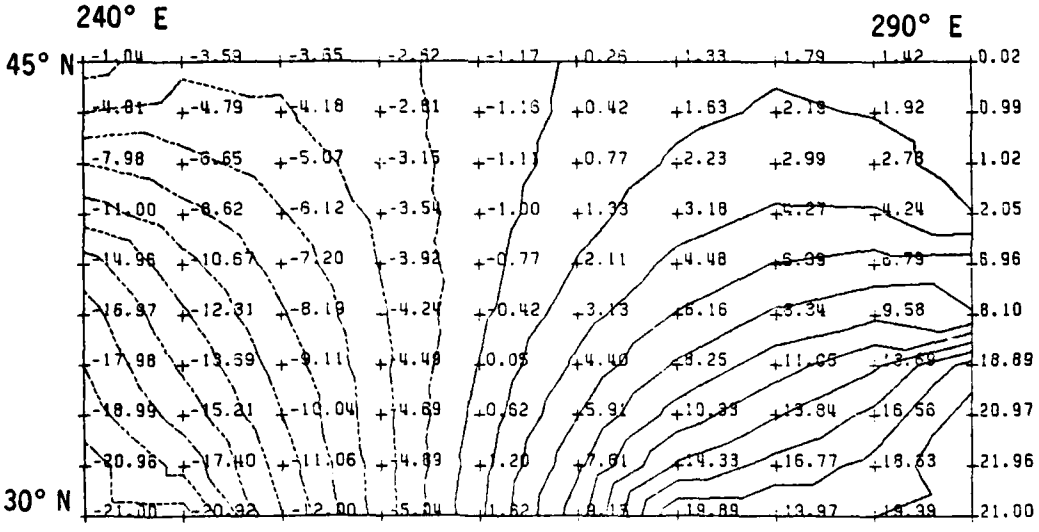

Figure 14. Contour map and the 3-D view of the distortion function d (eq. 3) for the case of the 10x10 Digital Surface Model.
The units are cm and contour interval is equal to 2 cm.

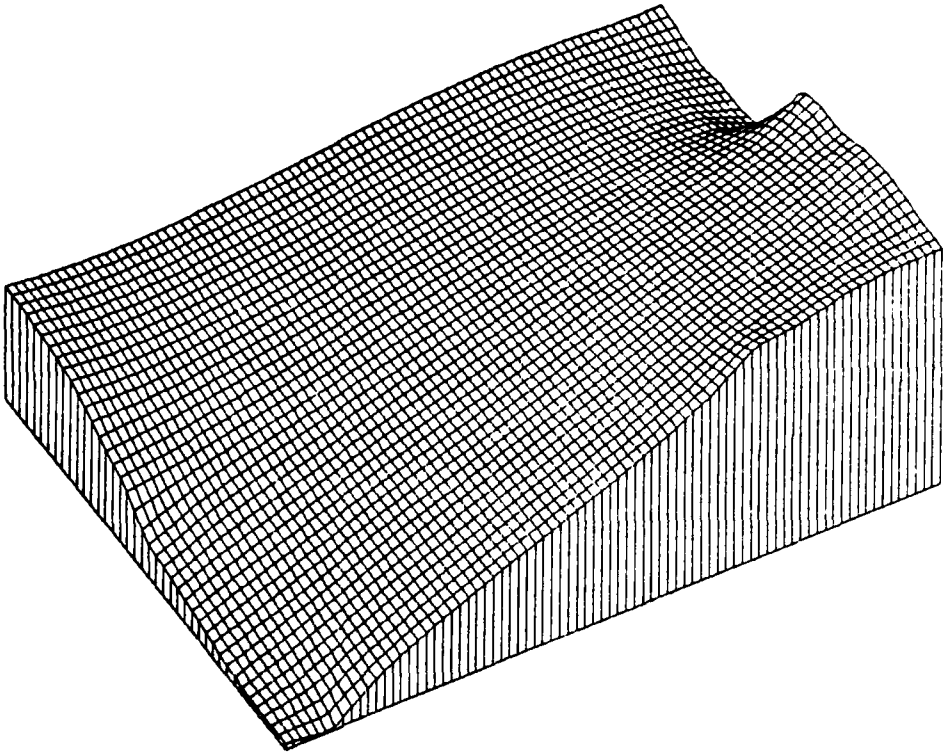

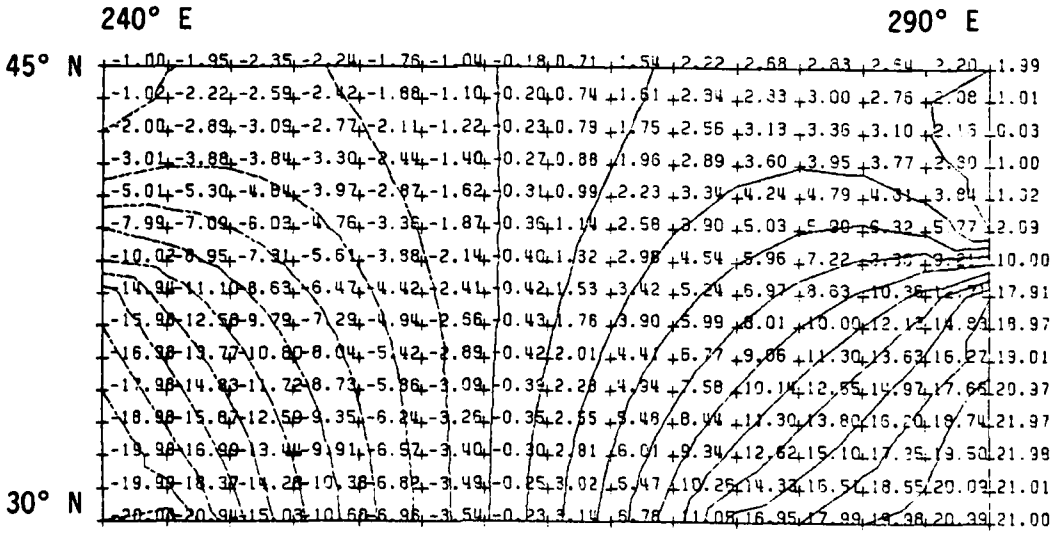

Figure 15. Contour map and the 3-D view of the distortion function d (eq. 3) for the case of the 15x15 Digital Surface Model.
The units are cm and contour interval is equal to 2 cm.

Of particular importance is the existence of the zone of no distortion. It indicates that along North-South span, right in the middle of the continent the heights are not affected by error due to the twist in the vertical datum. In other words, the equipotential surface implied by the zero-height for points inside this zone could represent the mean regional geoid for the North American continent. At all other points heights refer to the different equipotential surfaces which deviate from the mean regional geoid exactly by the particular value of the distortion function d. It means that on adding the distortion function d, all heights on the continent would refer to a single equipotential surface.

4.4 The Proper Procedure for the Adjustment of a Levelling Network and the Definition of the Geoid

In Section 4.2 it was shown that forcing the zero-height at more than one tide gauge introduces errors in the adjusted heights of the order of the variation of SST at tide stations chosen. In order to avoid this effect we should allow for a minimum-constraints solution, where a single point is assigned an a priori value. After the network is adjusted the computed heights of tidal stations should be statistically tested against the MSL heights determined by the oceanographic method. Next, the vertical translation of all adjusted heights could be designed in order to minimize the differences between the MSL values and the adjusted heights at tidal stations in some least squares sense. Heights obtained that way would refer to a single equipotential surface. This surface could be regarded as the definition of the geoid in the regional sense. It would have the property of minimizing the Sea Surface Topography variations over the given set of tidal stations. Therefore, such a regional geoid would depend on the particular configuration of tide gauges used. The conceptual difference between the regional geoid introduced here and the geoid itself is the following: The geoid (at least in the oceanographic sense) is the equipotential surface of the earth's gravity field that most closely (in some more or less formalized sense) approximates the MSL in the global context. The regional geoid (for a given continent) is that equipotential surface of the earth's gravity field that most closely approximates in the least squares sense the MSL variation over the discrete set of coastal points (tide gauge locations). The vertical datum implied by the regional geoid would define the zero-level that on average agrees with the MSL along the oceanic coasts of the region. Essentially one-dimensional information on the MSL variation along the coastal line (sampled at the tide gauge locations) is needed to define the regional geoid, whereas the areal distribution in the two-dimensional global sense is required to define geoid.

Another way to avoid distortions in the adjusted vertical datum is to perform an unconstrained adjustment. Of course the linear system that arises from this problem is singular and can not be solved by standard methods of normal equations. On the other hand the Householder orthogonal decomposition (presented in Section 4.2.1) is well suited for rank-deficient systems. In such case the algorithm produces

the so-called minimum length solution which is unique in this sense. Next, this solution could be block-shifted in vertical direction to meet certain conditions at tide gauges, which were described in the last paragraph.

In order to find out the differences between those two methods a synthetic network of 7 by 7 grid points was adjusted exactly the same way as described in Section 4.1. The only difference was, that a single zero-constraint was imposed on point at the North-West corner of the net, just to keep the full rank of linear system. At the same time an unconstrained minimum length solution was obtained for the same case of the 7x7 network. Then, this solution was block-shifted so that the height at North-West corner of the net became zero (exactly like in the single-constraint solution). Figure 16 shows the difference between the no-constraints and the single-constraint solution. The units are 10^{-12} m. The maximum difference was $4 \cdot 10^{-12}$ m, which indicates that solutions differ only on the order of round-off errors.

The above example indicates that both methods produce equivalent results. Either one can be applied in real-life situations.

5. THE DESIGN OF THE MODEL HEIGHT-ERROR FUNCTION DUE TO THE INCONSISTENCIES IN THE GLOBAL VERTICAL DATUM

Now we are in the position of constructiong the global model of the height-inconsistency function $\Delta h(\phi, \lambda)$ caused by the inconsistency between the different vertical datums in the world. In the spatial sense $\Delta h(\phi, \lambda)$ is understood to be a function of geodetic latitude ϕ and longitude λ. We are interested only in the effects related to the uncertainties in the Sea Surface Topography values or due to the improper numerical procedure during the adjustment of levelling networks.

The reference surface for the construction of $\Delta h(\phi, \lambda)$ is the equipotential surface implied by the Lisitzin's global average value of 280 dyn.cm of the SST variation (Lisitzin, 1965). This value was derived based on the 4000 dbar isobaric depth.

The function Δh is modeled as the patchwise step function assuming constant values over specific vertical datums. Such constant values refer to the sea surface topography at a particular tide gauge which was constrained to zero during the general adjustment of levelling net. In case where more than one tide gauge were constrained to zero (N. America) the average sea surface topography at all such tide gauges was chosen to represent the correction Δh over this particular vertical datum. This value was estimated based on the particular distribution of SST around the perimeter of the continental levelling network. The Lisitzin's deep-ocean Sea Surface Topography as shown on Figure 1 was extrapolated towards the locations of tide gauges which took part in the adjustment of the levelling net.

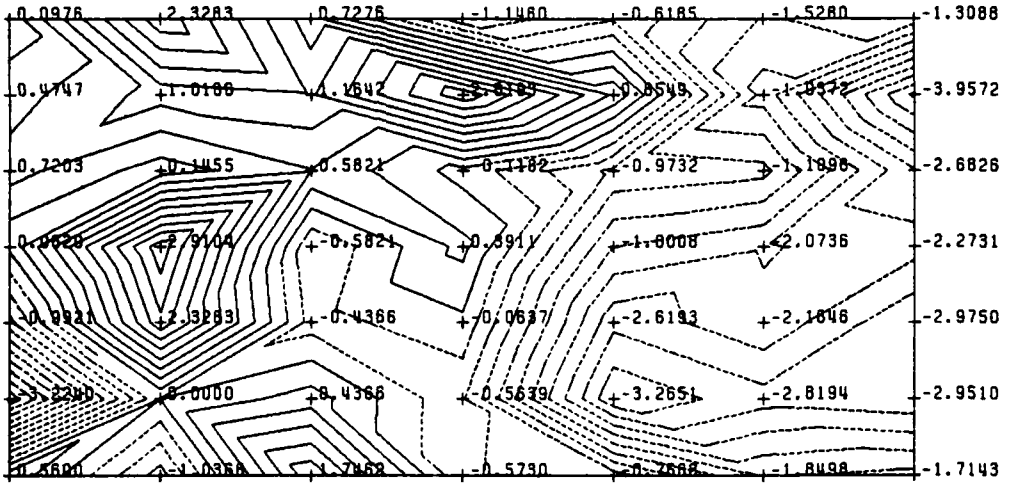

Figure 16. The difference between the unconstrained (rank-deficient) solution and the minimum constraints (full-rank) solution for the case of 7x7 Digital Surface Model. Units are pm=10^{-12}m and contour interval is 0.3 pm

At the ocean areas the Lisitzin's Sea Surface Topography values are assumed to represent the discrepancy Δh between the MSL and our reference geoid implied by the 280 dyn.cm global average.

More specifically, over the continental plates we imposed the following constant values for $\Delta h(\phi, \lambda)$:

a) North America
In the 1929 levelling net adjsustment 26 Primary Tide Stations were used as the reference zero-level. The average value of Sea Surface Topography over those 26 stations is -4 cm. The Sea Surface Topography variation and the location of the tide gauges is shown on Figure 4. Therefore, the value of $\Delta h(\phi, \lambda)$ over the North American Continent was chosen as -4 cm. The choice of the constant value of the distortion for the case of the American continent should be understood as merely an approximation. Due to irregular distribution of SST and improper numerical procedure in the 1929 adjustment the distortion function is not constant but actually reflects an irregular internal warp in the continental vertical datum. This will be studied in the sequel.

b) South America
No information is available on vertical datum or datums on this continent. However, since we are interested in the general effect of discrepancies of the order of variations of the SST, it is sufficient to numerically simulate a particular value of Δh in this area. Let us assume that the unified continental levelling net was constructed and the adjustment was done with a single zero- constraint at a given tidal station. Suppose this tide gauge was located in Buenos Aires where the Sea Surface Topography with respect to 280 cm reference is -40 cm (see Figure 10). In such case the value of $\Delta h(\phi, \lambda)$ over the S. American Continent will be -40 cm. The choice of the master tide gauge in Buenos Aires is quite arbitrary. From Figure 10, we see that if we chose any other location along the coastal line we would get the values ranging from -80 cm to +20 cm.

c) Europe
The adjustment of the United European Levelling Net was carried out with respect to a single fixed datum point in the Netherlands: Normal Amsterdam Peil (NAP). At this tide station the sea Surface Topography with respect to 280 cm reference is -55 cm (Figure 8). Therefore, the value of $\Delta h(\phi, \lambda)$ over Europe could be taken as -55 cm (Lisitzin, 1974, p. 163).

d) Africa
There is no information on the levelling net adjustment on this continent. Therefore, assume the unified continental levelling net was adjusted with a single zero constraint at the tide gauge at Lagos. The Sea Surface Topography at Lagos with respect to 280 cm reference is -10 cm (Figure 11). Therefore, the $\Delta h(\phi, \lambda)$ can be taken as -10 cm over the whole African Continent. The choice of master tide gauge at Lagos is again arbitrary. If we pick at random a point on the coast line we would get the values for the distortion function ranging from -60 cm to about +60 cm (Figure 9).

e) Asia

There is no information on the levelling net adjustment on this continent. There, assume the unified continental levelling net was adjusted with a single zero-constraint at Leningrad. The Sea Surface Topography at Leningrad with respect to 280 cm reference is approximately -30 cm (Figure 9). Therefore, the value of $\Delta h(\phi, \lambda)$ over Asia will be taken as -30 cm. If we pick any other location for the master tide gauge we would obtain different values for the distortion function ranging from about -120 cm to about +80 cm.

f) Australia

The adjustment of the Australian Height Datum (1971) was carried out with the heights fixed to zero at 30 tide gauges around the coast of the continent. The Sea Surface Topography average over those tide gauges (with respect to 280 cm reference) is +35 cm (Figure 6). Therefore, the value of $\Delta h(\phi, \lambda)$ over Australia could be taken as +35 cm.

On the other hand, the free network has been calculated (Mitchell, 1972) with a single constraint at Jervis Bay, where the SST is equal to 30 cm. Since a single constraint approach is more accurate than the overconstrained problem (as was shown in Chapter 4) we will use the value of +30 cm to represent Δh at this area.

g) Antarctica

There is no information on the vertical datum on this continent, neither is there on Sea Surface Topography below the latitude 60 South. Therefore, Antarctica will be treated as the ocean area. The constant value of $\Delta h(\phi, \lambda)$ over Antarctica will be taken as zero cm.

In order to study separately the effects of different components of the height-error function $\Delta h(\phi, \lambda)$, we constructed three different global models of this function Δh_1, Δh_2, Δh_3, proceeding from the simplest to the more complicated one.

Numerically, all our models are constructed as a set of 64800 mean values based on the 1°x 1° blocks covering the earth's surface in a regular equiangular grid. The continental outline with the 1°x 1° resolution was obtained based on the set of 1°x 1° mean land elevations and ocean depths provided by the Defense Mapping Agency Aerospace Center in 1979 (archived as file no. 11 on the GS160 magnetic tape, Department of Geodetic Science and Surveying, The Ohio State University).

Figure 17 shows the three-dimensional view of function Δh_1 which is a simple patchwise step function assuming constant value over different continental plates:

-4 cm	over	N. America
-40 cm	over	S. America
-55 cm	over	Europe
-10 cm	over	Africa
-30 cm	over	Asia
+30 cm	over	Australia
0 cm	over	Antarctica

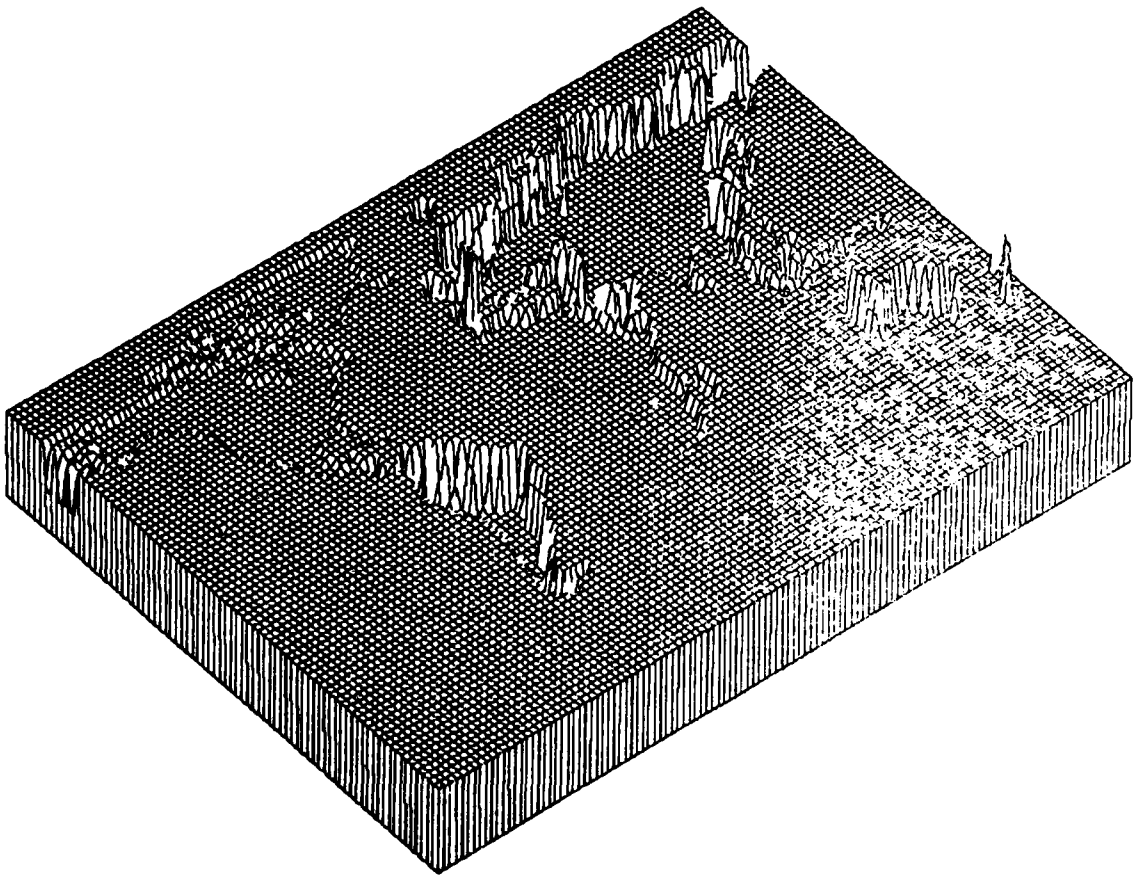

Figure 17. 3-D view of the model function Δh_1.
- the patchwise-step function over continents
- zero over oceans

The reasoning for such values was given above. In the ocean areas our step function Δh_1 is set to zero, which amounts to the assumption that the mean sea level coincides with our model geoid. The purpose of this first model is to reflect the relative displacements between different continental vertical datums. The individual vertical datums are considered here the undisturbed flat reference surfaces. The range of Δh_1 values used in this numerical model is from -55 to +30 cm.

In our second model-function Δh_2 , we introduce the SST variation over the ocean regions. The continental values of Δh_2 are exactly the same as in the first model. The purpose of this model is to reflect the relative displacements of different vertical datums, understood as the rigid vertical shiftings between the undisturbed continental reference planes, against the slowly varying SST over the oceans. Figure 18 shows the 3-dimensional view of the model 2 error function. The magnitude of Δh_2 varies within the interval (-160 cm, +120 cm). The values of the Sea Surface Topography were generated using the subroutine LISITZ by Kostas Katsambalos, of the Ohio State University in 1977. This subroutine uses the digitized values of SST from the Lisitzin's world chart (Lisitzin, 1974, Figure 1) on the 10°x 10° grid. The method of linear interpolation is used, and the Lisitzin's global average of 280 dyn. cm was removed. Katsambalos (ibid.) estimates the accuracy of the routine as +10 dyn.cm. The subroutine LISITZ gives values of SST only between Latitudes +60 and -60. Therefore, beyond this range we assume the zero value to represent our Δh_2 function (Figure 18.).

The third and most complex model is shown in Figure 19. It differs from model 2 function only in the values over the N. Americal continent. Instead of the constant reference level, the vertical datum distortion function d introduced in Section 4.3 was used to represent Δh_3 over this continent. The values of the distortion function d were constructed based on the grid of 15x15=225 values shown on Figure 15. Between grid points, the 1°x 1° values were estimated using the six-point weighted moving-average prediction method (Davis, 1973). The purpose of this third model is to reflect simultaneously all three possibile sources of vertical datum inconsistencies: the relative rigid displacements between the continental flat reference levels, the SST effect over oceans, and the internal vertical datum distortion due to improper numerical procedure during the levelling-data adjustment. The range of Δh_3 values falls in the interval (-160 cm, +120 cm).

We can expect, that all three components of the height inconsistency function will contribute to the errors in various gravimetric quantities. The next section will discuss that problem.

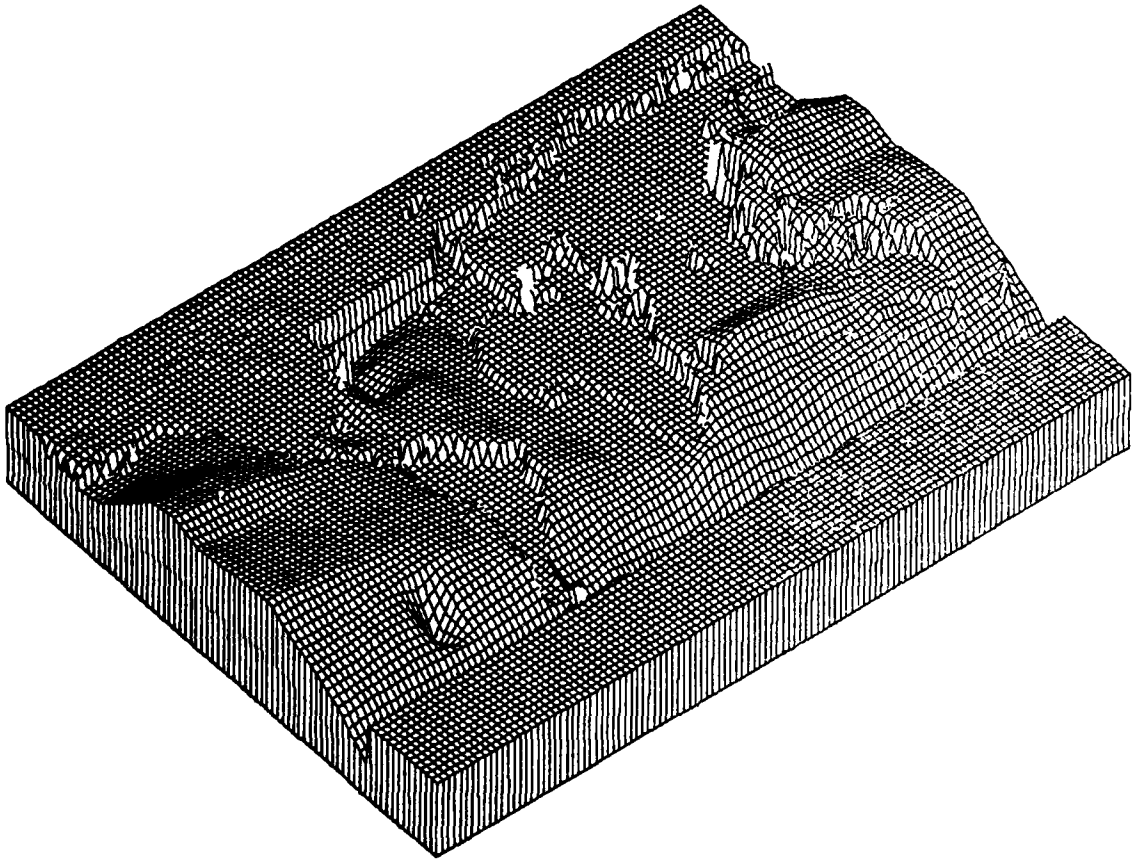

Figure 18. 3-D view of the model function Δh_2.
- the patchwise-step function over continents
- Sea Surface Topography over oceans

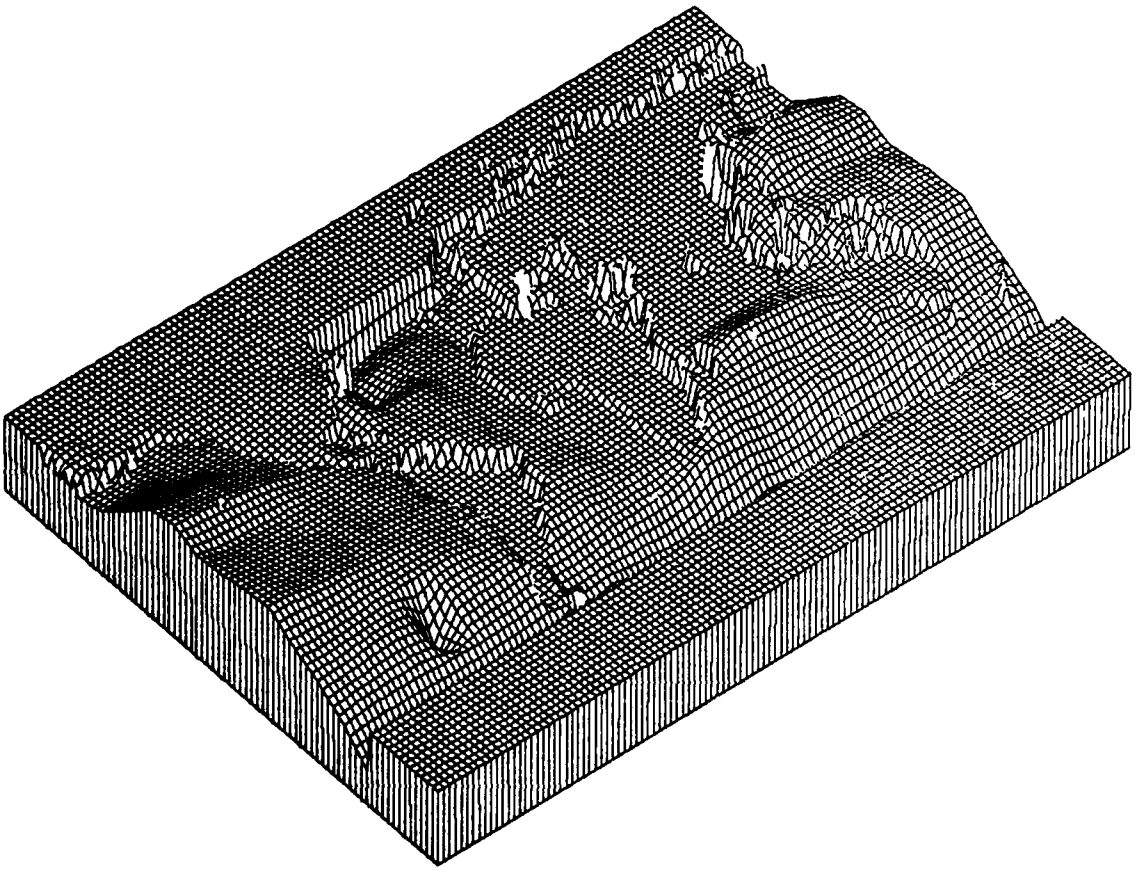

Figure 19. 3-D view of the model function Δh_3.
- the patchwise-step function over continents (excluding N. America)
- the values of distortion function d (eq. 3) over N. America
- Sea Surface topography over oceans

6. THE EFFECT OF THE INCONSISTENCIES IN THE GLOBAL VERTICAL DATUM ON THE DETERMINATION OF SPHERICAL HARMONIC COEFFICIENTS OF THE GEOPOTENTIAL FROM GRAVITY DATA - THE MODELLING STUDIES

In this section we evaluate the effects of vertical datum inconsistencies on spherical harmonics coefficients of the Earth's gravitational potential. The three different models of height inconsistency function (developed in the previous chapter) will be used as the basis for this study.

6.1 The Spherical Harmonic Analysis of Different Models of the Height Inconsistency Function Δh

First, we compute the set of corrections to the spherical harmonic coefficients of Earth's gravitational field based on the spectral analysis of the three model functions Δh_1, Δh_2, and Δh_3.

Consider the spherical harmonic expansion of Earth's gravitational field in the form

$$V = \frac{kM}{r}\left(1 + \sum_{n=2}^{\infty}\left(\frac{a}{r}\right)^n \sum_{m=0}^{n}\left(\bar{C}_{nm}\cos(m\lambda) + \bar{S}_{nm}\sin(m\lambda)\right)\bar{P}_{nm}(\sin\phi)\right) \qquad (7)$$

where (Heiskanen and Moritz, 1967):

$$\begin{Bmatrix} \bar{C}_{nm} \\ \bar{S}_{nm} \end{Bmatrix} = \frac{1}{4\pi G(n-1)} \iint_{\sigma} \Delta g^{*}\, \bar{P}_{nm}(\sin\phi) \begin{Bmatrix} \cos(m\lambda) \\ \sin(m\lambda) \end{Bmatrix} d\sigma \qquad (8)$$

G - average value of gravity (979.8 gals; Gravity Formula 1980)

Δg^{*} - mean gravity anomaly in blocks whose size is $d\sigma$.

kM - geocentric gravitational constant

r - the distance from the coordinate origin to the point of evaluation

a - a nominal earth radius

λ, ϕ - longitude and geocentric latitude of the point of evaluation

$\bar{P}_{nm}$ - fully normalized associated Legendre function of degree n and order m.

In formula (7) we assume that the coordinates origin coincides with the center of mass of the earth (no first degree term in the expansion).

Values of the potential coefficients are most currently found from the analysis of satellite data or through a combination of gravimetric and satellite data (Rapp, 1973). However, we assume here that the coefficients are computed from terrestrial gravity anomalies using formula (8).

Let's assume Δg^* refers to the idealized geoid - for the purpose of this modelling study it will be taken as one implied by the Lisitzin's average sea surface topography of 280 dyn.cm. Equation (8) produces coefficients centered with respect to a reference field implied by the normal potential of the level ellipsoid which most closely approximates our idealized geoid.

Actually, instead of the theoretical Δg^*, we have access only to anomalies Δg which were reduced from observed surface anomalies to a 'geoid' in a best possible way. The problem is, that such a'geoid' is not unique but is implied by the zero-level of a local vertical datum. Since the zero-height is established in connection with mean sea level surrounding a given continent, and since mean sea level differs from the equipotential surface of the true geoid by irregular Sea Surface Topography, different vertical datums in the real world define different equipotential surfaces of the actual gravitational field V. In other words, the zero-height implied by different vertical datums is not unique but varies from datum to datum by the amount probably in the order of sea surface topography variation. From the above, we can conclude that available global mean gravity anomaly data Δg should be further reduced to our model goid by the height difference between the zero-height implied by each vertical datum and the zero-height implied by our model geoid. Let us denote this height difference by Δh. Since for most of the world too little information is available on actual vertical datums, their interrelation with respect to our model geoid can not be precisely determined. Therefore, for the purpose of this study we will use the three models of our discrepancy function constructed in the previous chapter. Functions Δh_1, Δh_2, Δh_3 will serve as the three different approximations to the actual height-inconsistency function Δh. Therefore, the results obtained should be considered as an approximation to the actual impact of the true vertical datum-error on geopotential. Suppose we had been given gravity anomalies Δg which are considered to be reduced to the geoid implied by an individual vertical datum D. Originally, Δg were computed from the formula (Heiskanen, Moritz, 1967):

$$\Delta g = g_{obs} - \frac{\partial g}{\partial h} h_D - \gamma \qquad (9a)$$

where

g_{obs} - observed value of gravity

$\frac{\partial g}{\partial h}$ - vertical gradient of gravity

h_D - height difference between the surface point of the measurement and corresponding point on the geoid (implied by the vertical datum D).

γ - normal gravity on the reference ellipsoid

On the other hand, introducing the height correction Δh from the particular local geoid implied by datum D to our model geoid implied by the Lisitzin's SST global average, we are interested in the more accurate reduction of gravity data given by tne formula:

$$\Delta g^* = g_{obs} - \frac{\partial g}{\partial h}(h_D + \Delta h) - \gamma \qquad (9)$$

where Δh is the height inconsistency function. The Δg^* values obtained from (9) should be used in eq. (8).

Now we can compute the change in gravity anomaly caused by the introduction of our additional height correction Δh:

$$\delta\Delta g = \Delta g^* - \Delta g = -\frac{\partial g}{\partial h}\Delta h \cong 0.3086\ \Delta h\ (\text{mgal})(\text{where } \Delta h \text{ in meters})$$

which has the form of the free-air correction. Here Δh represents the values of our height correction function $\Delta h(\phi, \lambda)$, and could be approximated by our model-functions Δh_1, Δh_2, Δh_3.

Now, we can compute the corrections $\overline{\delta C}_{nm}$, $\overline{\delta S}_{nm}$ to potential coefficients implied by the assumed inconsistencies in vertical datums Δh:

$$\begin{Bmatrix} \overline{\delta C}_{nm} \\ \overline{\delta S}_{nm} \end{Bmatrix} = \frac{0.3086E\text{-}5}{4\pi G(n-1)} \iint_\sigma \Delta h(\phi, \lambda)\, \overline{P}_{nm}(\sin\phi) \begin{Bmatrix} \cos m\lambda \\ \sin m\lambda \end{Bmatrix} d\sigma \qquad (10)$$

where $\Delta h(\phi, \lambda)$ (in meters) is height inconsistency function described in Section 5. The other symbols are explained after formula (8).

Instead of the theoretical function Δh the approximations Δh_1, Δh_2, and Δh_3 described in Chapter 5 were used. The actual integration was carried out using Fast Fourier Transform method implied in the FORTRAN subroutine HARMIN described by Colombo (1981). The subroutine was

run using integrated associated Legendre functions for geocentric latitudes, and the optimum smoothing factors recommended by Colombo. The advantage of HARMIN is its very efficient calculation procedure. Using this program a discrete spectral analysis up to degree 180 was performed on the three different sets of 64800 1°x 1° block-values representing our model height-inconsistency functions Δh_1, Δh_2, and Δh_3. As a result three different sets of correction coefficients $\overline{\sigma C}_{nm}$, $\overline{\sigma S}_{nm}$ were generated.

The magnitude of the computed correction coefficients was tested against the magnitude of potential coefficient obtained by Rapp (1981) from the combination of the terrestrial gravity data, SEASAT altimeter data, and other satellite-derived data (see formula (8)). The degree variances of correction coefficients up to n=180 were evaluated according to the formula:

$$\sigma^2_{n,\delta} := \sum_{m=0}^{n} (\overline{\delta C}^2_{nm} + \overline{\delta S}^2_{nm}) \qquad (11)$$

The relative magnitude of corrections with respect to the reference coefficient (Rapp, 1981) can be expressed by the ratio:

$$R_n := \sqrt{\frac{\sigma^2_{n,\delta}}{\sigma^2_n}} \qquad (12)$$

where,

$$\sigma^2_n := \sum_{m=0}^{n} (\overline{C}^2_{nm} + \overline{S}^2_{nm})$$

represents the degree variances of reference coefficients $\overline{C}_{nm}$, $\overline{S}_{nm}$.

Figures 20, 21, and 22 show the relative magnitude of correction coefficients R_n obtained for our model datum-inconsistency functions Δh_1, Δh_2, and Δh_3 respectively. In all three cases the correction coefficients bear significant contribution to the original coefficients only up to degree 60. Above degree 60 the spectrum flattens, and the individual relative errors do not exceed the magnitude 0.002 for the case of Δh_2 and Δh_3, and 0.001 for Δh_1. We conclude that the effect of vertical datum inconsistency is mostly of long wavelength nature, and that for higher frequencies the relative error in the coefficients is on the order of the background noise. The distribution of the relative errors in the frequency domain for models Δh_2 and Δh_3, as shown on Figures 21 and 22 respectively, is very much alike,

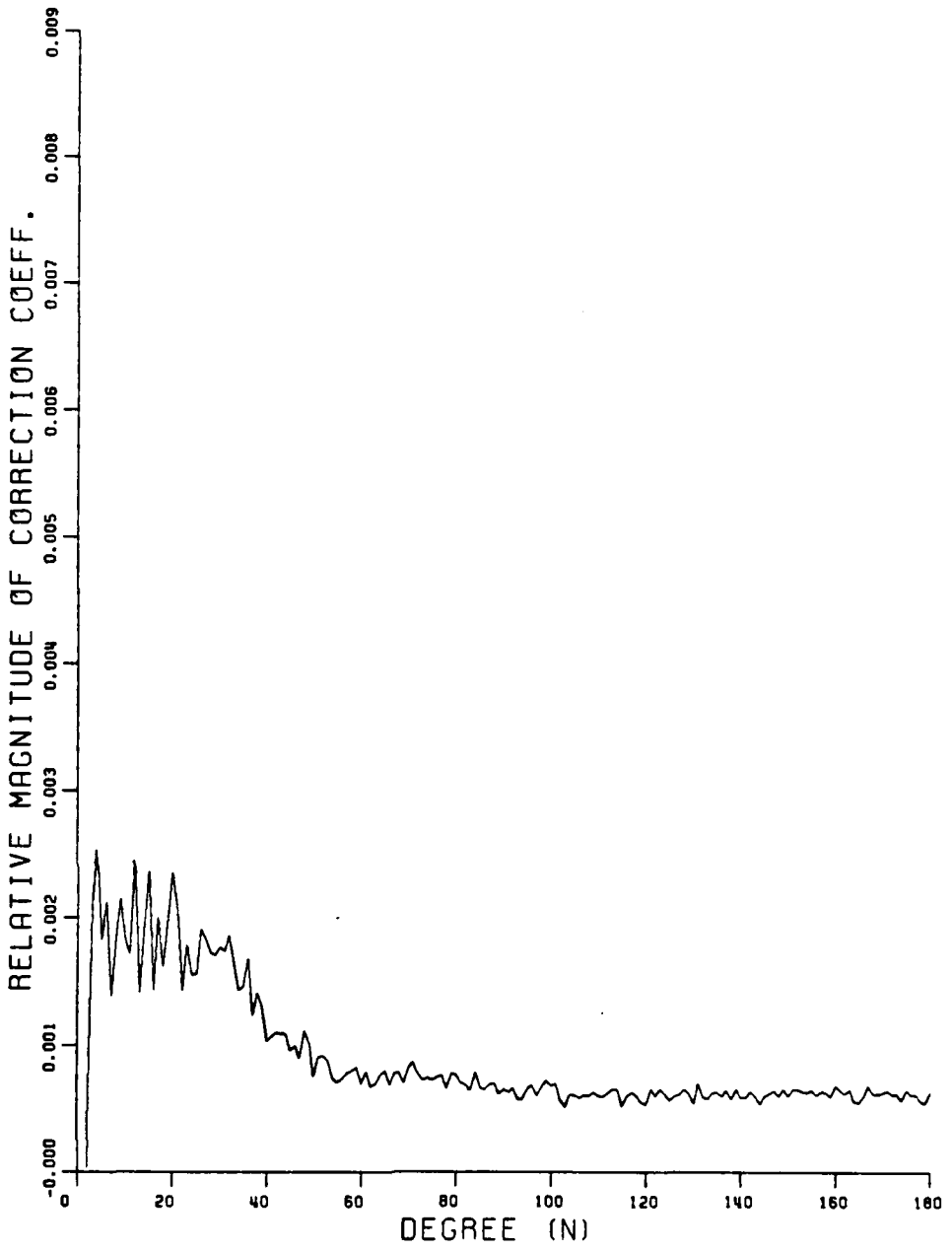

Figure 20. Relative magnitude of error coefficients (by ratio of degree variances) computed for the vertical datum inconsistency model Δh_1 (see eq. 12).

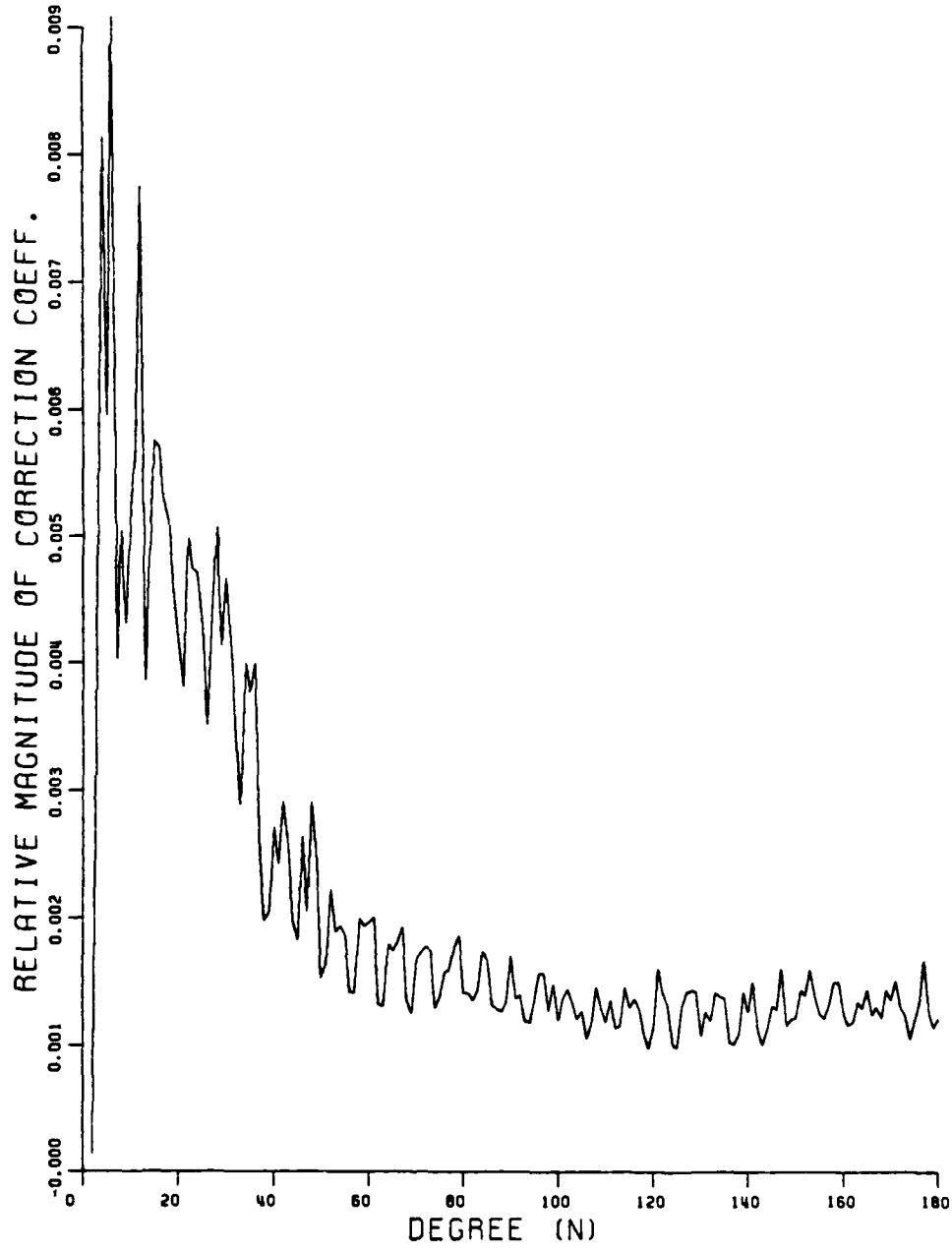

Figure 21. Relative magnitude of error coefficients (by ratio of degree variances, eq. 12) computed for the vertical datum inconsistency model Δh_2.

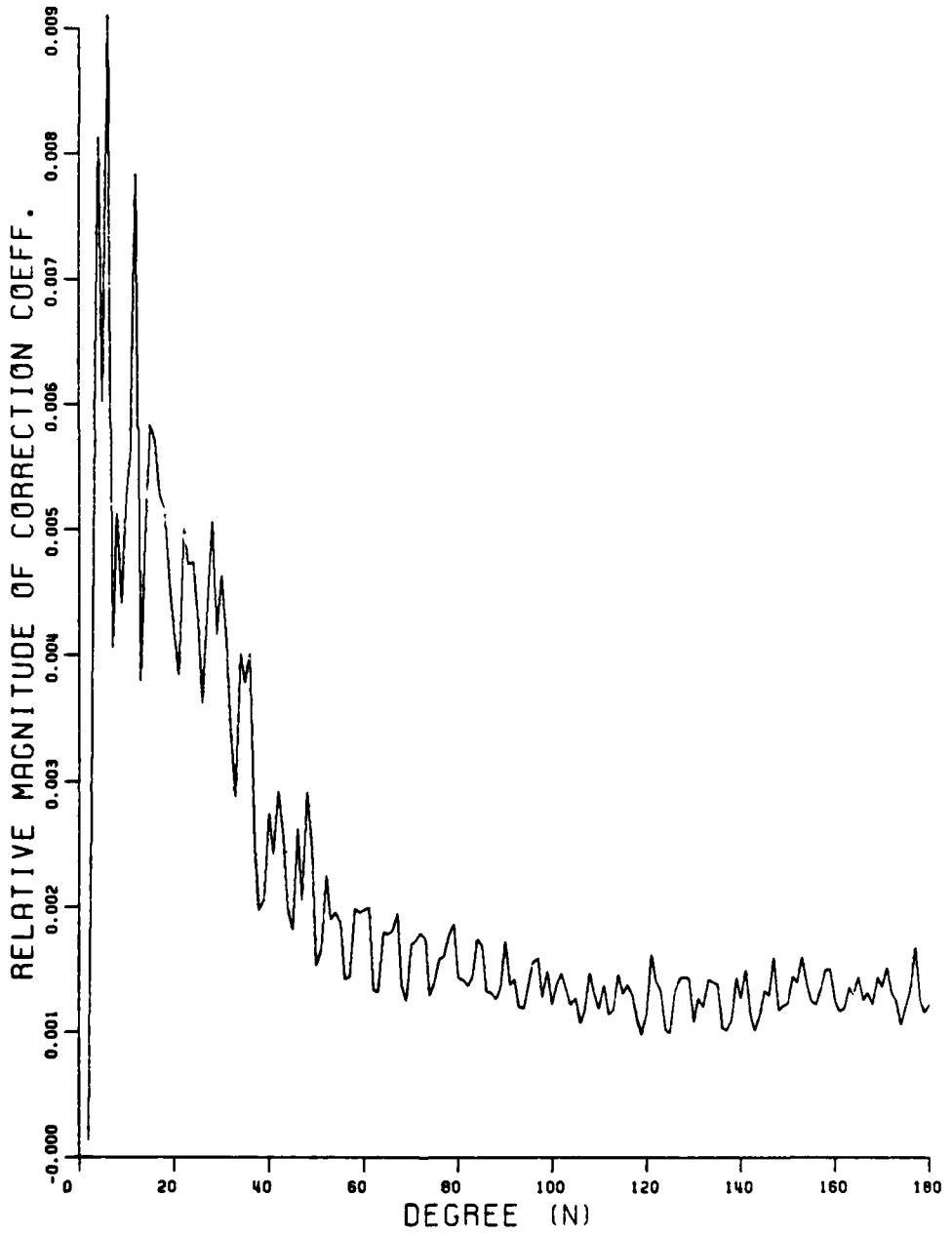

Figure 22. Relative magnitude of error coefficients (by ratio of degree variances, eq. 12) computed for the vertical datum inconsistency model Δh_3.

although the inclusion of the internal distortion of the North American datum (function Δh_3) caused slightly higher relative errors for most degree variances (see also Table 1).

Table 1 shows the comparison between the magnitude of relative errors in potential coefficients expressed by formula (12) for three different models of vertical datum inconsistencies represented by functions Δh_1, Δh_2, and Δh_3. The maximum individual relative error (by degree) in coefficients for the simplest model represented by Δh_1 (no SST included) occurs at degree 4 and has the magnitude of 0.00253 (0.253%). For the other two models which include SST the maximum relative error is about 0.009 (0.9%) and occurs at degree 6. Comparing the effects of Δh_1 (simple step-function, no SST) with those of Δh_2 or Δh_3 (SST included) we conclude that the variation of SST over oceans brought about a significant increase of power spectrum of correction coefficients. The models containing SST produce the spherical harmonics coefficients that are much larger in magnitude than those produced by a simple step-function Δh_1 . The addition of Sea Surface Topography had a very large effect of magnifying the errors more than 3 times. The oceans cover more than 70% of our globe, and therefore the variations over oceans determine the overall character of the inconsistency model. If we multiply (12) by 100 we obtain the average percentage correction to potential coefficients due to the datum inconsistency. From Table 1 we conclude that the global datum inconsistency can produce a significant error in the determination of potential coefficients. For low degree harmonics the relative error can be on the order of 1 percent. By significant we understand the error of the relative magnitude reaching 1% level.

The spectral analysis of our three models of the spatial inconsistencies in the global vertical datum (as represented on Figures 20, 21 and 22) shows significant effect only on the low degree harmonics. This is a result of the specific nature of our approximating functions Δh_1, Δh_2, and Δh_3 (see Figures 17, 18 and 19). All of them represent a flat or slowly varying surface, showing no local features of short-wavelength characteristics (except perhaps discontinuities along continental edges). Therefore, the particular distribution of energy in the spectrum could have been expected. We should mention also that the digital model of SST used in the computations was based on the rather crude 10°x 10° grid, and this certainly could add up to the overall smoothing of the distortion spectrum (high-cut filter effect).

More than two thirds of the entire energy in the spectrum comes from the discrepancy between MSL and the geoid over the oceans, as could be seen by comparing the first column with the second or third columns in Table 1. The relative error due to the internal distortion in the N. American vertical datum contributes very little to the cumulative effect; however, it may be significant in some applications.

6.1.1 The Error (by Degree Variances) in Geoid Undulations, Gravity Anomalies, and Deflections of Vertical due to Vertical Datum Inconsistency Models

The magnitude of correction coefficients $\overline{\delta C}_{nm}$, $\overline{\delta S}_{nm}$ can also be expressed in terms of the geoid undulation degree variances.

Table 1

The Relative Error in Potential Coefficients (by Ratio of Square Root Degree Variances, eq. 12) due to the three Vertical Datum Inconsistency Models: Δh_1, Δh_2, and Δh_3. (Unitless quantities)

DEGREE(N)	Δh_1	Δh_2	Δh_3
2	3.62E-05	1.37E-04	1.36E-04
3	2.11E-03	4.76E-03	4.83E-03
4	2.53E-03	8.14E-03	8.13E-03
5	1.83E-03	5.96E-03	6.02E-03
6	2.13E-03	9.08E-03	9.10E-03
7	1.39E-03	4.03E-03	4.05E-03
8	1.79E-03	5.04E-03	5.12E-03
9	2.15E-03	4.31E-03	4.42E-03
10	1.83E-03	5.22E-03	5.26E-03
11	1.72E-03	5.70E-03	5.65E-03
12	2.44E-03	7.75E-03	7.84E-03
13	1.42E-03	3.86E-03	3.80E-03
14	1.90E-03	4.82E-03	4.92E-03
15	2.37E-03	5.75E-03	5.83E-03
16	1.43E-03	5.70E-03	5.71E-03
17	2.00E-03	5.30E-03	5.29E-03
18	1.61E-03	5.12E-03	5.14E-03
19	2.00E-03	4.58E-03	4.56E-03
20	2.35E-03	4.19E-03	4.19E-03
21	2.05E-03	3.81E-03	3.84E-03
22	1.43E-03	4.98E-03	5.02E-03
23	1.79E-03	4.74E-03	4.72E-03
24	1.55E-03	4.70E-03	4.73E-03
25	1.56E-03	4.28E-03	4.26E-03
26	1.91E-03	3.52E-03	3.62E-03
27	1.83E-03	4.37E-03	4.40E-03
28	1.72E-03	5.07E-03	5.06E-03
29	1.71E-03	4.13E-03	4.17E-03
30	1.77E-03	4.66E-03	4.63E-03
31	1.74E-03	4.09E-03	4.11E-03
32	1.86E-03	3.42E-03	3.41E-03
33	1.65E-03	2.89E-03	2.88E-03
34	1.44E-03	3.99E-03	4.01E-03
35	1.46E-03	3.76E-03	3.78E-03
36	1.68E-03	4.00E-03	4.01E-03
37	1.24E-03	2.47E-03	2.48E-03
38	1.41E-03	1.98E-03	1.98E-03
39	1.30E-03	2.05E-03	2.06E-03
40	1.03E-03	2.72E-03	2.75E-03
41	1.07E-03	2.43E-03	2.43E-03
42	1.10E-03	2.91E-03	2.92E-03
43	1.09E-03	2.57E-03	2.56E-03
44	1.09E-03	1.99E-03	2.00E-03
45	9.63E-04	1.83E-03	1.83E-03
46	9.96E-04	2.64E-03	2.64E-03
47	9.00E-04	2.05E-03	2.06E-03
48	1.11E-03	2.91E-03	2.92E-03
49	1.01E-03	2.45E-03	2.47E-03
50	7.58E-04	1.53E-03	1.53E-03

$$x_n := R^2 \sum_{m=0}^{n} (\overline{\delta C}_{nm} + \overline{\delta S}_{nm}) \qquad (13)$$

where R denotes the mean earth radius. The contribution to the geoid undulation in terms of the square roots of undulation degree variances due to our three models of the inconsistencies in global vertical datum is shown in Figures 23, 24 and 25 respectively. In Table 2 we compare the effects (up to degree 50) on geoid undulation produced by our three models of vertical datum inconsistencies Δh_1, Δh_2 and Δh_3. The maximum square root of undulation degree variance was computed as 11.16 cm (at degree 2) for the first model, 42.38 cm (at degree 2) for the second model and 42.05 cm (at degree 2) for our third model.

The existence of the zero degree unulation term in the error spectrum can be interpreted in the following way. Theoretically, if we evaluated the anomalous gravity potential T with respect to the reference normal potential of the level ellipsoid, which is chosen to have a mass equal to the mass of the Earth and potential equal to that associated with the geoid, then the zero-degree coefficient in the spherical harmonic expansion of T or undulation N would vanish. This is true only if the terrestrial gravity data used were properly reduced to the geoid. The geoid is approximated by a given level ellipsoid which induces normal gravity used in the gravity data reduction. Geometrically this approximation means that the average (over the unit sphere) deviation of the geoid from the reference ellipsoid is zero, and the origin of the ellipsoid coincides with the center of mass of the Earth.

In practice however we deal with the gravity data that have been reduced not to the idealized geoid, but to some nearby surface which is not necessarily the equipotential surface. Let us for the moment call this surface a pseudogeoid. The height error function Δh described in the previous chapter represents precisely the deviation of pseudogeoid from the geoid. In the frequency domain, this deviation is represented by the error power spectrum x_n, that is by the various harmonic components of the difference:

$$\{\text{pseudogeoid undulation}\} - \{\text{geoid undulation}\} := \delta N$$

The non-vanishing zero degree undulation term in the error spectrum shows that the average height of the pseudogeoid with respect to our reference normal ellipsoid does not reduce to zero. The detailed interpretation of the zero-degree term can be found for example in Heiskanen and Moritz (1967). In geometric terms the semimajor axis of the mean best fit ellipsoid associated with the pseudogeoid differs from the semimajor axis of the normal ellipsoid associated with the geoid by the amount expressed by the zero degree term in the error spectrum. By the best-fit ellipsoid implied by the pseudogeoid we understand the

Table 2

The Error in Geoid Undulation (by Square Root Degree Variances up to Degree 50, see eq. 13) due to the three Vertical Datum Inconsistency Models: Δh_1, Δh_2, and Δh_3. Units are cm.

DEGREE(N)	Δh_1	Δh_2	Δh_3
0	10.562	3.369	3.738
2	11.162	42.384	42.051
3	3.996	9.008	9.239
4	2.562	8.241	8.229
5	1.350	4.406	4.453
6	1.218	5.192	5.204
7	0.675	1.957	1.970
8	0.551	1.554	1.580
9	0.582	1.167	1.195
10	0.414	1.179	1.188
11	0.292	0.969	0.962
12	0.258	0.818	0.828
13	0.206	0.560	0.551
14	0.164	0.416	0.425
15	0.191	0.464	0.471
16	0.136	0.540	0.541
17	0.151	0.401	0.399
18	0.112	0.356	0.358
19	0.125	0.286	0.285
20	0.111	0.198	0.198
21	0.104	0.194	0.196
22	0.086	0.298	0.300
23	0.082	0.217	0.216
24	0.064	0.193	0.194
25	0.068	0.187	0.186
26	0.065	0.119	0.123
27	0.058	0.139	0.140
28	0.063	0.184	0.184
29	0.055	0.132	0.133
30	0.062	0.163	0.163
31	0.048	0.113	0.114
32	0.049	0.090	0.090
33	0.048	0.084	0.083
34	0.047	0.131	0.131
35	0.042	0.109	0.110
36	0.041	0.098	0.098
37	0.040	0.080	0.080
38	0.040	0.057	0.056
39	0.041	0.064	0.065
40	0.029	0.075	0.076
41	0.031	0.070	0.070
42	0.030	0.081	0.081
43	0.027	0.064	0.064
44	0.030	0.054	0.054
45	0.025	0.047	0.047
46	0.024	0.064	0.064
47	0.024	0.055	0.055
48	0.025	0.065	0.066
49	0.023	0.055	0.055
50	0.019	0.039	0.039

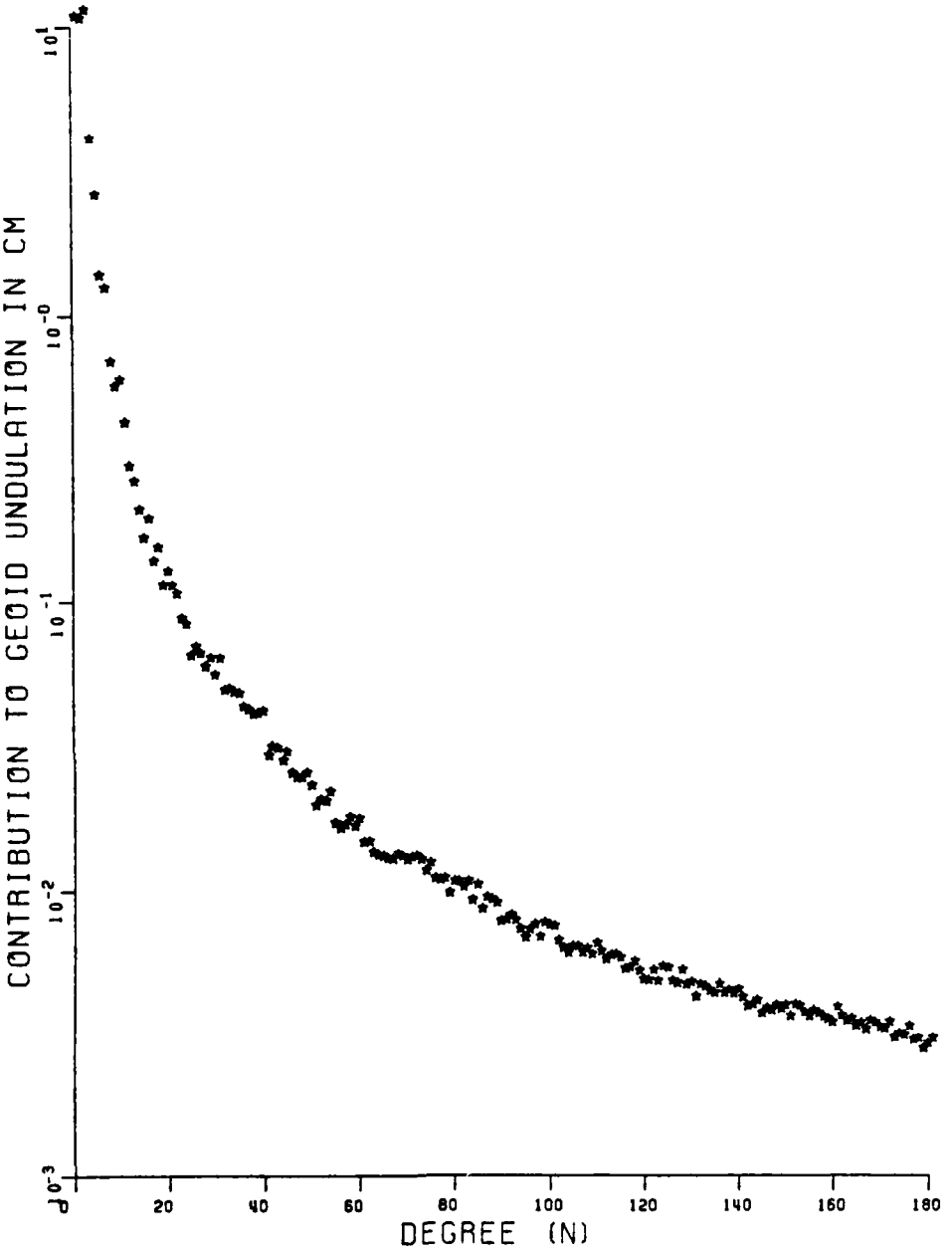

Figure 23. The error in geoid undulation (by square root degree variances, eq. 13) due to the vertical datum inconsistency model Δh_1.
Units are cm.

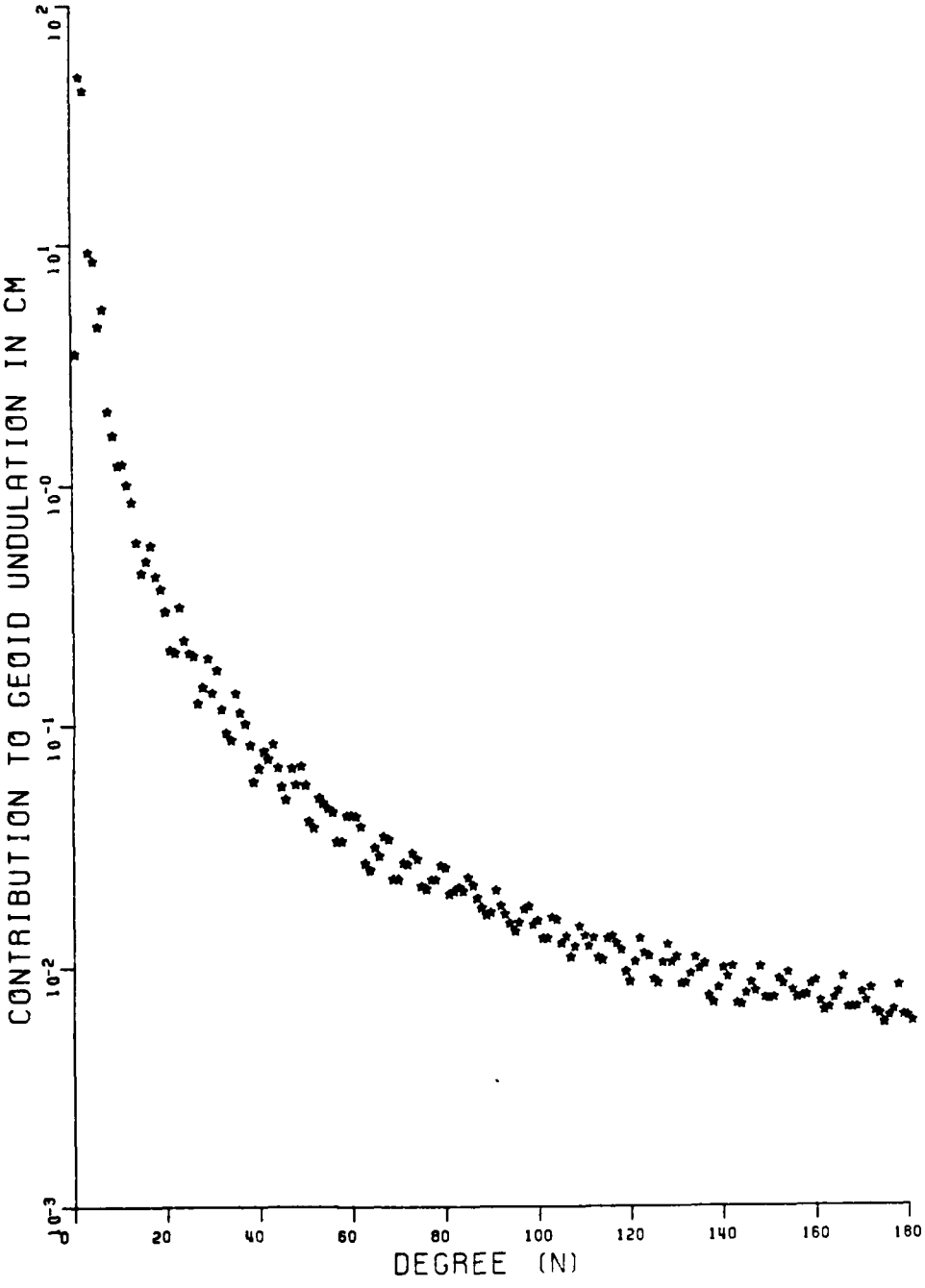

Figure 24. The error in geoid undulation (by square root degree variances, eq. 13) due to the vertical datum inconsistency model Δh_2.
Units are cm.

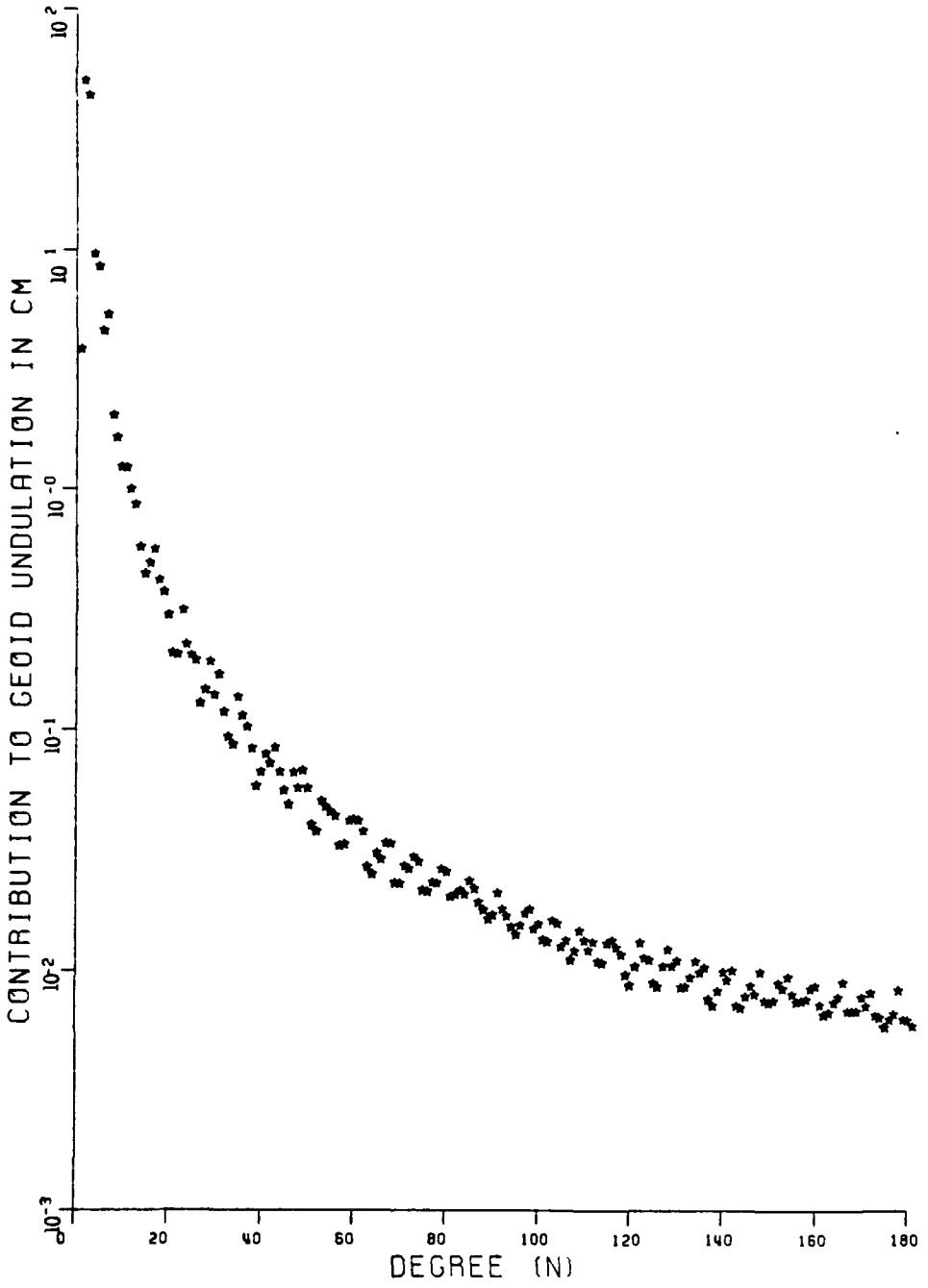

Figure 25. The error in geoid undulation (by square root degree variances, Eq. 13) due to the vertical datum inconsistency model Δh_3.
Units are cm.

Table 3

The Error in Gravity Anomalies (by Square Root Degree Variances, eq. 15) due to the Three Vertical Datum Inconsistency Models: Δh_1, Δh_2 and Δh_3. Units are micro-gals.

DEGREE(N)	Δh_1	Δh_2	Δh_3
0	16.24	5.18	5.75
1	15.96	74.57	74.34
2	17.16	65.18	64.67
3	12.29	27.71	28.42
4	11.62	38.02	37.97
5	8.30	27.10	27.39
6	9.36	39.92	40.02
7	6.22	18.06	18.18
8	5.93	16.72	17.00
9	7.17	14.36	14.70
10	5.72	16.31	16.45
11	4.49	14.91	14.80
12	4.37	13.84	14.00
13	3.80	10.33	10.16
14	3.28	8.32	8.49
15	4.11	10.00	10.14
16	3.14	12.46	12.47
17	3.72	9.86	9.83
18	2.93	9.31	9.35
19	3.46	7.92	7.89
20	3.24	5.78	5.79
21	3.21	5.97	6.01
22	2.77	9.62	9.70
23	2.77	7.33	7.31
24	2.25	6.82	6.87
25	2.51	6.91	6.88
26	2.49	4.58	4.72
27	2.33	5.56	5.59
28	2.60	7.64	7.63
29	2.35	5.69	5.74
30	2.77	7.29	7.25
31	2.23	5.23	5.25
32	2.33	4.28	4.28
33	2.34	4.12	4.10
34	2.38	6.63	6.66
35	2.21	5.71	5.74
36	2.22	5.27	5.29
37	2.22	4.43	4.45
38	2.29	3.22	3.21
39	2.39	3.76	3.77
40	1.72	4.52	4.58
41	1.89	4.29	4.29
42	1.92	5.09	5.11
43	1.77	4.16	4.15
44	1.95	3.56	3.58
45	1.69	3.21	3.20
46	1.67	4.43	4.42
47	1.70	3.89	3.90
48	1.80	4.72	4.74
49	1.66	4.03	4.07
50	1.44	2.91	2.92

Table 4

The Error in Deflections of the Vertical (by Square Root Degree Variances, eq. 17) due to the Vertical Datum Inconsistency Model Δh_3. Units are Seconds of Arc.

DEGREE(N)	Δh_3
2	3.38E-02
3	1.04E-02
4	1.19E-02
5	7.90E-03
6	1.09E-02
7	4.77E-03
8	4.34E-03
9	3.67E-03
10	4.03E-03
11	3.58E-03
12	3.35E-03
13	2.41E-03
14	1.99E-03
15	2.03E-03
16	2.09E-03
17	2.26E-03
18	2.14E-03
19	1.20E-03
20	1.31E-03
21	1.36E-03
22	2.19E-03
23	1.64E-03
24	1.34E-03
25	1.34E-03
26	1.05E-03
27	1.25E-03
28	1.69E-03
29	1.27E-03
30	1.61E-03
31	1.16E-03
32	9.44E-04
33	9.04E-04
34	1.47E-03
35	1.25E-03
36	1.16E-03
37	9.75E-04
38	7.02E-04
39	8.25E-04
40	1.00E-03
41	9.37E-04
42	1.12E-03
43	9.06E-04
44	7.03E-04
45	6.97E-04
46	9.61E-04
47	8.45E-04
48	1.03E-03
49	3.85E-04
50	6.84E-04

ellipsoid producing no zero-degree undulation term (Heiskanen, Moritz, 1967, eq. (2-194a)). In geometric terms, the pseudogeoid encloses a slightly different volume than the geoid does. In other words the volume of a thin irregular layer described by our height error function Δh does not average to 0.

This does not necessarily contradict the fact that the average SST used as a primary component in Δh was claimed to be zero. First of all the Lisitzin's 280 dyn.cm average of SST variation was implied by data irregularly distributed between latitudes +60° and -60°. Near the poles there was no data at all.

Secondly, the 280 dyn.cm average pertains only to the oceanic part of Earth's surface, whereas our model height error function covers the entire globe.

In the next step of this analysis, for each model we computed the cumulative effect on geoid undulation up to degree 180:

$$\sqrt{\sum_{n=0}^{180} R^2 \sum_{m=0}^{n} (\overline{\delta C}^2_{nm} + \overline{\delta S}^2_{nm})} \qquad (14)$$

This effect is 16.24 cm for function Δh_1, 44.90 cm for Δh_2 and 44.67 cm for model-function Δh_3. Again almost two-thirds of the total effect comes from the SST variation over oceans, while the contribution from the relative rigid displacements of the flat continental datums (function Δh_1) amounts only to about 16 cm. The inclusion of the internal distortion of the N. American vertical datum had a cumulative effect on the order of millimeters.

The computed effect of inconsistencies in the global vertical datum can also be expressed in terms of the gravity anomaly degree variances:

$$c_n := G^2 (n-1)^2 \sum_{m=0}^{n} (\overline{\delta C}^2_{nm} + \overline{\delta S}^2_{nm}) \quad , \quad n \neq 1 \qquad (15)$$

$$c_1 := G^2 \sum_{m=0}^{1} (r_m^2 + q_m^2), \qquad \text{where} \qquad (15a)$$

$$\begin{Bmatrix} r_m \\ q_m \end{Bmatrix} := \frac{0.3086E\text{-}5}{4\pi G} \iint_{\sigma} \Delta h\,(\phi,\lambda)\, \overline{P}_{1m}(\sin\phi) \begin{Bmatrix} \cos m\lambda \\ \sin m\lambda \end{Bmatrix} d\sigma$$

where G := the average value of gravity.

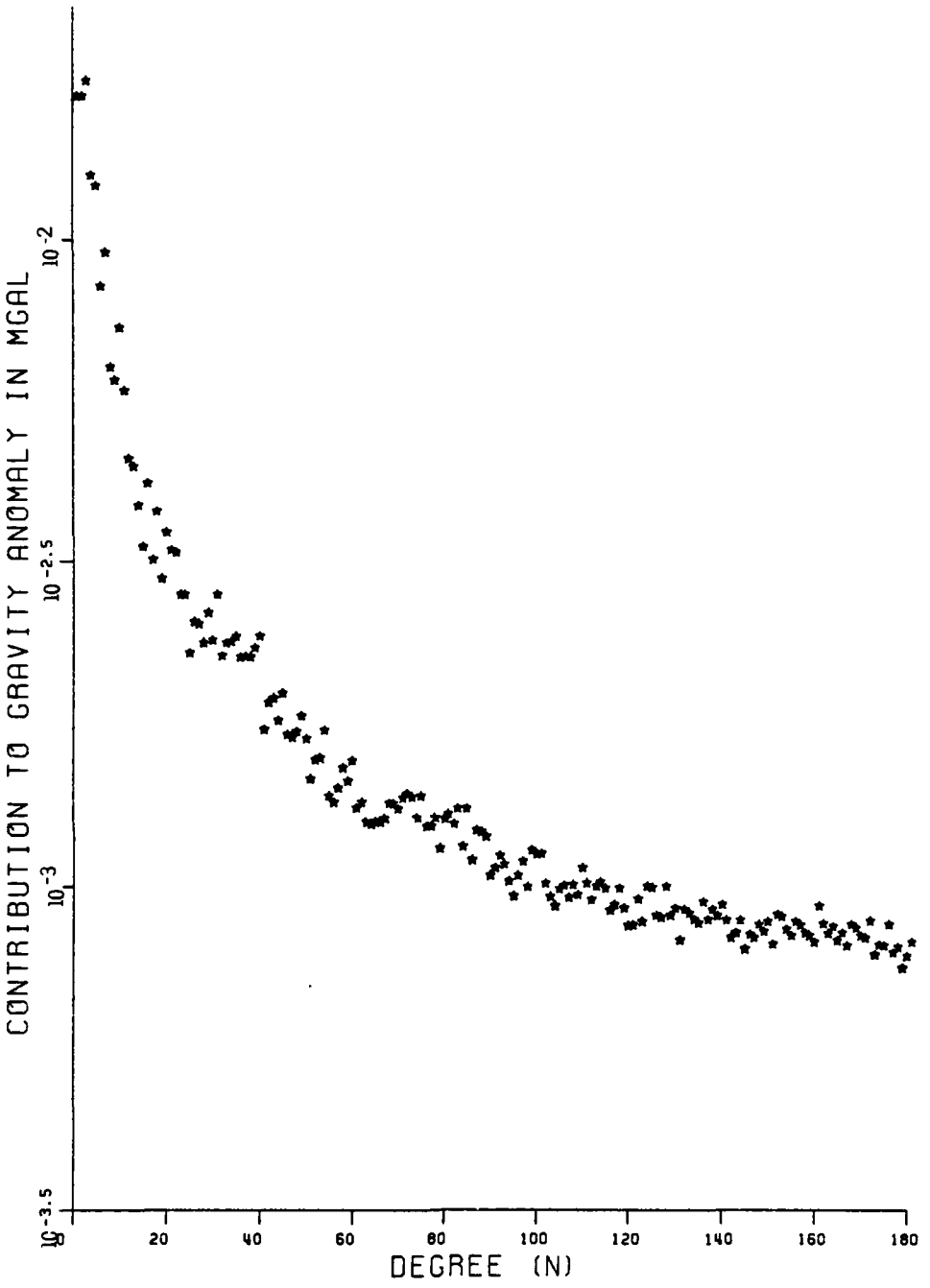

Figure 26. The error in gravity anomaly (by square root degree variances, eq. 15) due to vertical datum inconsistency model Δh_1. Units are mgals.

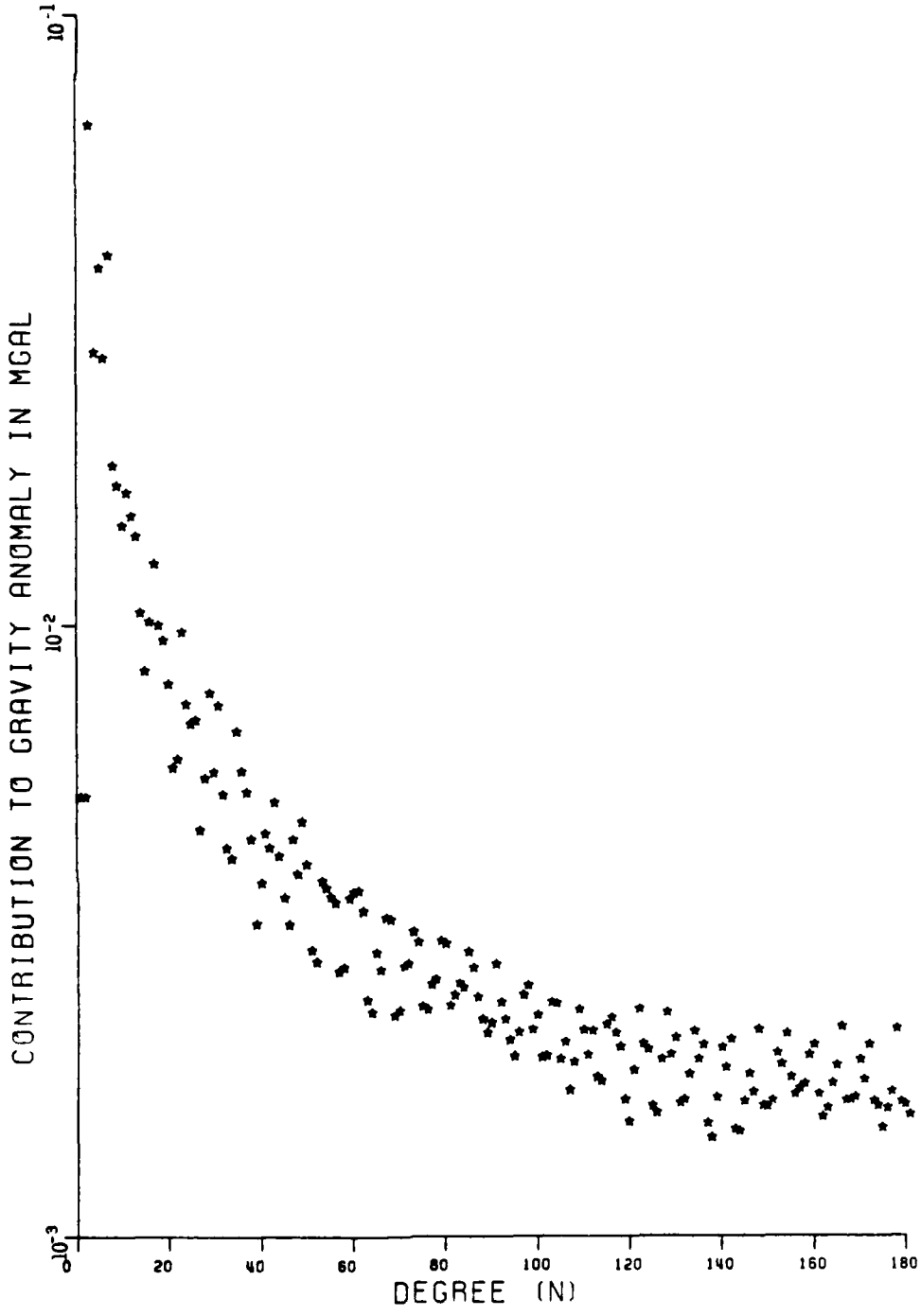

Figure 27. The error in gravity anomaly (by square root degree variances, eq. 15) due to vertical datum inconsistency model Δh_2. Units are mgals.

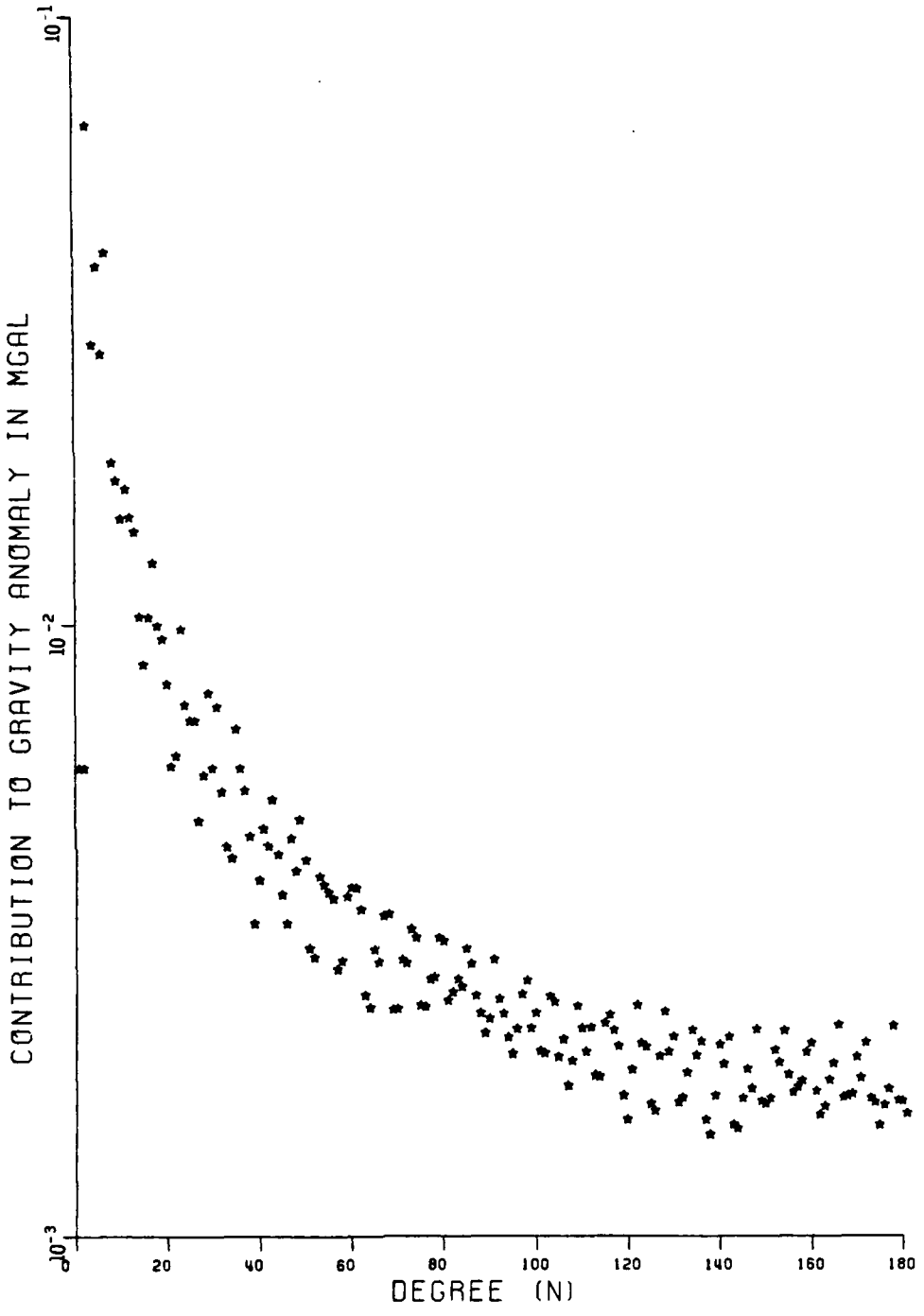

Figure 28. The error in gravity anomaly (by square root degree variances, eq. 15) due to the vertical datum inconsistency model Δh_3. Units are mgals.

Figures 26, 27, and 28 show the contribution to gravity anomaly by the square root of c_n (formula (15)) produced by model 1, 2, and 3. Table 3 compares the errors in the gravity anomaly represented by the above three figures for our model functions Δh_1, Δh_2 and Δh_3 respectively. The maximum individual errors (by degree) reach the magnitude 0.017 mgal at degree 2 for the case of the simplest model Δh_1, up to 0.074 mgal (at degree 1) for the most complex one. Also, we computed the cumulative error in gravity anomaly expressed by the formula:

$$\sqrt{\sum_{n=0}^{180} G^2(n-1)^2 \sum_{m=0}^{n} (\overline{\delta C}^2_{nm} + \overline{\delta S}^2_{nm})} \qquad (16)$$

This error is 0.043 mgal for the simplest model Δh_1, 0.13 mgal for model Δh_2 and 0.13 mgal for the most complicated model. Again the dominant error comes from the Sea Surface Topography variation over oceans. The effect of distortions in N. Americal vertical datum is only on the order of 1E-4 mgal.

We also computed the effect of the global vertical datum inconsistency in terms of deflections of vertical degree variances:

$$\theta_n := n(n+1) \sum_{m=0}^{n} (\overline{\delta C}^2_{nm} + \overline{\delta S}^2_{nm}) \qquad (17)$$

Figure 29 shows the frequency spectrum decomposition of the error in the deflection of vertical (by degree) generated by our most complex model-function Δh_3, reflecting the rigid relative shiftings of the continental reference-planes, SST over oceans, and internal distortion of the N. American vertical datum. The individual values were computed as square roots of the deflection of vertical degree variances given by formula (17). The units are seconds of arc. Also, in Table 4 we show those results up to degree 50. The maximum individual error occurs at degree 2 and has the magnitude of 3.33E-2 sec of arc, whereas the cumulative effect up to degree 180:

$$\sqrt{\sum_{n=0}^{180} \theta_n}$$

is 5.2E-2 sec of arc.

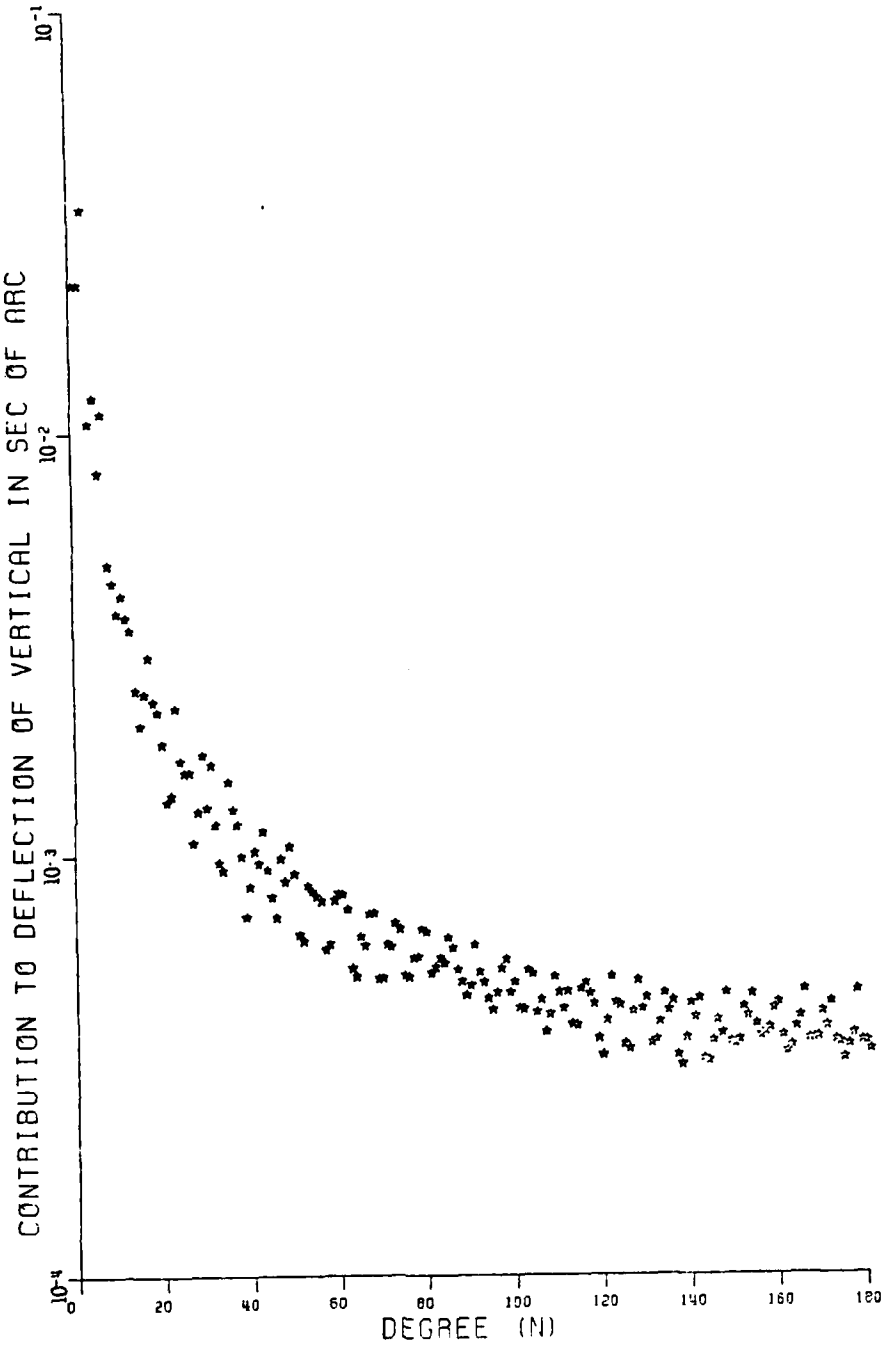

Figure 29. The error in deflections of vertical (by square root degree variances, eq. 17) due to the vertical datum inconsistency model Δh_3.
Units are seconds of arc.

6.2 Some Remarks on the Present Procedures for Determination of Spherical Harmonics Coefficients of Geopotential

In the previous section we studied the effects of vertical datum inconsistencies on the determination of geopotential, as if the only information available was the terrestrial gravity data. However, the most current procedure of computing the potential coefficients is through a combination of gravimetric and satellite-derived data (Rapp, 1973). Those procedures use satellite data to derive low degree coefficients and terrestrial data to supply information for the higher frequency part of the spectrum. Therefore, only part of the error estimated in the previous chapter will actually contribute to the error in the determination of the spherical harmonic coefficients. This part comes only from the higher degree error coefficients, produced by our models of inconsistencies in the global vertical datum.

It might be of interest to estimate the cumulative error in coefficients due to the datum inconsistencies only above certain degree. It would reflect the fact that only higher degree coefficients are affected by errors of that nature, and that low degree harmonics are derived in some different way. However, the satellite-derived coefficients are affected by different sources of errors and generally are less accurate for higher degrees. Therefore, this type of analysis could provide an additional insight into the nature of this combined procedure. Also, it could suggest the specific degree beyond which the terrestrial information can safely be incorporated into the combined solution. The idea is to balance the errors in the satellite-derived coefficients with those inherent in the terrestrial data.

Figure 30 shows the cumulative error in the geoid undulation due to our third model (Δh_3) of datum inconsistency. The 6 curves on this figure represent the cumulative contribution to the undulation (as a function of degree n) beyond the specified degree. This truncation degree can be found at the intersection with the horizontal axis. To construct the curves we used the formula:

$$\text{CUMULAT.ERROR.N}^{p}(n) = R\sqrt{\sum_{i=p}^{n}\sum_{m=0}^{i}(\overline{\delta C}^2_{im} + \overline{\delta S}^2_{im})} \quad ; \; p \leq n \leq 180 \qquad (18)$$

where the starting degree p takes on the values 10, 20, ..., 60. From Figure 30 we learn that the cumulative error undulation, when the summation starts at degree 10, can amount to almost 2 cm at degree 180 (the highest curve on Figure 30). If we start the summation from degree 40 this cumulative error can reach 0.3 cm and for the summation starting at 60 it is only 0.15 cm at degree 180 (the lowest curve on Figure 30).

The similar type of analysis for gravity anomalies is shown in Figure 31. The curves were constructed according to the formula:

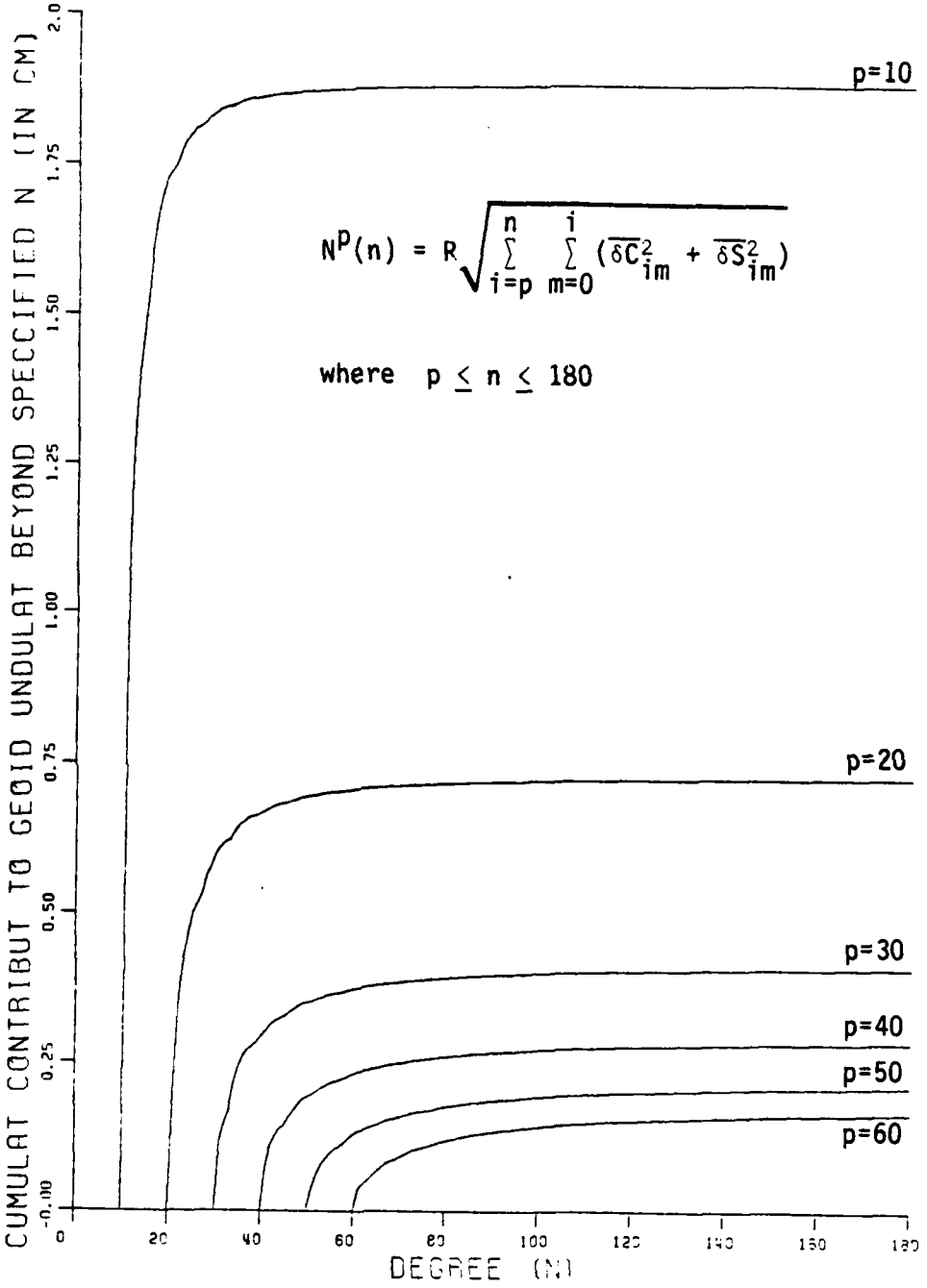

Figure 30. Cumulative error contribution to geoid undulation (eq. 18) beyond specified degree due to the vertical datum inconsistency model Δh_3.
Units are cm.

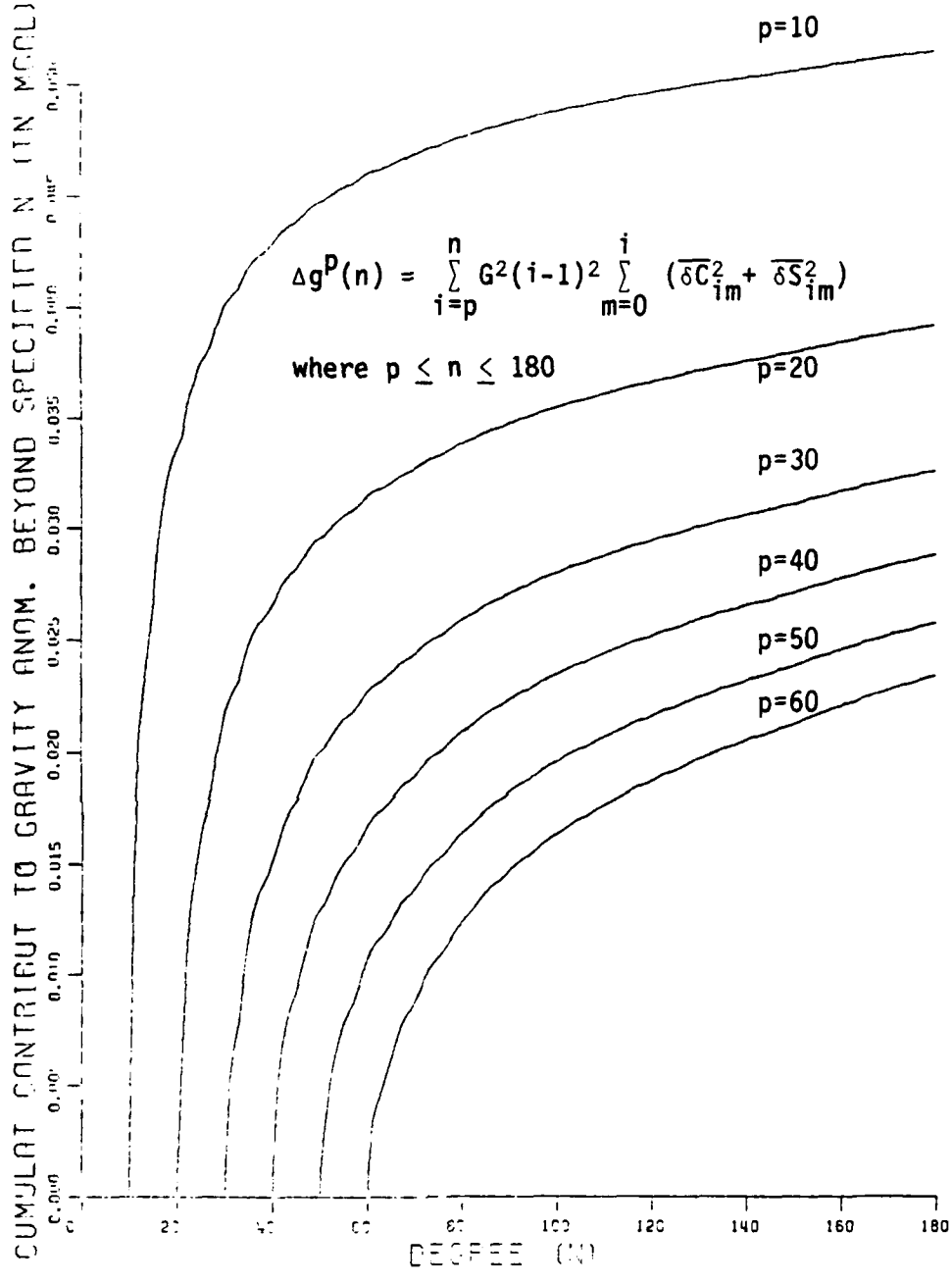

Figure 31. Cumulative error contribution to gravity anomalies (eq. 19) beyond specified degree due to the vertical datum inconsistency model Δh_3.
Units are mgal.

$$\text{CUMULAT.ERROR. } \Delta g^p(n) := \sqrt{\sum_{i=p}^{n} G^2(i-1)^2 \sum_{m=0}^{i} (\overline{\delta C}^2_{im} + \overline{\delta S}^2_{im})} \quad ; \qquad (19)$$

$p \leq n \leq 180$ for $p = 10, 20, \ldots, 60$.

The correction coefficients $\overline{\delta C}_{nm}$, $\overline{\delta S}_{nm}$ produced by our third model (Δh_3) of datum inconsistency were used. From the highest curve in Figure 31 we see that neglecting the errors in the first 10 degrees the cumulative effect (19) of errors at the remaining part of the spectrum can reach 0.053 mgal at the degree 180. On the other hand neglecting the errors of coefficients having degree less or equal 60, the cumulative error in the gravity anomaly due to datum inconsistency beyond this degree can only reach 0.023 mgal for n=180 (see formula (19)).

7. THE EFFECT OF VERTICAL DATUM INCONSISTENCIES ON THE DETERMINATION OF GEOID UNDULATION FROM A COMBINATION OF SPHERICAL HARMONIC COEFFICIENTS AND GRAVITY IN CAP

In practice, the geoidal undulation are often computed using Stokes' equation where the global data set of gravity anomalies has been truncated to form a spherical cap surrounding the point computation. Additionally this truncated terrestrial data is usually supported by the long wavelength global information in the form of low degree harmonic expansion of geopotential. The theory of this combination of satellite-derived and terrestrial data to obtain the geoid undulation (or disturbing potential) originates with M.S. Molodenskii (Molodenskii et al., 1962) and was further developed by (Heiskanen and Moritz, 1967), (Meissl, 1971), (Jekeli, 1980) and others.

The general idea came from the fact that global gravity data is needed in the classical Stokes' equation:

$$N = \frac{R}{4\pi G} \iint_{\sigma} \Delta g \, S(\psi) \, d\sigma \qquad (20)$$

In the equation the symbol $S(\psi)$ denotes the Stokes' function:

$$S(\psi) = \sum_{n=2}^{\infty} \frac{2n+1}{n-1} P_n(\cos \psi)$$

where

ψ - the spherical distance between the variable surface element $d\sigma$ and the point at which the formula is evaluated

$P_n(\cos\psi)$- Legendre's polynomial

Normally, if we do not associate any additional assumptions with Δg in equation (20) the left hand-side quantity N represents the geoid undulation from which the zero and first degree harmonics have been removed (Heiskanen and Moritz, 1967, eq. (2-1636)), even if Δg contains the zero and first degree harmonic components. In other words those two components in Δg actually do not contribute to the geoid undulation produced by eq. (20).

Usually, the information on the zero-degree undulation term N must be supplied to equation (20) in the form of a separate term

$$N = N_0 + \frac{R}{4\pi G} \iint_\sigma \Delta g \, S(\psi) \, d\sigma \qquad (21)$$

where (Heiskanen and Moritz, 1967, p. 102):

$$N_0 = -\frac{R}{2G} \Delta g_0 + \frac{k\delta M}{2GR} \qquad (22)$$

where

R - mean radius of earth

G - mean value of the normal gravity over the earth

δM - mass difference between the earth and reference ellipsoid

k - gravitational constant

Δg_0 - the zero-degree component possibly present in the spherical harmonic expansion of Δg field.

If we are using gravity anomalies in a spherical cap surrounding the point of computation, a special correction term is needed to account for the effect of truncation of the data domain. More specifically, the gravity anomaly data in the cap are used with the ordinary Stokes' kernel $S(\psi)$.

$$\frac{R}{4\pi G} \iint_{\sigma_c} \Delta g \; S(\psi) \; d\sigma_c \tag{23}$$

where

σ_c - spherical cap around the point of computation,

then the truncation error can be expressed by (Jekeli, 1980)

$$\delta N_1 = \frac{R}{2G} \sum_{n=2}^{\infty} Q_{1n} \; \Delta g_n \tag{24}$$

where

$$\Delta g = \sum_{n=0}^{\infty} \Delta g_n$$

denotes the expansion of the terrestrial gravity anomalies in to the series of Laplace spherical harmonics,

$$Q_{1n}(\psi_c) = \int_{\psi_c}^{\pi} S(\psi) \; P_n(\psi) \; \sin\psi \;\; d\psi$$

(Molodensky truncation coefficients), and

ψ_c - the radius of spherical cap.

If the gravity anomaly data in the cap are used with the modified kernel $S(\psi) - S(\psi_c)$:

$$\frac{R}{4\pi G} \iint_{\sigma_c} \Delta g \; (S(\cos\psi) - S(\cos\psi_c)) \; d\sigma_c \tag{25}$$

then the truncation error can be expressed (Molodenskii et al., 1962) as

$$\delta N_2 = \frac{R}{2G} \sum_{n=2}^{\infty} Q_{2n}(\psi_c) \; \Delta g_n \tag{26}$$

where

$$Q_{2n}(\psi_c) = \int_{\psi_c}^{\pi} (S(\psi) - S(\psi_c))\, P_n(\psi) \sin\psi \, d\psi + \int_{0}^{\pi} S(\psi_c)\, P_n(\psi) \sin\psi \, d\psi$$

are known as the modified Molodenskii truncation coefficients.

The Δg_n terms above are the Laplace surface harmonics of the gravity anomaly field Δg. This representation can be obtained from a priori given set of potential coefficients according to the formula:

$$\Delta g_n = G(n-1) \sum_{m=0}^{n} (\bar{C}^*_{nm} \cos m\lambda + \bar{S}_{nm} \sin m\lambda)\, \bar{P}_{nm}(\cos\theta) \qquad (27)$$

where

$\bar{C}^*_{nm}$, $\bar{S}_{nm}$ - anomalous potential coefficients relative to the potential field implied by the assumed reference ellipsoid

λ, θ - polar coordinates of the point of computation

The actual computational procedure for the evaluation of geoid undulation based on the above method is given by Rummel and Rapp (1976, eq. 21) (excluding atmospheric effect) as:

$$N = \bar{N}_0 + \frac{R}{4\pi G} \iint_{\sigma_c} S(\psi)\, \Delta g \, d\sigma_c + \frac{R}{2G} \sum_{n=2}^{n_0} Q_{in}(\psi_c)\, \Delta g_n \qquad (28)$$

where

$$\bar{N}_0 = N_0 - \frac{R}{4\pi G} \iint_{\sigma_c} S(\psi)\, \Delta g_0 \, d\sigma_c \qquad (29)$$

Substituting for N_0 (eq. 22) and using the identity (Jekeli, 1980, eq. 123, 124):

$$-\frac{R}{4\pi G} \iint_{\sigma_c} S(\psi)\, \Delta g_0 \, d\sigma_c = \frac{R}{2G} Q_{10}\, \Delta g_0 \qquad (30)$$

we rewrite equation (29) in more explicit form:

$$\bar{N}_0 = \frac{k\delta M}{2GR} - \frac{R}{2G} \Delta g_0 \ (1-Q_{10}) \tag{31}$$

In order to evaluate the contribution of Δg_0 term to $\bar{N}_0$ we need values of Q_{10} and Q_{20} (Q_{20} must be used in eq. (31) if the modified kernel was used in Stokes' integral).

It can be shown that (Molodenskii et al., 1962)

$$Q_{10}(\psi_c) = -4t + 5t^2 + 6t^3 - 7t^4 + (6t^2 - 6t^4) \ln(1+t) \tag{32}$$

where

$$t = \sin \frac{\psi_c}{2}$$

Also, it can be shown that (Jekeli, 1980 eq. 65)

$$Q_{20}(\psi_c) = Q_{10} + S(\psi_c) \ (1 - \cos \psi_c) \tag{33}$$

In the previous section we noted that the zero-degree harmonic component in the error in gravity anomaly field due to the inconsistency in the vertical datum can reach the magnitude (Table 3):

$$\Delta g_0 = 0.57 \times 10^{-2} \text{ mgal} \tag{34}$$

This error component, in turn, will be responsible for the truncation effect in the zero-degree undulation term when the anomalies in the cap are used in the equation (28) with unmodified kernel $S(\psi)$ or with modified one: $S(\psi) - S(\psi_c)$.

First we define the truncation effects on zero degree undulation term which contribute to the quantity defined by equation (31) as:

$$\delta N_1^0 = \frac{R}{2G} Q_{10} \Delta g_0 \tag{35}$$

or

$$\delta N_2^0 = \frac{R}{2G} Q_{20} \Delta g_0 \tag{36}$$

depending on the kernel used in the Stokes' integral

Figure 32 shows the absolute values of these effects plotted as functions of the truncation angle. We see that for small caps (truncation radius $\psi_c < 38°$) the modified Molodenski kernel (25) produces smaller truncation effect than the unmodified kernel (23). For the cap radius $\psi_c = 38$ degrees both methods produce the same truncation effect of about 2.1 cm. If we consider larger caps ($\psi_c > 38°$) the truncation effect of modified kernel is generally speaking greater than that associated with unmodified one, and can reach 3.6 cm for the cap 72° in radius and 11.4 cm for the full cap 180° in radius. This last number has no practical meaning since the global set of data is required so in fact there is no truncation at all. It merely reflects the nominal limit of the expression (36) when ψ_c approaches 180°. We rewrite equation (36) in the equivalent form (Jekeli, 1980):

$$\delta N_2^0 = -\frac{R}{4\pi G}\Delta g \iint_{\sigma_c} S(\cos\psi)\, d\sigma + \frac{R}{4\pi G}\Delta g\, S(\psi_c) \iint_{\sigma_c} d\sigma \qquad (37)$$

where σ_c denotes the spherical cap of radius ψ_c.

We see that in the limit for $\sigma_c \to \sigma_{180°} := \sigma$ (the area of the unit sphere) the integral in the first term goes to 0 from the orthogonal properties of Legendre polynomials and the integral in the second term goes to 4π which is the area of the unit sphere. Therefore, for $\psi_c = 180°$ we get the nominal value

$$\lim_{\psi_c \to 180°} \delta N_2^0 = \frac{R\Delta g_0}{G} S(180°) = 11.4 \text{ cm}.$$

This is equivalent to computing the undulation correction from Stokes' equation. in which the Stokes' function $S(\psi)$ was replaced by the constant $S(180°)$.

However, for all practical applications small spherical caps are in use. In our example the truncation effects for some typical values of ψ_c are:

truncation angle	truncation effect	
ψ_c	unmodified kernel	modified kernel
5°	0.4 cm	0.2 cm
10°	0.8 cm	0.4 cm
15°	1.1 cm	0.6 cm
20°	1.5 cm	0.9 cm

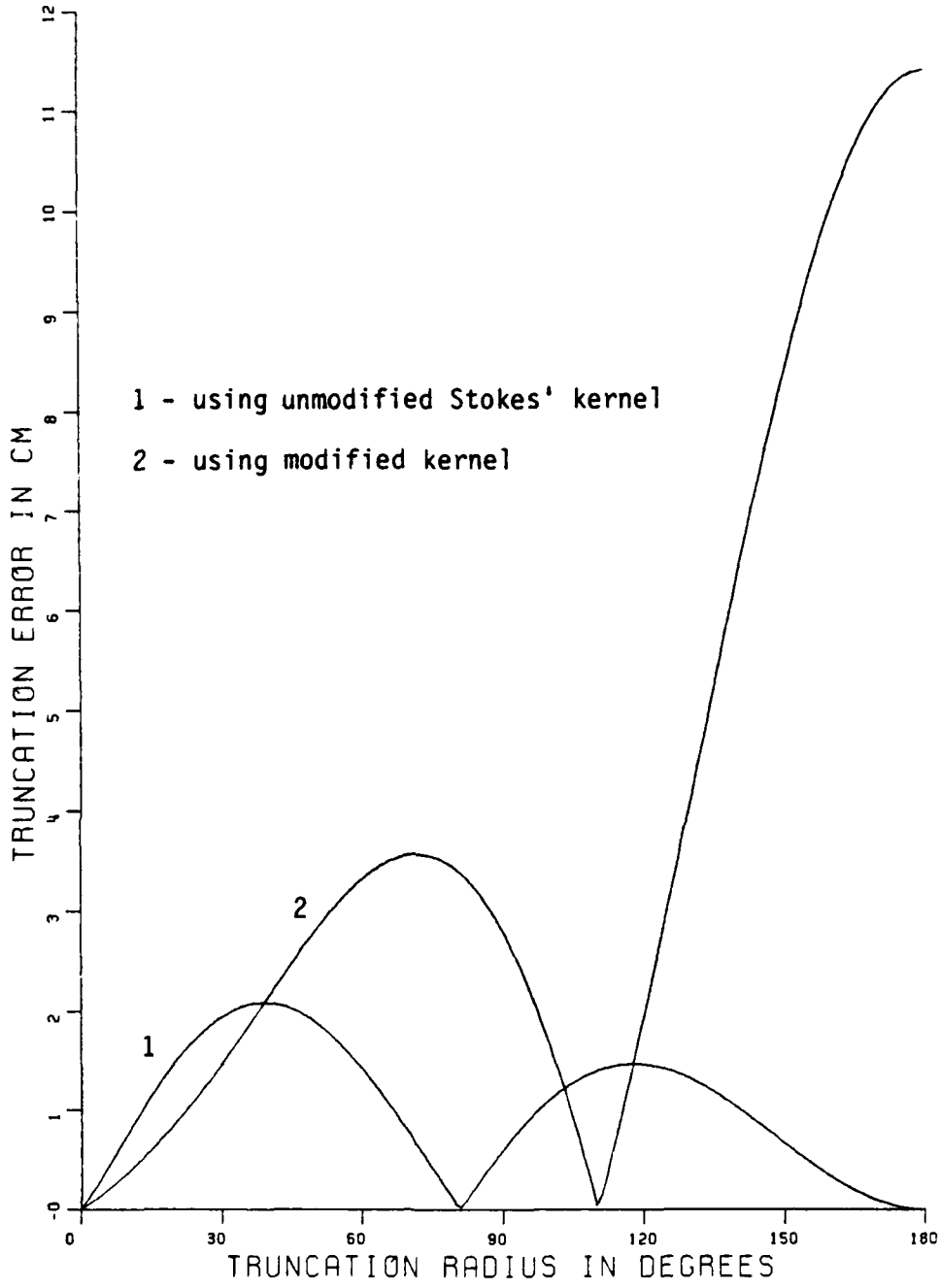

Figure 32. Truncation effect on the zero-degree undulation term (formulae 35 and 36) computed for the zero-degree component of gravity anomaly Δg_0 (eq. 34) due to vertical datum inconsistency model Δh_3.
Units are cm.

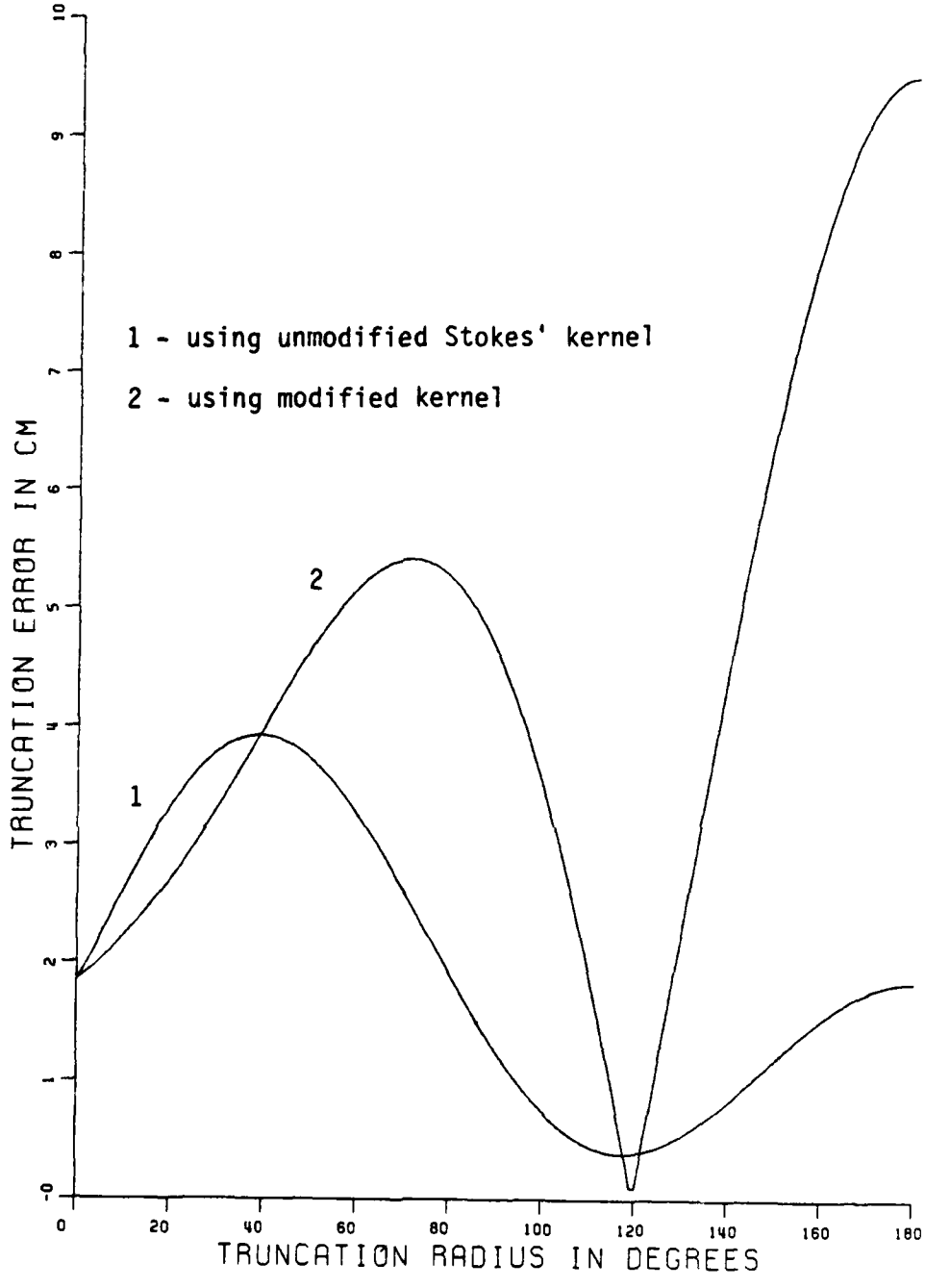

Figure 33. Truncation effect (absolute value) on the zero-degree undulation term computed according to formula 38, using the zero-degree component of gravity anomaly Δg_0 (eq. 34) due to vertical datum inconsistency model Δh_3. Units are cm.

We see that the modified kernel produces much smaller truncation effects than the unmodified one. In fact up to ψ_c=15° the effect of unmodified procedure can be twice the effect due to the modified one.

We can also evaluate the total magnitude of the effect on the zero-degree undulation according to formula (31). We will not consider

$$\frac{k\delta M}{2GR}$$

term, since δM is not known. The second term in equation (31) can be evaluated using the constants of GRS1980 used in previous sections.

$$G = 9.797644 \ (m/s^2)$$

$$R = 6371008.7714 \ m$$

The Δg_0 effect due to the inconsistencies of vertical datum was computed in the previous chapter as 0.57×10^{-2} mgal (eq. 34). Using the above constants we first find:

$$-\frac{R}{2G}\Delta g_0 = -1.85 \text{ cm}$$

Now we can evaluate the joint effect of Δg_0 on $\overline{N_0}$ (eq. 31), that is:

$$-\frac{R}{2G}\Delta g_0(1-Q_{10}) \qquad (38)$$

for different values of the truncation radius ψ_c. Figure 33 shows this effect for the case the simple Stokes' kernel is used exactly as in the basic eq. (28), and for the case a modified kernel is used in the integral term of formula (28).

Now we will evaluate the effect of datum inconsistency, which exists in a given set of terrestrial gravity anomalies for the case the geoid undulations are computed according to equation (28) using idealized values of Laplace harmonics of gravity anomaly field implied by potential coefficients (equation 28) and a given set of surface gravity anomalies in a cap possibly contaminated by vertical datums inconsistency. In other words we postulate that a given set of terrestrial gravity anomalies data can be split into two parts:

$$\Delta g = \Delta g_I + \delta\Delta g \tag{39}$$

where

Δg_I - idealized, consistent set of gravity anomalies

$\delta\Delta g$ - the effect due to inconsistencies in vertical datum.

We also assume that the idealized set of terrestrial data Δg_I is that implied by the potential coefficients:

$$\Delta g_I = \sum_{n=2}^{\infty} \Delta g_n \tag{40}$$

where Δg_n are given by formula (27).

Substituting for Δg in equation (28) we have

$$N = \overline{N}_0 + \frac{R}{4\pi G} \iint_{\sigma_c} S(\psi)\ (\Delta g_I + \delta\Delta g)\ d\sigma_c + \frac{R}{2G} \sum_{n=2}^{n_0} Q_{1n}(\psi_c)\ \Delta g_n \tag{41}$$

or

$$N = \overline{N_0} + \frac{R}{4\pi G} \iint_{\sigma_c} S(\psi)\ \Delta g_I\ d\sigma_c + \frac{R}{2G} \sum_{n=2}^{n_0} Q_{1n}(\psi_c)\ \Delta g_n + \delta N \tag{42}$$

where

$$\delta N = \frac{R}{4\pi G} \iint_{\sigma_c} S(\psi)\ \delta\Delta g\ d\sigma_c \tag{43}$$

Therefore, we can rewrite (42) in the form:

$$N = N_I + \delta N \tag{44}$$

where

N_I - idealized set of geoid undulation implied by Δg_I.

Now we will evaluate the δN term (eq. 43) which can be attributed to the effect of datum inconsistencies implied by the computational method (28).

Introducing the Molodenskii's truncation coefficients (eq. 24) we can rewrite (43) as:

$$\delta N = \frac{R}{4\pi G} \iint_{\sigma} S(\psi)\, \delta\Delta g\, d\sigma - \frac{R}{2G} \sum_{n=2}^{\infty} Q_{1n}\, \delta\Delta g_n \qquad (45)$$

The ordinary Stokes' integral in (45) represents the total effect of datum inconsistencies in terms of geoid undulation which was already evaluated in Chapter 6 (eq. 13) and is given in Table 2 in terms of degree variances (we will use data in the third column of Table 2 as pertaining to the most complete third model of datum inconsistencies). The quantities $\delta\Delta g$ were also evaluated in Chapter 6 in the form of degree variances (eq. 15). They simply represent the spherical harmonic decomposition of the effect of vertical datum inconsistencies described in terms of gravity anomalies. Now we can rewrite eq. (45) using the explicit spherical harmonic decomposition of the integral term in formula (45) and substituting for $\delta\Delta g_n$ by means of correction coefficients $\overline{\delta C}_{nm}$ and $\overline{\delta S}_{nm}$ already found in Chapter 6 (eq. 10):

$$\delta N = \sum_{n=2}^{\infty} R \sum_{m=0}^{n} (\overline{\delta C}_{nm} \cos m\lambda + \overline{\delta S}_{nm} \sin m\lambda)\, \overline{P}_{nm}(\cos\theta) +$$

$$- \sum_{n=2}^{\infty} Q_{1n}(\psi_c)\, \frac{R(n-1)}{R} \sum_{m=0}^{n} (\overline{\delta C}_{nm} \cos m\lambda + \overline{\delta S}_{nm} \sin m\lambda)\, \overline{P}_{nm}(\cos\theta) \qquad (46)$$

or

$$\delta N = \sum_{n=2}^{\infty} \left(R \sum_{m=0}^{n} (\overline{\delta C}_{nm} \cos m\lambda + \overline{\delta S}_{nm} \sin m\lambda)\, \overline{P}_{nm}(\cos\theta)\right)\left(1 - \frac{n-1}{2} Q_{1n}(\psi_c)\right) \qquad (47)$$

We can rewrite (47) as follows:

$$\delta N = \sum_{n=2}^{\infty} N_n \left(1 - \frac{n-1}{2} Q_{1n}(\psi_c)\right) \qquad (48)$$

where

$$N_n = R \sum_{m=0}^{n} (\overline{\delta C}_{nm} \cos m\lambda + \overline{\delta S}_{nm} \sin m\lambda) \overline{P_{nm}}(\cos \theta)$$

denotes the undulation Laplace spherical harmonic of n-th degree due to vertical datum inconsistencies. Note that in the formula (48) the Laplace harmonics are modified by the cap-size dependent factor

$$(1 - \frac{n-1}{2} Q_{1n}(\psi_c))$$

which reflects the truncation effect.

Since we are interested mostly in the magnitude of the effect described by eq. (48) we will rewrite this equation in terms of degree variances which reflect the average effect due to the specific degree. Then, the cummulative effect up to degree 180 may be defined as:

$$\sqrt{\overline{\delta N^2}} := \sqrt{\sum_{n=2}^{180} x_n (1 - \frac{n-1}{2} Q_{1n}(\psi_c))^2} \qquad (49)$$

where

x_n - denotes the undulation error degree variance (Chapter 6, eq. 13).

The numbers $\sqrt{x_n}$ were computed in Chapter 6 and are given in Table 2. We will use the last column in Table 2 as being implied by our most complete model of datum inconsistencies.

Now, equation (49) can be evaluated for different values of cap-radius ψ_c with upper summation index n =180. Figure 34 shows this effect plotted for the two cases: Curve 1 was constructed exactly like in formula (49) using unmodified Molodenskii's coefficients $Q_{1n}(\psi)$. Curve 2 was constructed using modified Molodenskii coefficients $Q_{2n}(\psi)$ which arise when the modified kernel $S(\psi) - S(\psi_c)$ was originally used in method (28).

From Figure 34 we see that maximum effect of datum inconsistencies occurs for the truncation angle ψ_c=180° (that is when global data is used). and reaches 44.51 cm. This result should be compared with 44.7 cm cumulative effect on geoid undulation computed in Chapter 6, eq. (14), which is based on the summation from 0 to 180 of the square roots of correction coefficients degree variances (eq. 10). The slight difference is due to the magnitude of the zero degree term which is not considered by formula (49).

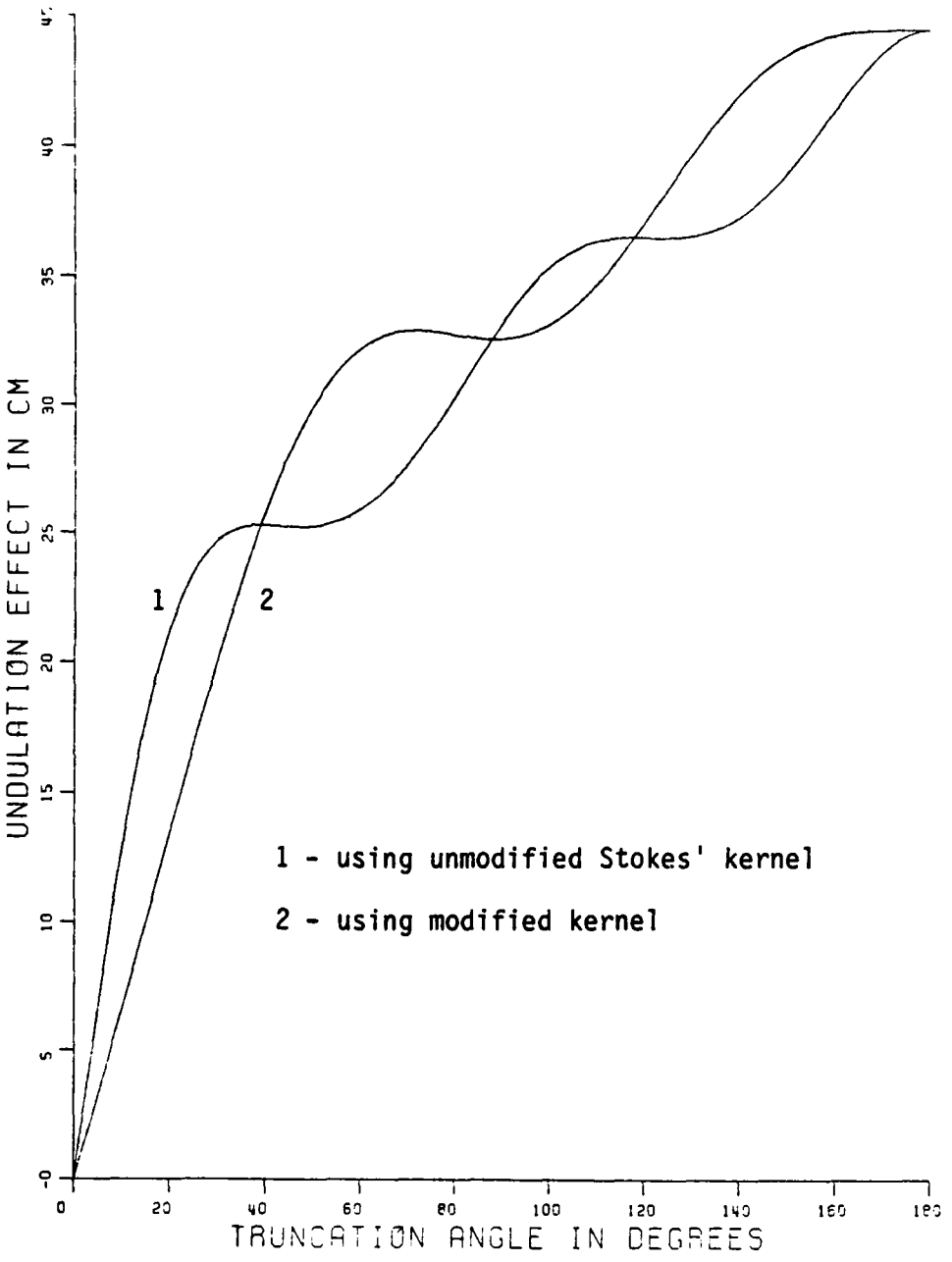

Figure 34. Cumulative effect on geoid undulation (excluding zero-degree term, see eq. 49) due to vertical datum inconsistency model Δh_3 for different truncation angles.

For the truncation angle $\psi_c=0°$ the effect due to eq. (49) is zero since no terrestrial gravity data is actually used. For spherical caps having radius $\psi_c \leq 39°$ the effect due to the modified Molodenskii kernel is considerably smaller than the effect due to the unmodified Stokes' kernel.

The caps used in most practical cases have radius varying from 10 to 15 degrees which can produce the effect varying from 6 to 11 cm for the case of modified kernel or from 13 to 19 cm for the case of simple Stokes' kernel (see Figure 34).

If we combine the cumulative effect on undulation due to harmonics having degree from 2 to 180 as computed from formula (49) (Figure 34) with the zero degree effect expressed by eq. (38) we will find the total effect due to vertical datum inconsistencies associated with our basic method for computation of geoid undulation (see eq. 28). Using equations (38) and (49) the magnitude of this todal effect can be expressed as follows:

$$\sqrt{\left(\frac{R}{2G}\right)^2 \Delta g_0^2 \,(1-Q_{10})^2 + \sum_{n=2}^{180} x_n \left(1 - \frac{n-1}{2} Q_{1n}\right)^2} \qquad (50)$$

Figure 35 shows this effect for the two cases: curve 1 is related to the unmodified Stokes' kernel, whereas curve 2 is related to the modified Molodenskii's kernel, depending which one is used in our basic method of geoid undulation computation (formula 28). From the figure we note that for the truncation angle $\psi_c=0°$ the total effect is 1.85 cm which represents the constant:

$$\frac{R}{2G} \Delta g_0$$

This constant is independent of the truncation angle ψ_c. It was originally introduced by the formula (22), and evaluated for the zero degree harmonic component of the error in gravity anomaly field due to the inconsistency in the vertical datums (see formula 34). For the truncation angle $\psi_c=180°$, that is for the global data set, the total effect reaches 44.55 cm for the ordinary Stokes' kernel and 45.52 cm for the modified one.

For the usual cap size ranging from 10 to 15 degrees the total effect shown on Figure 35 varies from 13 to 19 cm for the ordinary Stokes' kernel and from 7 to 11 cm for the modified one. Since in many applications there is a need for the determination of the geoid to the accuracy of 10 cm, the effects computed here cannot be neglected.

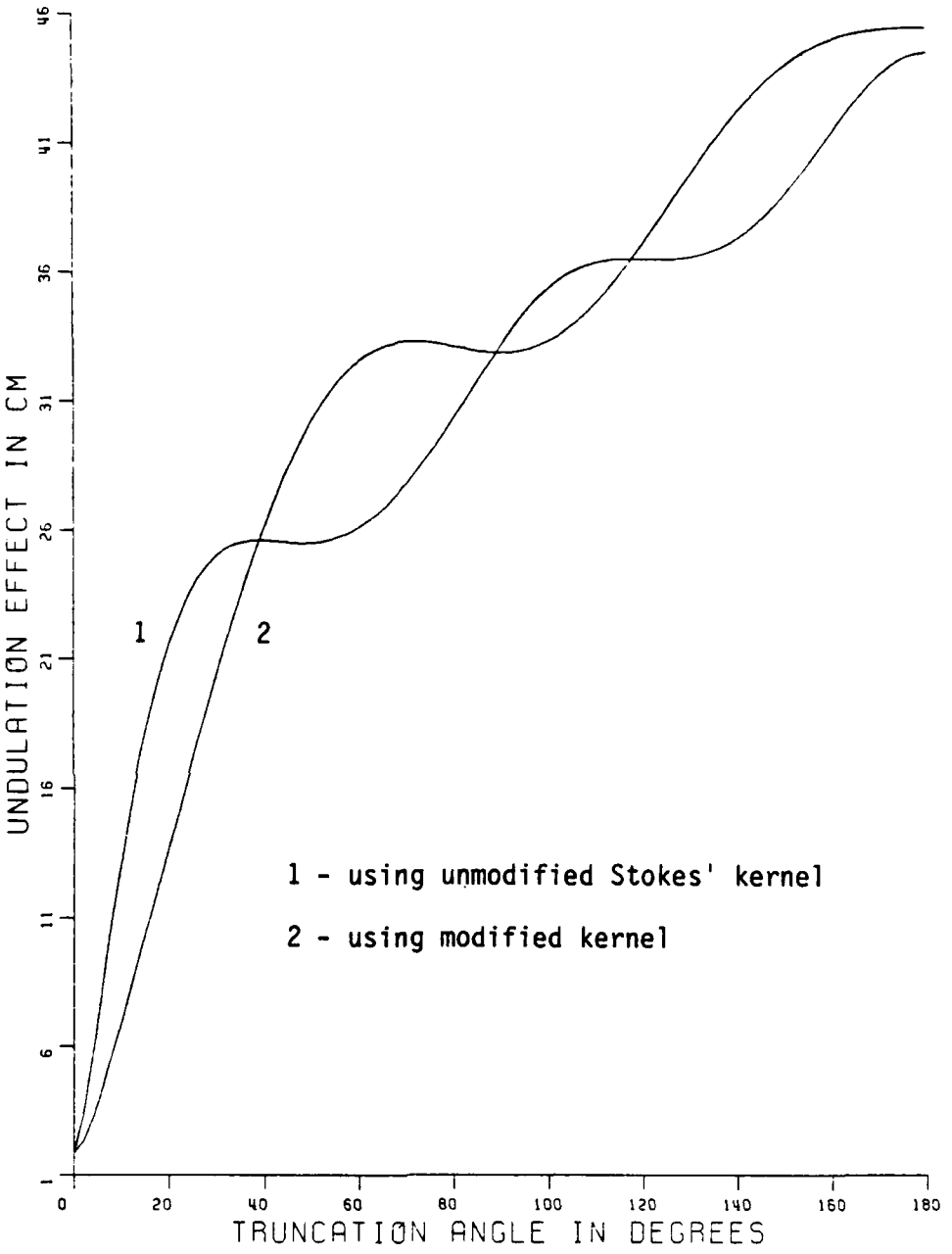

Figure 35. The total cumulative effect on geoid undulation (including zero-degree component, see eq. 50) due to vertical datum inconsistency model Δh_3 for different truncation angles.

8. SUMMARY AND CONCLUSIONS

The Sea Surface Topography determines the deviation of the Mean Sea Level from the geoid. This deviation causes different vertical datums existing in different parts of the world to refer to slightly different zero-levels. Those zero-levels define different equipotential surfaces of Earth's gravitational potential or surfaces that are not even equipotential (due to overconstrained adjustment of levelling net). Therefore, the terrestrial gravity data that were reduced 'to the geoid' are in fact in an inconsistent system. These inconsistencies in the global vertical datum can be modeled to the accuracy the SST is known, provided sufficient information on variety of existing vertical networks and procedures is available.

Today, our knowledge on the SST variation is far from complete. The same pertains to the information on actual vertical datums on most of the land areas on our globe. Therefore, the approach presented in this work can be classified as the numerical simulation technique. We constructed three different approximations of the hypothetic vertical datum inconsistencies as shown on Figures 17, 18 and 19. In order to evaluate the propagated error in potential coefficients due to the vertical datum inconsistencies we carried out the spectral analysis of those approximating function (formula (10)). The correction coefficients produced in this way represent the errors in potential coefficient due to datum inconsistency, provided geopotential is determined using only terrestrial gravity anomaly data.

Table 1 shows that global datum inconsistency can produce a significant relative error in potential coefficients that, for low degree harmonics, can reach almost 1 percent. In terms of geoid undulation this error translates to the average of almost half a meter at first degree harmonics. The cumulative error up to degree 180 (see formula (14)) was computed as 44.67 cm, which means it can easily reach the full amplitude of the SST variation.

Beyond degree 60 the effect of vertical datum inconsistency is of the order of background noise and can be neglected. The most significant contribution is in the low degree harmonics. As can be estimated from Figure 30 the low order correction coefficients within the first 10 degrees carry as much as 92.6 percent of the total energy of the error-spectrum (if we confine our study up to degree 180). Beyond degree 60 there is only about 1 percent of the total energy in the error-spectrum.

The conclusion is that by supplying the low degree harmonics of geopotential (say up to degree 10) from other sources than the terrestrial gravity data we can avoid as much as 90 percent of the error introduced by the inconsistencies in vertical datum. From that point of view the combination of satellite-derived low degree coefficients with the high degree coefficients derived from terrestrial data is

highly recommended. Plots similar to those of Figure 30 or Figure 31 can provide the estimate of the optimal 'splitting degree', so that the errors over the whole spectrum are minimized.

The internal warp in the North Americal vertical datum as modeled in Figure 15 seems to have a negligible effect on the determination of spherical harmonics coefficients of gravitational potential. In terms of the error in geoid undulation, this effect can be estimated to be of the order of millimeters.

Finally, the effect due to the computational procedures such as the one proposed by Rummel and Rapp (1976) (see eq. 28) is of a great practical importance. It was shown that due to the inconsistency in the world vertical datum the frequency content of a given terrestrial gravity anomaly data may differ from the frequency content of an idealized anomalies implied by a consistent vertical reference. This discrepancy in turn will propagate on geoid undulation as determined by the computational method such as the one of Rummel and Rapp (eq. 28). The magnitude of that effect is a function of size of spherical cap used in the computations. For the usual cap size ranging from 10 to 15 degrees in spherical radius this effect ranges from 7 cm to 11 cm or from 13 cm to 19 cm depending on the modified kernel or unmodified one was used in the computations. In the near future the 10 cm accuracies will be required for the determination of geoid. We conclude that due to vertical datums inconsistencies the 10 cm level is actually the highest possible resolution that could be achieved using the terrestrial gravity data. One cannot go beyond that limit without solving the vertical datum problem.

References

Angus-Leppan, P.V., Rizos, C., (1980), The Need for a High Accuracy Geoid on Land and Sea, 4th International Symposium on Geodesy and Physics of the Earth, G.D.R. Karl-Marx-Stadt, May 12-17, p. 211-225.

Colombo, O. (1981), Numerical Methods for Harmonic Analysis on the Sphere, Report No. 310, Department of Geodetic Science and Surveying, The Ohio State University, Columbus.

Davis, J.C., (1973), 'Statistics Data Analysis in Geology, John Wiley and Sons, Inc.

Defant, A., (1941), Quantitative Untersuchungen zur Statik und Dynamic des Atlantischen Ozeans. 5. Lief. Die absolute Topographie des physikalischen Meeresniveaus und der Druckflächen, sowie die Wasserbewegung in Atlantischen Ozean. Wissensch. Ergebn. Dtsch. Atlant. Exped. "Meteor", 6, p. 191-260.

Dietrich, G., (1937), Die Lage der Meeresoberfläche im Druckfeld von Ozean und Atmosphere, mit besonderer Berücksichtigung des westlichen Nordatlantischen Ozeans und des Golfs von Mexico.II. Über Bewegung und Herkunft des Golfstromwassers. Veröff. Inst. Meeresk. Berlin, N. F. Geogr. - Naturw, Reihe, 33, p. 1-52.

Frasetto, R., (1970), The Subsidence and Storm Surge Effects in Venice - Italy. Rep. Symp. Coastal Geodesy, Munich, pp. 527-535.

Golub, G.H. and Businger, P.A. (1965), Linear Least Squares Solutions by Householder Transformations, Numer. Math., H.B. Series Linear Algebra pp. 269-276.

Hanson, R.H. and Lawson, C.L. (1969), Extensions and Applications of the Householder Algorithm for Solving Linear Least Squares Problems, Math. Comp., 23, No. 108, p. 787-812.

Heer, R., Niemeir, W., (1982), Levelling Network and 'Height Truth' around the North Sea, Mitteilung Nr. 166, Des Instituts Angewandte Geodasie, Frankfurt am Main.

Heiskanen, W. and H. Moritz, (1967), Physical Geodesy, W.H. Freeman and Co., San Francisco.

Householder, A.S. (1958), Unitary Triangularization of a Nonsymmetric Matrix, J.ACM, 5, pp. 339-342.

AD-A137 881 THE EFFECT OF VERTICAL DATUM INCONSISTENCIES ON THE DETERMINATION OF GRAV..(U) OHIO STATE UNIV COLUMBUS DEPT OF GEODETIC SCIENCE AND SUREEYI.. P LASKOWSKI

2/2

UNCLASSIFIED AUG 83 OSU/DGSS-349 AFGL-TR-83-0228 F/G 8/5 NL

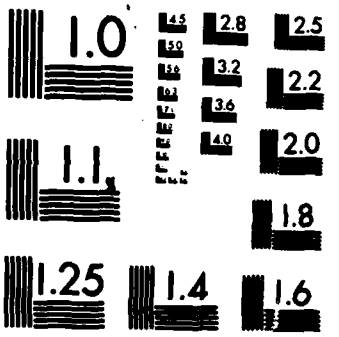

MICROCOPY RESOLUTION TEST CHART
NATIONAL BUREAU OF STANDARDS-1963-A

Jekeli, C., (1980), Reducing the Error of Geoid Undulation Computations by Modifying Stokes' Function, Report No. 301, Department of Geodetic Science and Surveying, The Ohio State University, Columbus Ohio.

Kok, J., Ehrnsperger, W., Rietveld, H., (1980), The 1979 Adjustment of the United European Levelling Network (UELN) and Its Analysis of Precision and Reliability, The Second International Symposium on Problems Related to the Redefinition of North American Vertical Geodetic Network (NAD 1980), Ottawa, p. 455.

Lachapelle, G., (1978), Status of the Redefinition of the Vertical Reference System in Canada, Proceedings: Second International Symposium on Problems Related to the Redefinition of North American Geodetic Networks. The Marriot Hotel, Arlington, Virginia April 24-28, p. 610.

Lacombe, H., (1951), Application de la méthode dynamique à la circulation dans l'océan Indien, au printemps boréal, et dans l'océan Antarctique, pendant l'été austral. Bull. Inf. C.O.E.C., 3, p. 459-468.

Lawson, C. and R. Hanson, (1974), Solving Least Squares Problems, Prentice-Hall Inc.

Leppert, K., (1974), The Australian Levelling Adjustment Progress to April 1970, Report on the Symposium on Coastal Geodesy, Munich 20-24 July, p. 223.

Levitus, S., (1982), Climatological Atlas of the World Ocean, NOAA Professional paper 13, 1982.

Lippold, H., (1980), Readjustment of the National Geodetic Vertical Datum, EOS, vol. 61, no. 24, June 10, pp. 489-490.

Lisitzin, E., (1965), The Mean Sea Level of the World Ocean. Comment. Phys.-Math. Helsingf., pp. 30-35.

Lisitzin, E., (1974), Sea-Level Changes, Elsevier Science Publishing Company, Amsterdam, New Jork.

Meissl, P., (1971), Preparations for the Numerical Evaluation of Second Order Molodensky - type Formulas, Report No. 163, Department of Geodetic science and Surveying, The Ohio State University.

Merry, C., and P. Vanicek, (1982), Investigation of Local Variations of Sea Surface Topography, paper submitted to Marine Geodesy.

Milbert, D., (1980), A Simulation of Random Error Propagation for the United States Levelling Network, 2nd International Symposium on Problems Related to the Redefinition of North American Vertical Geodetic Networks (NAD 1980), Ottawa.

Mitchell, H., (1972), An Australian Geopotential Network Based on Observed Gravity, Unisurv. G18, University of New South Wales, Australia, p. 35-50.

Molodenskii, M.S., et al., (1962), Methods for the Study of the External Gravitational Field and Figure of the Earth, translated from Russian (1960), Israel Program for Scientific Transactions, Jerusalem, 1962.

Powell, M.J.D., and J.K. Reid, (1968), On Applying Householder's Method to Linear Least Squares Problems, Proc. IFIP Congress.

Rapp, R.H., (1973), Numerical Results from the Combination of Gravimetric and Satellite Data Using the Principles of the Least Squares Collocation, Reports of the Department of Geodetic Science, No. 200, The Ohio State University, Columbus, Ohio.

Rapp, R.H., (1981), The Earth's Gravity Field to Degree and Order 180 Using Seasat Altimeter Data, Terrestrial Gravity Data, and Other Data, Reports of the Department of Geodetic Science and Surveying, No. 322, The Ohio State University, Columbus, Ohio.

Rapp, R.H., and R. Rummel, (1975), Methods for the Computation of Detailed Geoids and their Accuracy, Reports of the Department of Geodetic Science, No. 233, The Ohio State University, Columbus, Ohio.

Reid, J.L.,(1961), On the Geostrophic Flow of the Surface of the Pacific Ocean with Respect to the 1000-decibar Surface. Tellus, 13, p. 489-502.

Rummel, R., and R. Rapp, (1976), The Influence of the Atmosphere on Geoid and Potential Coefficient Determinations from Gravity Data, Journal of Geophysical Research, Vol. 81, No. 32.

Stommel, H., (1965), The Gulf Stream, a Physical and Dynamical Description. Univ. Calif. Press, Berkeley, Calif., 2nd ed., 248 pp.

Sturges, W., (1974), Sea Level Slope Along Continental Boundaries, Journal of Geophysical Research, vol. 79. No. 6, p. 825-830.

Vanicek, P., Castle, R., Balazs, E., (1980), Geodetic Levelling and Its Applications, Reviews of Geophysics and Space Physics, vol. 18, No. 2, May, pp. 505-524.

END

FILMED

3-84

DTIC